STRUCTURE OF BEDROCK OFFSHORE FROM POINT ACONI, CAPE BRETON ISLAND, NOVA SCOTIA

James Patrick Duggan

Submitted in Partial Fulfilment of the Requirements
for the Degree of Bachelor of Science, Honours
Department of Earth Sciences
Dalhousie University, Halifax, Nova Scotia
April, 1995

Distribution License

DalSpace requires agreement to this non-exclusive distribution license before your item can appear on DalSpace.

NON-EXCLUSIVE DISTRIBUTION LICENSE

You (the author(s) or copyright owner) grant to Dalhousie University the non-exclusive right to reproduce and distribute your submission worldwide in any medium.

You agree that Dalhousie University may, without changing the content, reformat the submission for the purpose of preservation.

You also agree that Dalhousie University may keep more than one copy of this submission for purposes of security, back-up and preservation.

You agree that the submission is your original work, and that you have the right to grant the rights contained in this license. You also agree that your submission does not, to the best of your knowledge, infringe upon anyone's copyright.

If the submission contains material for which you do not hold copyright, you agree that you have obtained the unrestricted permission of the copyright owner to grant Dalhousie University the rights required by this license, and that such third-party owned material is clearly identified and acknowledged within the text or content of the submission.

If the submission is based upon work that has been sponsored or supported by an agency or organization other than Dalhousie University, you assert that you have fulfilled any right of review or other obligations required by such contract or agreement.

Dalhousie University will clearly identify your name(s) as the author(s) or owner(s) of the submission, and will not make any alteration to the content of the files that you have submitted.

If you have questions regarding this license please contact the repository manager at dalspace@dal.ca.

Grant the distribution license by signing and dating below.

_____ _____

Name of signatory Date

Dalhousie University

Department of Earth Sciences
Halifax, Nova Scotia
Canada B3H 3J5
(902) 494-2358
FAX (902) 494-6889

DATE April 25,1995

AUTHOR James Patrick Duggan

TITLE STRUCTURE OF BEDROCK OFFSHORE FROM POINT ACONI,

CAPE BRETON ISLAND, NOVA SCOTIA

Degree Honours BSc Convocation May Year 1995

Permission is herewith granted to Dalhousie University to circulate and to have copied for non-commercial purposes, at its discretion, the above title upon the request of individuals or institutions.

Signature of Author

Abstract

The Prince Colliery is a major offshore coal mine operated by the Cape Breton Development Corporation (DEVCO) in the Hub coal seam of the Sydney Mines Formation (Upper Carboniferous). This thesis presents the results of a multibeam swath bathymetry and high resolution seismic survey in the area offshore from Point Aconi, Cape Breton Island. The multibeam bathymetric data set generally shows the surface expression of the MacKenzie Syncline, a major structural feature in the study area. The Atlantic Geoscience Centre (AGC, Geological Survey of Canada) designed the seismic survey to delineate more precisely the geological structure of bedrock in the area of anticipated mine development. Seafloor morphology influences the interpretation of the seismic data by producing drawdown effects on the seismic record. The seismic data extend the surface structural trends downwards, defining the three dimensional geometry of the bedrock. In addition, two coal seams (Lloyd Cove and Point Aconi coal seams) correlate with specific bedrock reflectors. The seismic data set shows no evidence of faulting. The conversion of the interpretation of structure from two-way time to depth can account for survey geometry and drawdown resulting from unconsolidated sediments. Mine planning at the Prince Colliery accounts for thickness of bedrock, which varies laterally with the depth of the Hub coal seam and thickness of unconsolidated sediments. This new interpretation is, therefore, of benefit to mine planning activities at the Prince Colliery.

Key Words: high resolution seismology, coal, Prince Colliery, mine planning, Sydney Mines Formation, Sydney Basin, multibeam sonar, seafloor morphology

Acknowledgements

The following is a list of persons the author wishes to acknowledge for help given during the progress of this thesis:

•facilities	.Bob Courtney
	.Kevin Coflin
•writing	.Barrie Clarke
	.Pat Ryall
•geophysics	.Brian Nicols
	.John Stewart
•geology	.Rob Naylor
	.Brendan McKenzie
	.Tom Martel
	.Ken Sanders
•diagrams	.Neil Tibert
•transportation	.Mark Stevens
•miscellaneous	.Kevin Giles
	.Gunter Muecke

Table of Contents

CHAPTER 3 DATA

CHAPTER 4 INTERPRETATION

CHAPTER 5 DISCUSSION

CHAPTER 6 CONCLUSIONS

REFERENCES

APPENDIX A MULTIBEAM SWATH BATHYMETRY SURVEY OPERATIONS

APPENDIX B SEISMIC SURVEY OPERATIONS

List of Figures

Chapter 4 Interpretation

Chapter 5 Discussion

Appendix B Seismic Survey Operations

List of Tables

CHAPTER 1 INTRODUCTION

1.1 Background

1.1.1 Sydney Coalfield and Prince Colliery

The Sydney Coalfield of Cape Breton Island contains large resources of coal of favourable rank and thickness. In size, production, and remaining resources, the Sydney Coalfield is the largest field in eastern Canada, and the present annual production of coal is between 2.7 and 3.6 million metric tonnes (Hacquebard 1993). The Sydney Coalfield crops out on land but is almost entirely submarine, extending from north-eastern Cape Breton Island to within 50 kilometres of southwestern Newfoundland. Currently, all mining operations are in the submarine area immediately adjacent to land.

The Sydney coalfield generally corresponds to the Sydney Mines Formation of the Morien Group. Figure 1.1 shows the onland portion of the Morien Group, and the offshore boundary between the Morien Group and unnamed redbeds (Sydney Basin). Onland exposure shows major folds of Sydney Basin strata at one to ten kilometres separation. The Bateson and Mountain faults define the southern and northern extents of the Sydney Basin, respectively (Fig. 1.1). Deposition of Morien Group strata (Westphalian B to Stephanian) occurred in an alluvial floodplain while motion continued on regional faults (Gibling et al. 1987). The Sydney Mines formation and overlying unnamed redbeds are generally not faulted (Bird 1987; Gibling et al. 1987). Figure 1.2 summarises the stratigraphy of the Sydney Basin, showing absolute ages, biostratigraphic units, lithological units, and regional tectonic control on deposition.

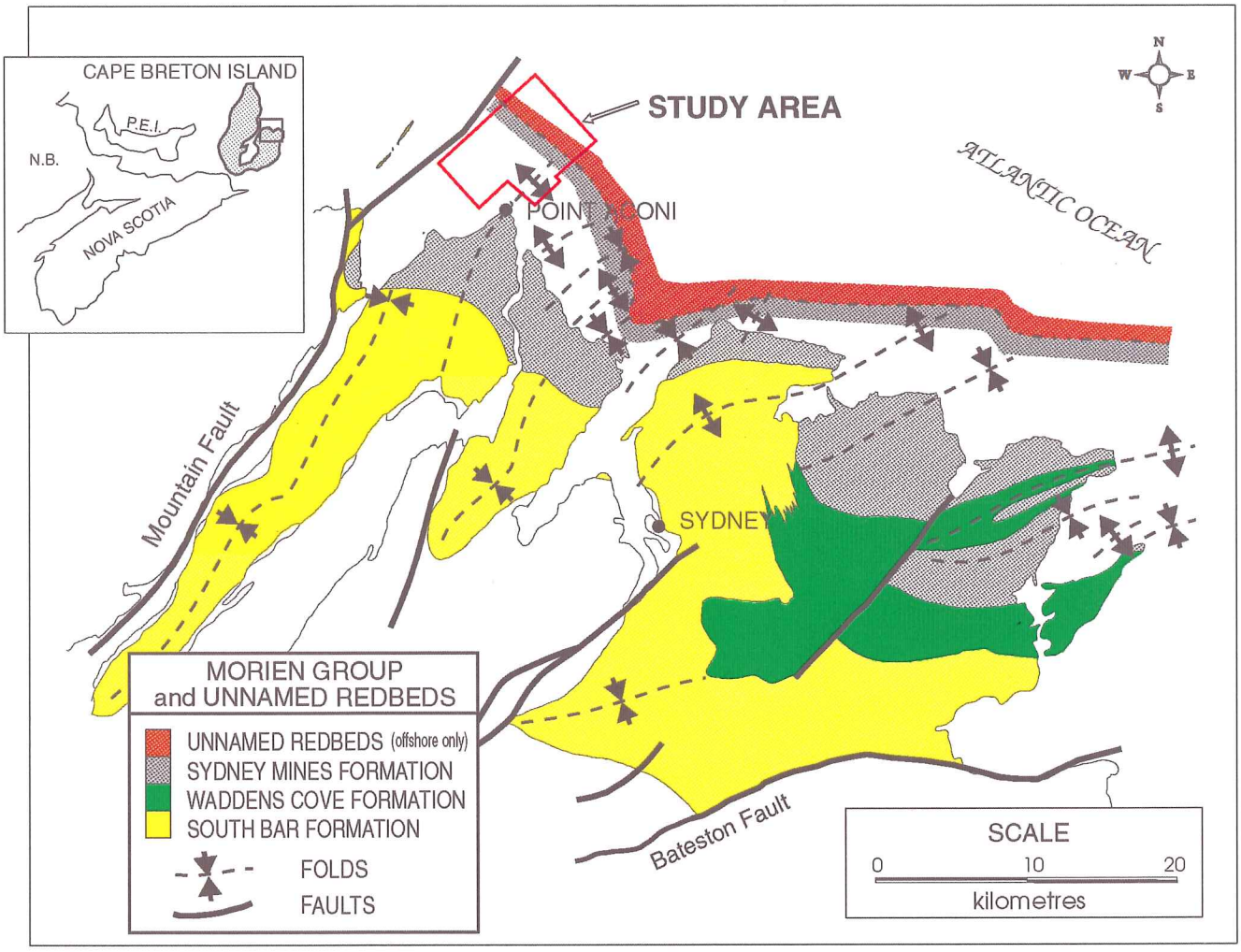

Figure 1.1 Location map of the study area showing major structural elements of the Morien Group. Point Aconi is located 25 kilometres northwest of Sydney. The Mountain and Bateston faults define the northern and southern boundaries of the onland portion of the Morien Group and unnamed redbeds. The Morien Group consists of the South Bar, Waddens Cove, and Sydney Mines Formations. Unnamed redbeds belong to the Pictou Group (Gibling et. al. 1992; after Boehner and Giles 1986, modified by Tibert 1994).

THE SYDNEY BASIN

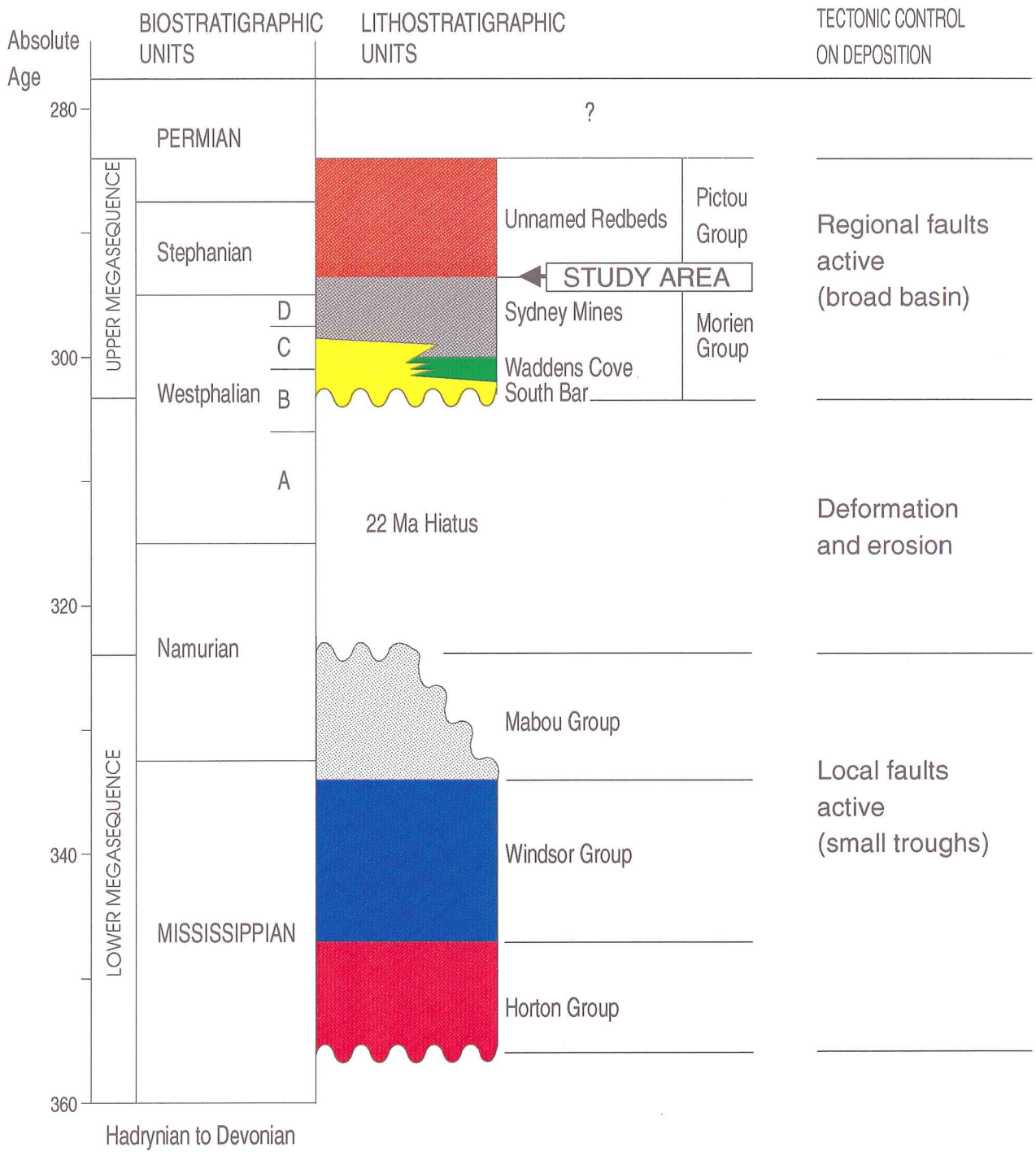

Figure 1.2 Stratigraphy of the Sydney Basin with generalised tectonic control on deposition. Bedrock in the study area offshore from Point Aconi is at the Westphalian/Stephanian boundary. The lower megasequence was deposited in small troughs accompanied by local fault movement. A 22 Ma hiatus separates the upper and lower megasequences. The upper megasequence was deposited in a broad basin accompanied by regional fault movement. As a result, strata of the upper megasequence are relatively undeformed and do not show evidence of faulting (Gibling et al. 1987, modified after Tibert 1994).

The Prince Colliery, a major working operated by the Cape Breton Development Corporation (DEVCO), is located at Point Aconi, 25 kilometres northwest of Sydney (Fig. 1.1). At Point Aconi, the Hub seam is the largest coal resource, estimated at 85 million tonnes (Hacquebard 1979). At present, workings begin onland and extend almost five kilometres offshore to a maximum depth of 240 metres below the seafloor. Figure 1.3 shows the study area of this thesis, with an overlay of mine workings as of August 1994. Anticipated development of the mine is to the northeast, as indicated by the arrows in Figure 1.3.

1.1.2 Geological Structure as an Aid in Mine Planning

Geological structure at various scales must be considered for reasons of mine planning. Prince Colliery mine workings follow the Hub coal seam, which varies laterally in its depth below the seafloor. The Prince Colliery uses the advanced longwall method of coal extraction. Two aspects arise from using the longwall method: 1) coal mining is restricted to strata that are relatively flat and free of faults; and 2) mine workings are restricted in width by an amount that varies with depth below the sea floor (B. McKenzie, pers. comm. 1995).

A coal seam disrupted by faulting or intense folding is not suitable for the advanced longwall method. Although faults are absent in mine and onland exposures, absence of faulting must be confirmed in the area of anticipated development.

Because operations are below the seafloor, mine planning is concerned with water infiltration into the mining area. With the advanced longwall method, bedrock collapses after the extraction of coal. Fractures result from collapse of bedrock, and fractures may produce conduits for water infiltration. The allowable width of a working is based on the nature of fracturing, as

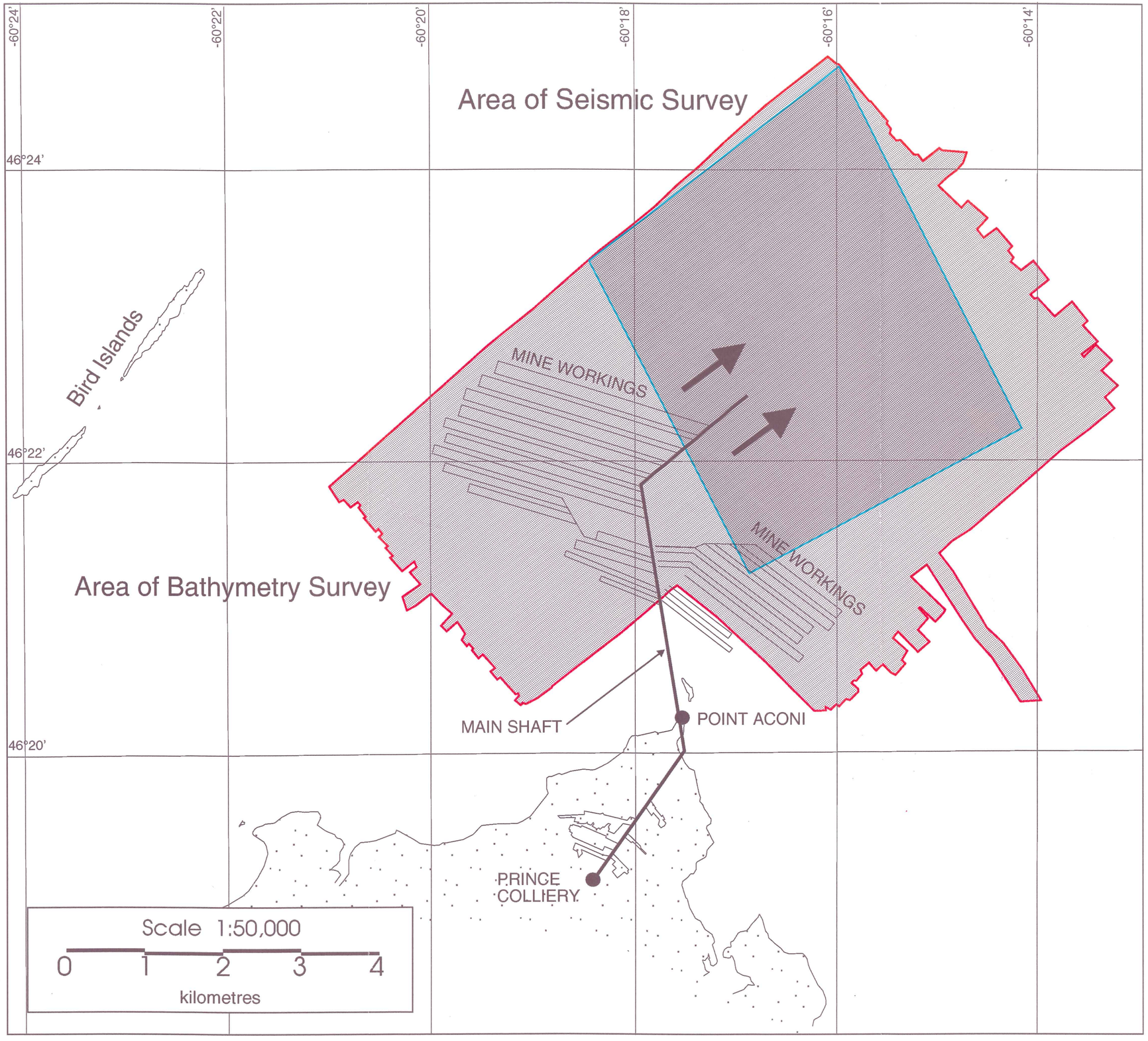

Figure 1.3 Study area offshore from Point Aconi, Cape Breton Island. The light gray area is surveyed by multibeam swath bathymetry; the dark gray area by single-channel seismics. Prince Colliery mine workings extend for five kilometres offshore to a maximum depth of 240 metres below the seafloor. The arrows indicate direction of anticipated development by the Prince Colliery.

controlled by the thickness of overlying bedrock and the weight on bedrock, which in turn depends on the thickness of unconsolidated sediments on the seafloor and the depth of water. The accuracy that describes each of the above three aspects (i.e., depth below seafloor, thickness of unconsolidated sediments, and depth of water) affects the allowable width of mine workings (B. McKenzie, pers. comm. 1995). Mine planning first takes geological structure into account, then involves other geological factors such as coal quality, thickness of the coal seam, and type of sediment immediately overlying the coal seam (R. Naylor, pers. comm. 1994).

1.1.3 Application of Marine Seismology and Definition of Geological Structure

A proven method of mapping three-dimensional geological structure below the seafloor is marine reflection seismology. With marine reflection seismology, a sound source behind the survey vessel produces a pulse that travels through the water column and reflects from the seafloor. Some energy penetrates the seafloor and reflects from layers within the bedrock (Fig. 1.4a) and hydrophone receivers record the returning sound signal. Increasing time for the arrival of the returning signal corresponds to deeper layers within the bedrock (bedrock reflectors). By repeating the signal as the ship moves along a straight line over the seafloor, bedrock reflectors and other features below the seafloor appear in two-dimensional space. A number of parallel, closely spaced lines delineates the third dimension (Fig. 1.4b).

This thesis presents an interpretation of seismic data from a recent survey offshore from Point Aconi. Seafloor morphology obtained by a multibeam sounding technique (Fig. 1.5) constrains this interpretation based on the seismic data. These two data sets (multibeam swath bathymetry and seismic surveys; Appendices A and B) provide new information offshore from

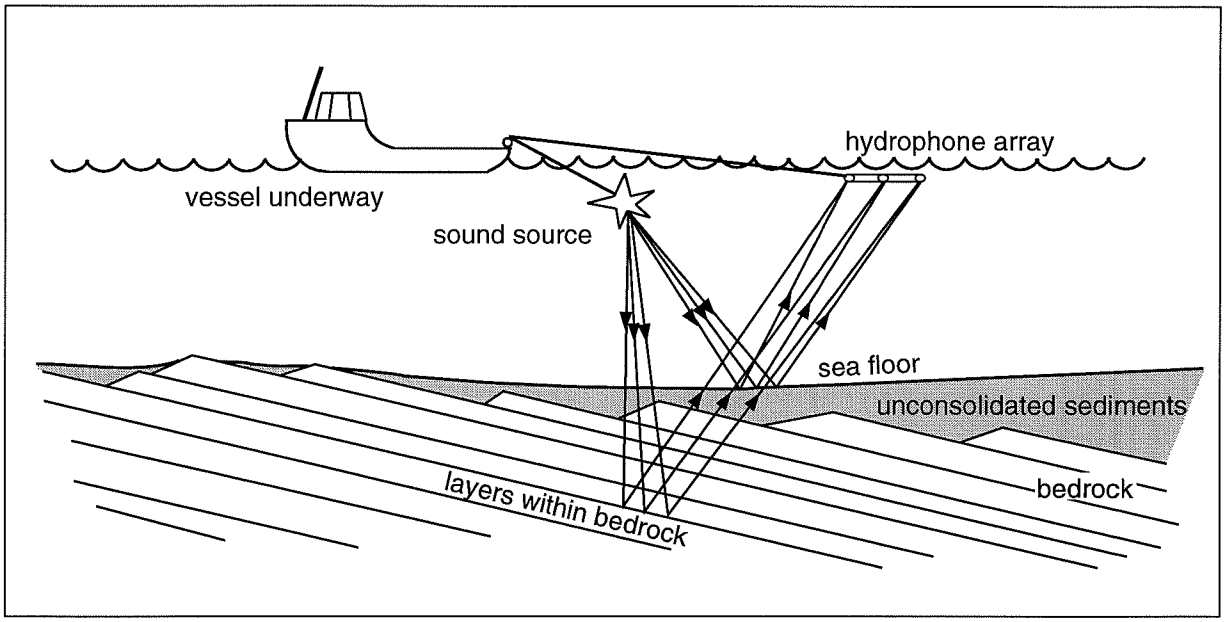

Figure 1.4a The survey set-up for single-channel seismic reflection profiling (after Kearney and Brooks 1991).

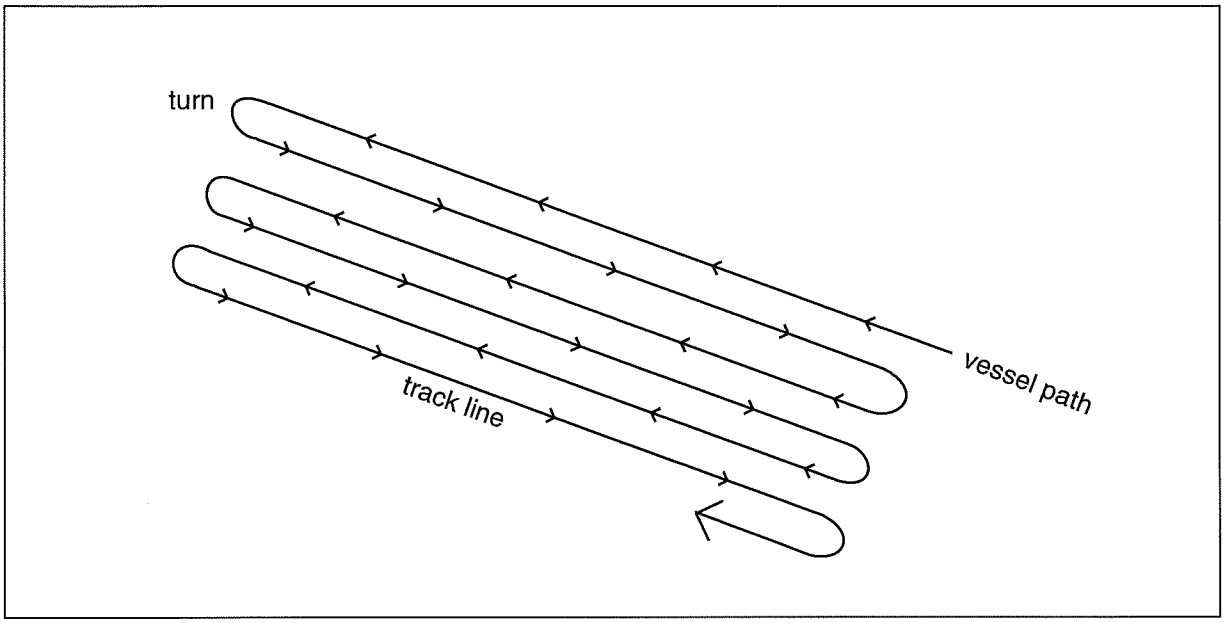

Figure 1.4b Map view of marine seismic survey consisting of a series of parallel track lines.

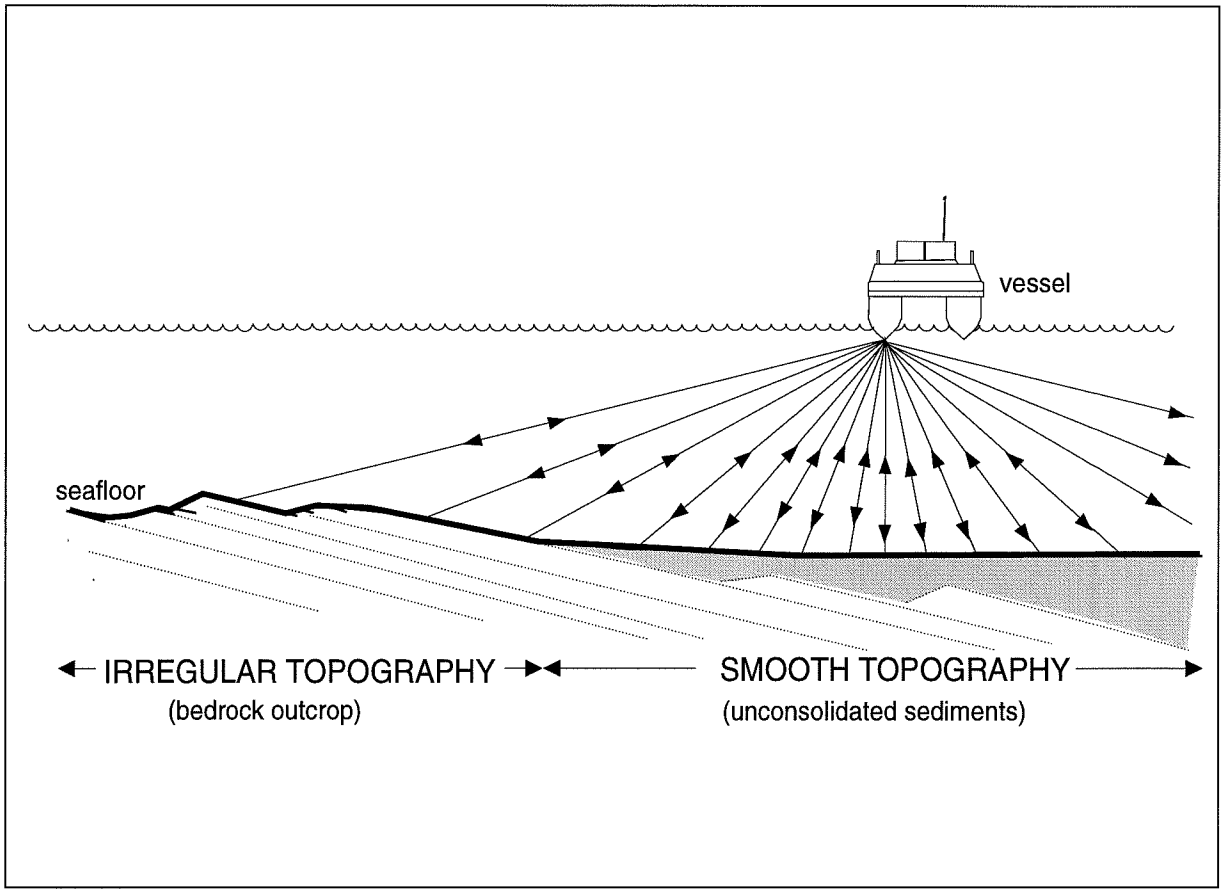

Figure 1.5 Configuration for multibeam swath bathymetry survey. Sonar does not penetrate more than a few millimeters into the seafloor. Irregular topography results from out cropping bedrock. Smooth topography results from unconsolidated sediments that overlie bedrock.

Point Aconi, and together they lead to a new interpretation of the three-dimensional geological structure in the area not yet developed by the Prince Colliery.

1.1.4 Previous Work

Stewart (1994) identified one fault (Mountain Fault) and two folds (Boisdale Anticline and MacKenzie Syncline), based on the data from two seismic surveys (one single-channel marine seismic survey conducted by the Nova Scotia Research Foundation (NSRF) in 1978, and one multi-channel marine seismic survey conducted by GeoTerrex in 1980) (Fig. 1.6). The Mountain Fault continues onland and defines the northern limit of the Sydney Basin. The Boisdale Anticline is exposed onland at Point Aconi and trends northeast. The major structural feature identified by Stewart (1994) in the study area is the MacKenzie Syncline, and it trends east-west in an orientation similar to the Hub seam contours (Fig. 1.6). The Boisdale Anticline converges towards the MacKenzie Syncline in the study area (Stewart 1994).

Stewart (1994) made a case for lack of faulting in the study area, based mainly on the NSRF data; however, this interpretation conflicts with the GeoTerrex data, which suggests the presence of an east-trending fault north of borehole H12 (Stewart 1994). Mine planning operations at the Prince Colliery, therefore, still consider the possibility of faulting (B. McKenzie, pers. comm. 1995).

1.2 Objectives

The primary objective of this thesis is to provide a better interpretation of the bedrock structure (Sydney Mines Formation and unnamed redbeds) in the offshore area to be developed

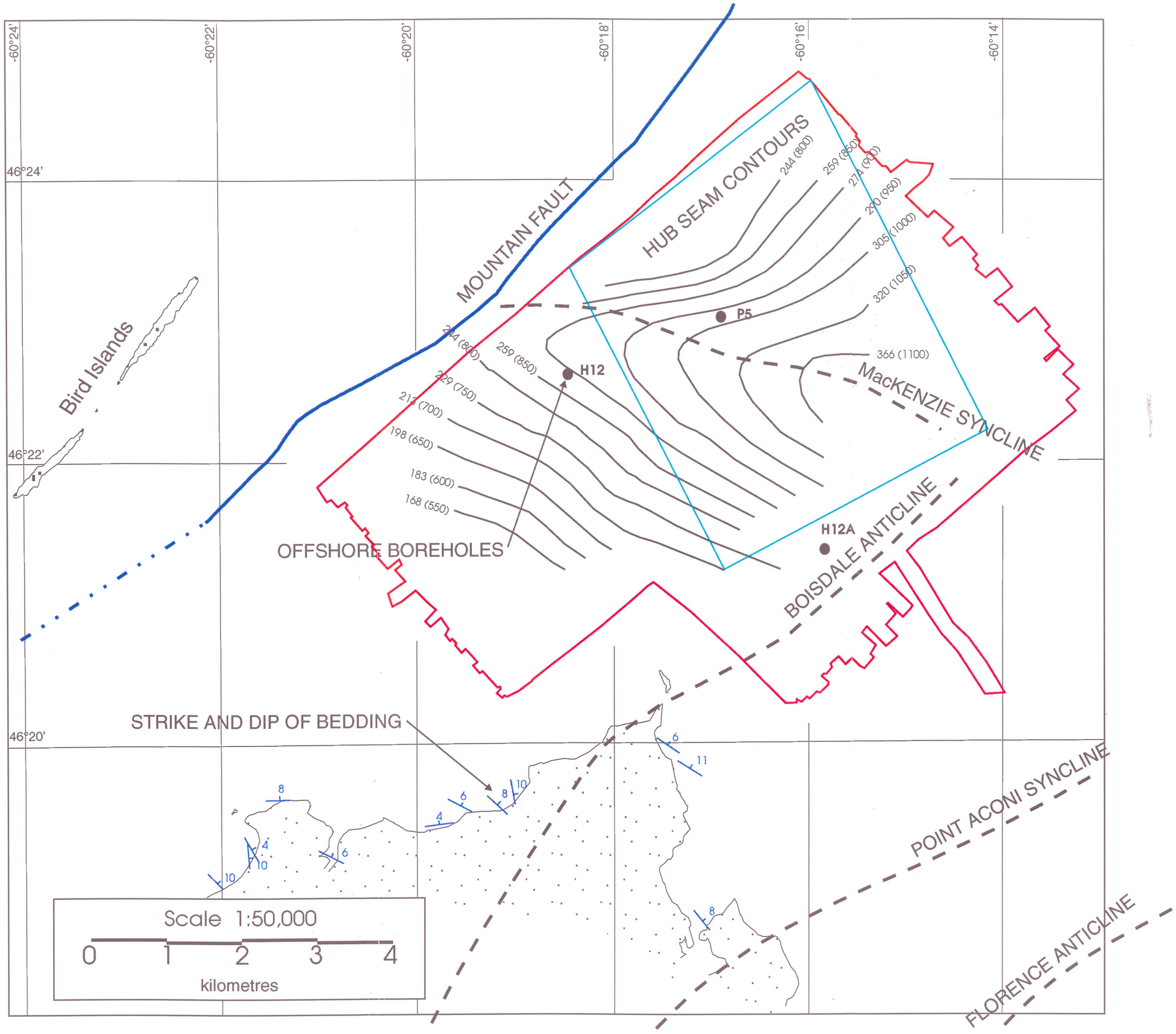

Figure 1.6 Summary of previous work in the Point Aconi area, showing geological structure at and offshore from Point Aconi with offshore borehole sites H12, H12A, and P5. MacKenzie Syncline and Mountain Fault show by Nova Scotia Research Foundation single-channel seismics. Hub seam contours are from mine exposure in metres (feet) below sea level and NSRF single-channel seismics. (after Stewart 1994; Boehner and Giles 1986)

by the Prince Colliery, using bathymetric and seismic data. The second objective to this thesis is to confirm the absence of faulting in the area of anticipated development.

This thesis is part of a larger investigation of the study area. The Geological Survey of Canada (GSC, Atlantic Geoscience Centre, Bedford Institute of Oceanography, Dartmouth), in conjunction with DEVCO and Canmet, is conducting a multi-faceted geophysical investigation offshore from Point Aconi (AGC project 94-011). Other aspects of the larger investigation include analysis of seafloor subsidence resulting from mining, mapping of unconsolidated sediments, determination of sediment type immediately above the Hub coal seam, and testing of new geophysical equipment.

1.3 Scope

Figure 1.3 defines the geographical limits of the study area. The two main data sets include: 1) EM-1000 multibeam swath bathymetry; and 2) shallow seismic with air-gun source (sleeve-gun). The onset of the first water bottom multiple limits the interpretation based on the seismic data to a maximum of 160 metres below the seafloor. New examination of two of the three boreholes (H12, H12A, and P5) helps to correlate bedrock reflectors to lithology. The comparison with onland geological structure relies on previously reported data, e.g., scientific literature and unpublished theses. Personal communication with geologists provided additional geological information specific to the Prince Colliery .

1.4 Organisation

This thesis consists of six chapters. Chapter 1 introduces the content of the thesis and orients the reader. After this introduction, subsequent chapters present the geological and geophysical data. Chapter 2 summarises the procedures for the interpretation of the multibeam sonar and seismic data sets. Chapter 3 presents the seismic and bathymetric data, and Chapter 4 presents the interpretation. Chapter 5 discusses the economic relevance of the thesis with emphasis on future work in converting the interpretation to depth. Chapter 6 summarises the conclusions of this study.

Two Appendices provide additional information related to this study. Appendix A describes the multibeam swath bathymetry survey. Appendix B describes the seismic survey and explains some of the physical aspects of reflection seismology.

CHAPTER 2 METHODOLOGY

2.1 Introduction

This thesis uses two geophysical data sets to define geological structure. Bathymetric data (multibeam swath bathymetry) show seafloor morphology, including bedrock structure where bedrock crops out. Reflection seismic data shows structure of bedrock below the seafloor. Seafloor morphology was considered during the interpretation of seismic data (single-channel marine reflection seismology). In addition, three boreholes constrain bedrock reflectors to corresponding depths below seafloor. Two of the three boreholes correlate bedrock reflectors with lithology.

2.2 Bedrock Structure Based on Seafloor Morphology

The bathymetric chart aids in the interpretation of the sub-surface, in much the same way that aerial photographs aid in the interpretation of geology on land. The interpretation of the seismic data considered local variations in topography; therefore, the bathymetric chart complements the interpretation otherwise based solely on seismic the seismic data.

Accuracy and resolution of bathymetric data are related to vessel positioning, depth of water, and the prediction of the path of the sonar ray. Vessel positioning is maintained in the long-term (vessel motion along track lines) by a differential geographic positioning system (DGPS), and in the short-term (changes in vessel orientation; heave, pitch, roll) by accelerometers and gyroscopes. The resulting horizontal accuracy is ±3 metres. Predicting the

path of the sonar ray is accomplished with velocity profiles of the water column, measured daily (Appendix A). The resulting bathymetric error is less than 1 % water depth, which corresponds to ±0.05 to ±0.60 metres in the study area.

A series of sub-parallel ridges crop out in areas of bedrock exposure. Ridges generally represent the intersection between bedding planes and the seafloor (ridge lines). The method of delineating fold axes on the seafloor uses all ridge lines of length greater than about 250 metres; no preference is given based on height of ridge or any other parameter that could describe ridges or ridge lines. The distribution of ridge lines on the seafloor generally shows structure based on visual association.

2.3 Defining Structure Below the Seafloor

2.3.1 Bedrock Reflectors

Single-channel marine seismics help to define the structure below the seafloor. Bedrock reflectors (horizons A, B, and C) were traced across a series of adjacent track lines. Two tie lines constrain the interpretation across adjacent track lines. Of the three horizons interpreted, horizons A and B are individual reflectors. Horizon C delineates a *succession* of reflectors defined by a pattern of reflectivity. For horizon C, the pattern may change across the entire survey area, but the pattern may not change noticeably between adjacent track lines.

2.3.2 Processing Technique

The processing technique included a band-pass frequency filter. The frequency filter passed energy between 100 to 800 Hz and rejected energy outside that range. The band-pass

process removed much of the low frequency noise that obscured bedrock reflectors; however, this process also removed much of the signature of unconsolidated sediments, making the interpretation of the sediment/bedrock interface more difficult.

The GSC made many attempts to deconvolve the data to suppress multiples. Yilmaz (1987) explained various deconvolution techniques. Suppression of multiples relies on predicting the multiple trace, based on the nature of the trace above the multiple (predictive deconvolution). Because of the shallow water in the survey area (20 to 60 metres), and the relatively small offset (distance from sound source to receiver of 52 metres; Appendix B), the shape of the multiple trace differs from the shape of the trace above the multiple (B. Nicols, pers. comm. 1995). As a result, multiples, particularly the first water-bottom multiple (FWBM; i.e., reflection from the seafloor upwards, from the water/air interface downwards, and from seafloor upwards again) could not be removed satisfactorily (Fig. 2.1).

2.3.3 Accuracy and Resolution

Accuracy of the seismic records is related to vessel and streamer positioning. Resolution of the seismic records is related to distance between shots (horizontal resolution) and frequency of the sound source (vertical resolution). Differential GPS provided horizontal positioning accuracy of the vessel to ±3 metres. However, streamer positioning is difficult to quantify because the streamer is towed by the vessel. As a result, positioning accuracy is likely ±10 metres. Horizontal resolution is controlled by spacing between lines (40 metres), and distance between successive shots (8 metres). However, horizontal resolution is compromised where track lines are absent, where distance between adjacent track lines is as large as 200 metres.

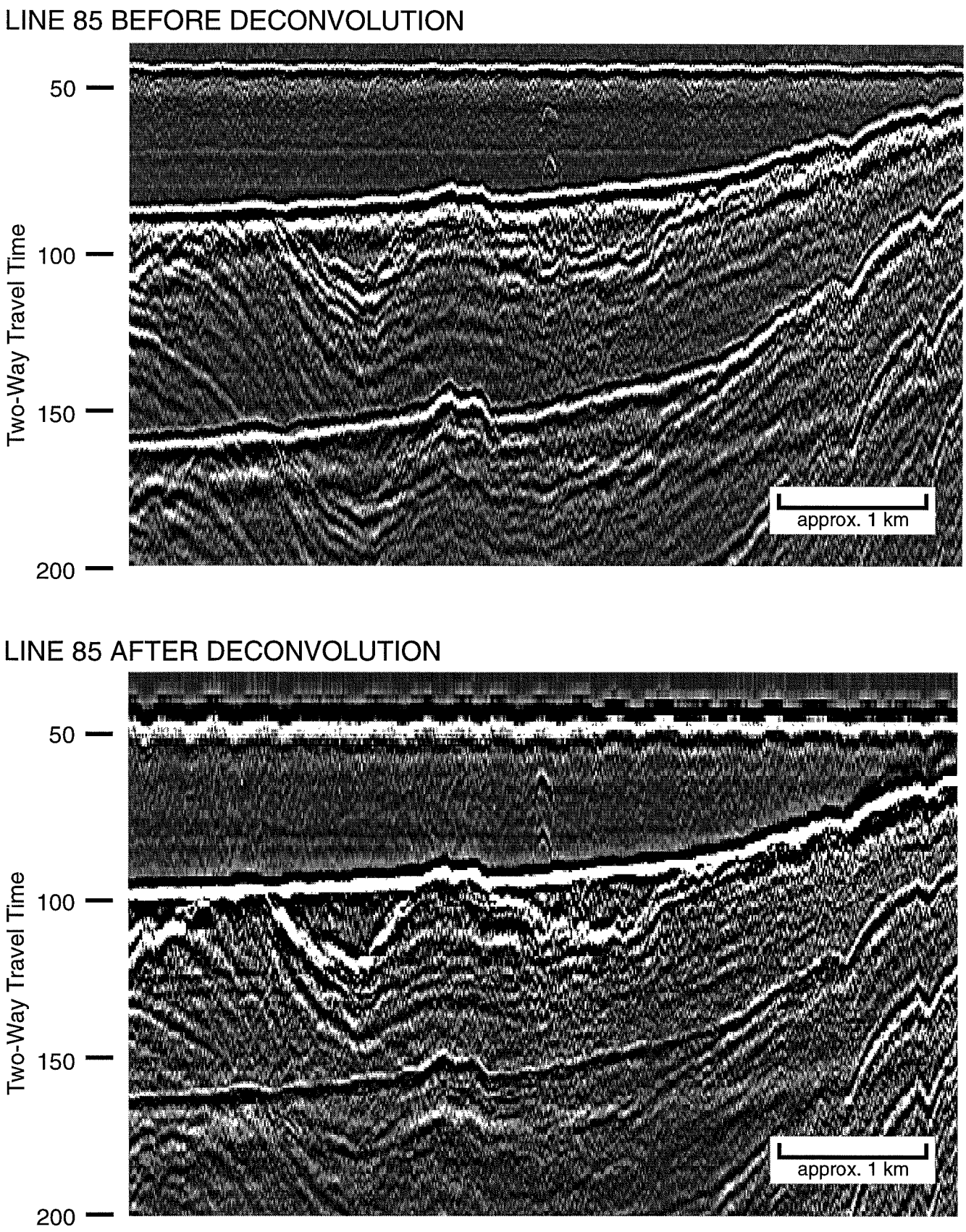

Figure 2.1 Example of attempt at deconvolving line 85. The FWBM is suppressed by approximately 70%. Two-way a travel time in milliseconds. Horizontal scale is shown in the insets.

2.3.4 Interpretation Software

SeisWorks 2D™ software (version 2.3) was used to interpret the seismic data. The software provides three different types of multi-tasking windows and includes:

1) the *seismic data window*, which shows the seismic data and the interpretation of the seismic data;

2) the *map view window*, which shows the progress of interpretation on a representation of the survey chart; and

3) the *perspective view window*, which shows a 3-dimensional representation of the interpretation.

The user changes the colour palette to emphasise features on the seismic record. Also, the user defines the window content so that parts of the interpretation temporarily disappear from view. Seismic windows show the intersections between lines as the interpretation progresses and intersections aid the interpreter in correlating bedrock reflectors across adjacent seismic lines.

2.4 Integrating Offshore Boreholes

Three offshore boreholes (boreholes H12, H12A, and P5) provide the sonic and lithological data used in this thesis. Synthetic seismograms correlate lithology (i.e., coal seams) with bedrock reflectors. Synthetic seismograms are produced from convolving seismic pulse with acoustic profiles H12 (to the level of the Point Aconi coal seam) and P5 (to the level of the Hub coal seam).

CHAPTER 3 DATA

3.1 Introduction

This chapter presents two geophysical data sets (the results of the multibeam bathymetric and high-resolution seismic surveys), two well history logs (boreholes H12 and H12A; well history logs describe lithology) and three borehole acoustic logs (boreholes H12, H12A, and P5). The GSC collected the two geophysical data sets in 1994 (Appendices A and B summarise the bathymetric and seismic surveys, respectively), and the Nova Scotia Department of Mines collected the borehole logs in 1978. In addition, this chapter summarizes all velocity data relevant to this thesis.

3.2 Multibeam Swath Bathymetry

The bathymetric survey covers approximately 45 km^2. Figure 3.1 is the resulting bathymetric chart, with bathymetry coloured at five metre intervals. Seafloor morphology is exaggerated by a false-shadowing technique (vertical exaggeration of 10) that shows contrast in brightness with topographic variations (Shaw et al., 1994). Courtney (in prep.) gives instructions for viewing small-scale detail on the bathymetric chart.

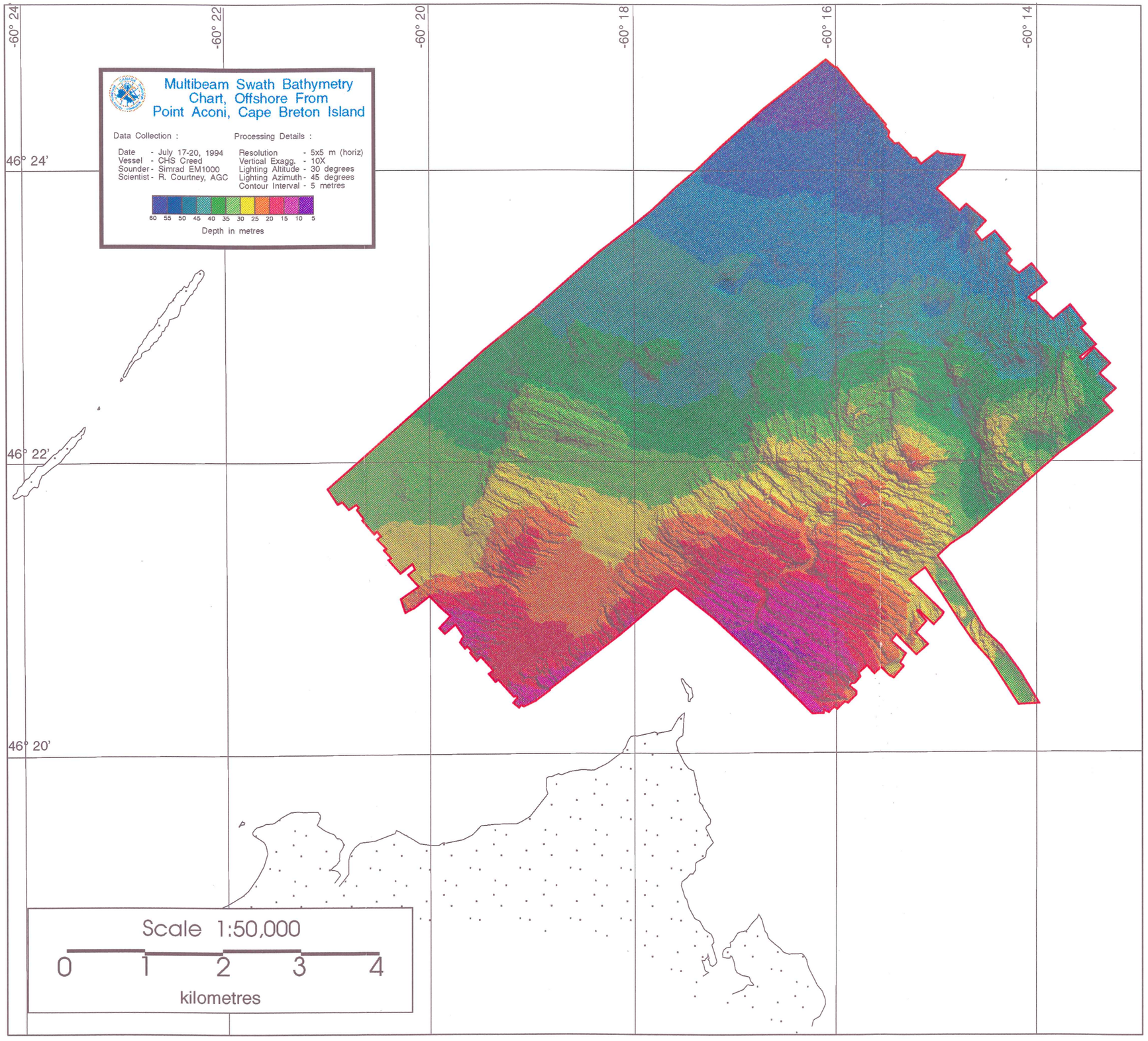

Figure 3.1 Multibeam swath bathymetry chart. Bathymetry is coloured at five metre intervals. False-shadows (i.e., variations in colour intensity) enhance seafloor morphology (approximate vertical exaggeration is 10X). Refer to Courtney (in prep.) for viewing small-scale detail.

3.3 Reflection Seismic Data

3.3.1 Survey Coverage

The seismic survey offshore from Point Aconi covers approximately 20 km^2 and consists of a series of parallel, closely-spaced track lines, running southeast. Spacing between track lines averages 40 metres (Appendix B), and the distance between successive shots along track lines is approximately 8 metres. Of one hundred lines in the main survey area, twelve are missing as a result of equipment failure and limitations in time (lines 6, 7, 8, 14, 24, 34, 35, 36, 46, 47, 48, and 52). Two addition lines intersect the main survey lines and run northeast (lines t1 and t2).

3.3.2 Representative Lines

Figure 3.2 shows the bathymetric chart with an overlay of fourteen representative seismic track lines and an overlay of mine workings. Twelve of the representative lines are at 225 to 500 metre spacing in the main survey area and run southeast (lines 1, 9, 16, 23, 42, 53, 64a, 75, 88, 94, and 100; Figs. 3.3 to 3.14). Two more representative lines run northeast and approximately perpendicular to all other lines (lines t1 and t2; Figs. 3.15 and 3.16). In addition, Figures 3.15 and 3.16 show tie-lines t1 and t2.

3.4 Velocity Data

3.4.1 Offshore Boreholes

Three borehole acoustic logs (boreholes H12, H12A, and P5) provide continuous velocity data with depth. Figures 3.17 and 3.18 show acoustic velocity profiles and corresponding lithology for boreholes H12 and H12A, respectively, to the depth of the Point Aconi coal seam.

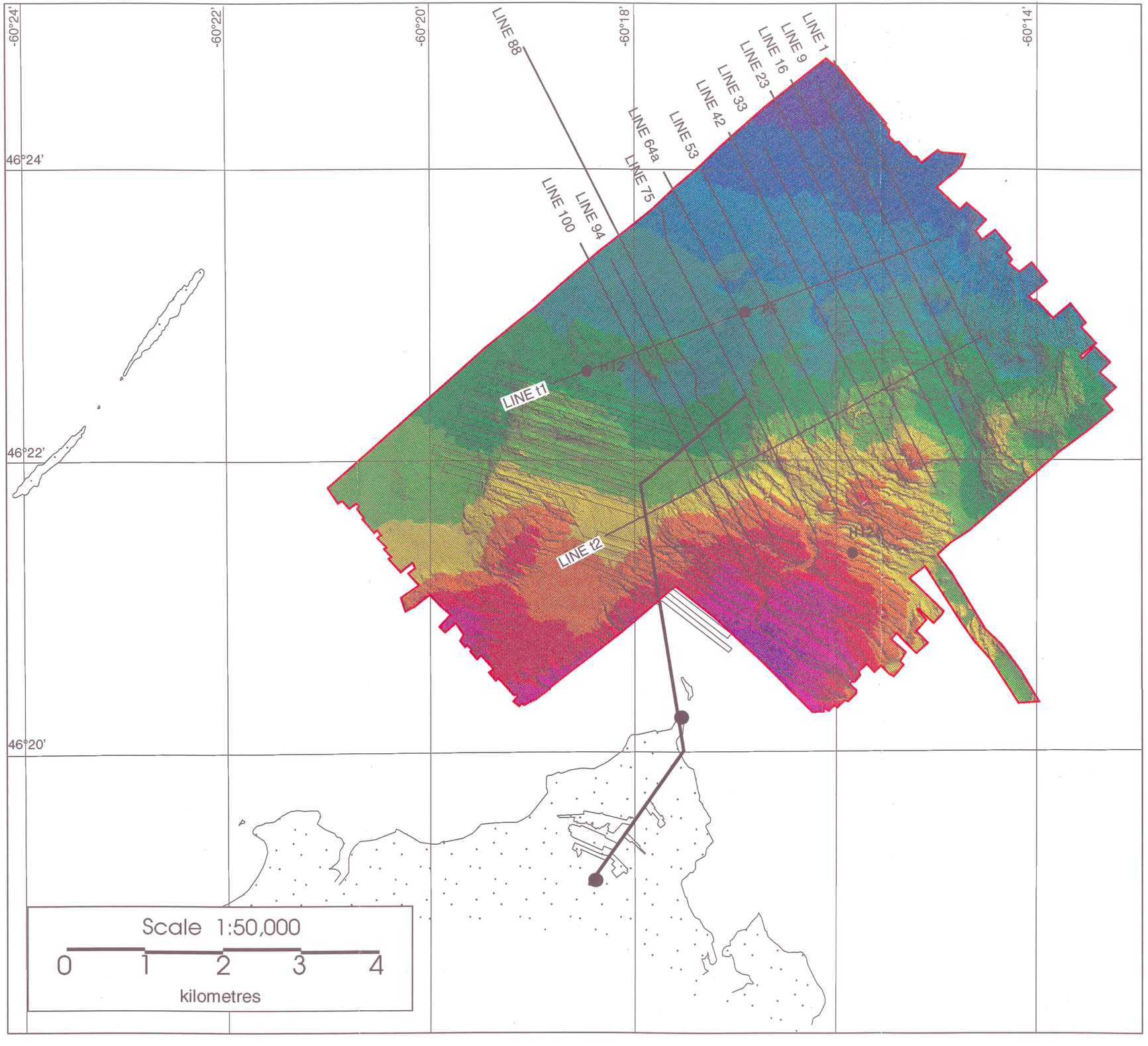

Figure 3.2 Multibeam swath bathymetry chart with overlay of mine working, representative seismic track lines, and boreholes H12, H12A, and P5.

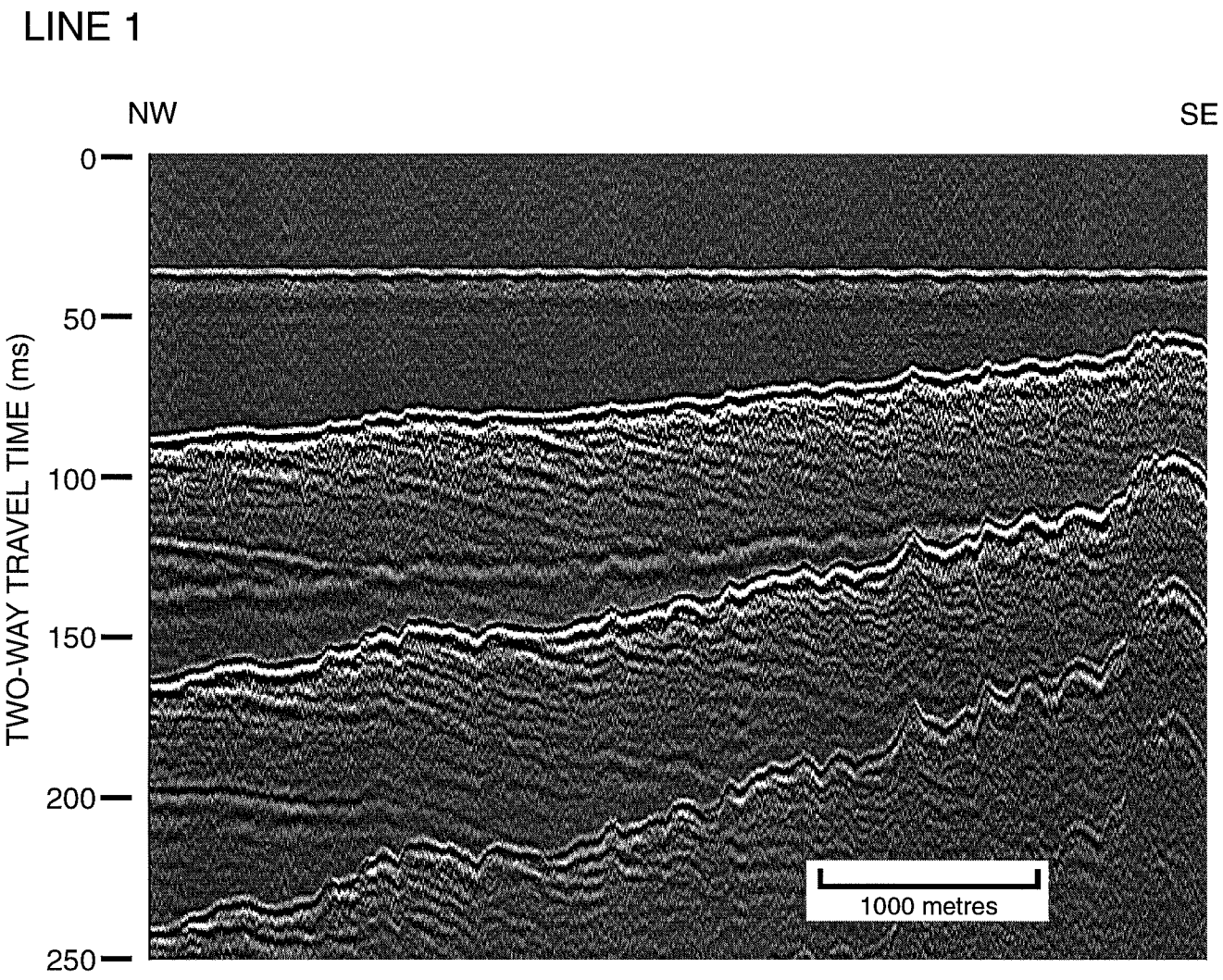

Figure 3.3 Seismic line 1 offshore from Point Aconi in two-way travel time. Two-way travel time is in milliseconds. Horizontal scale is shown in the inset.

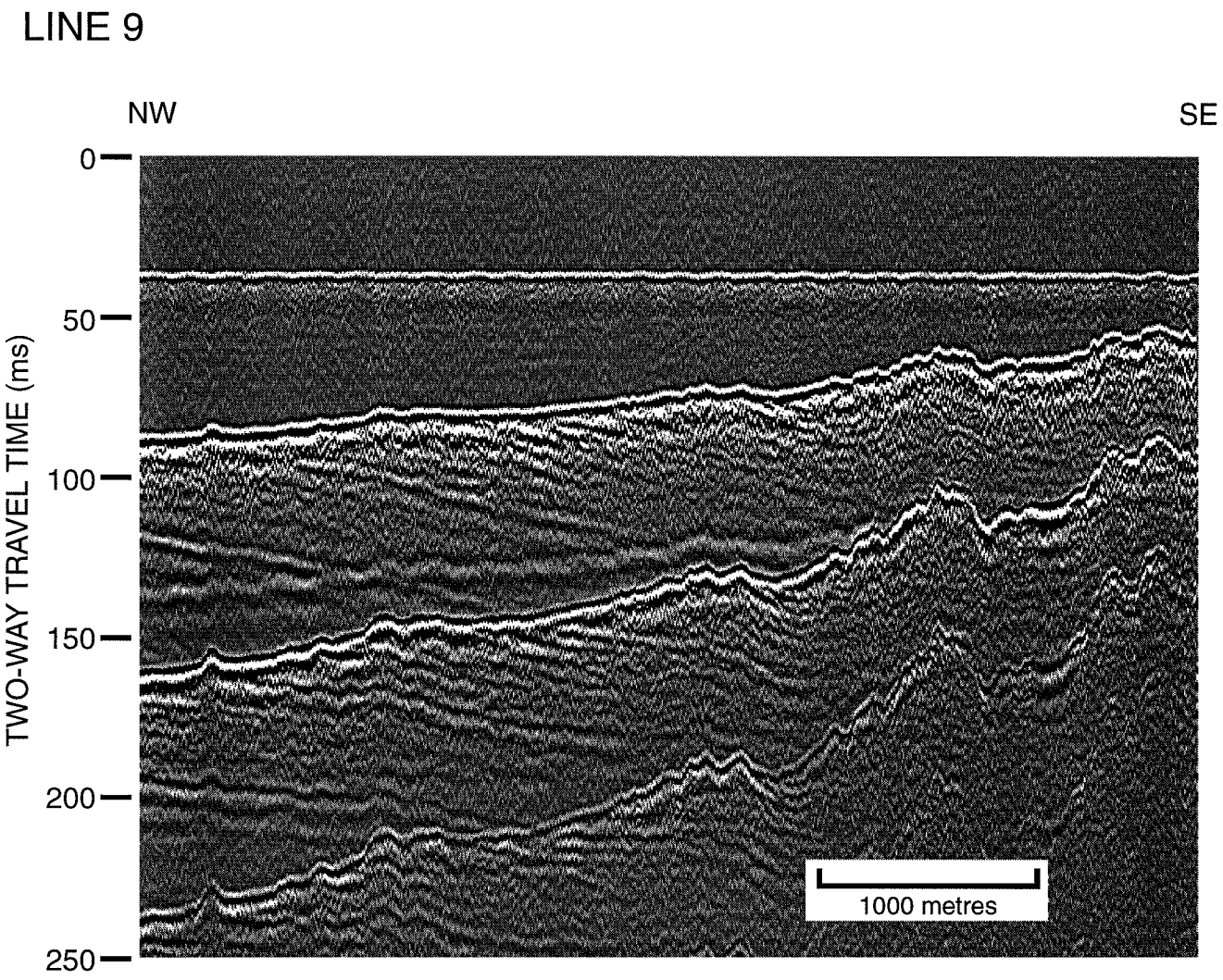

Figure 3.4 Seismic line 9 offshore from Point Aconi in two-way travel time. Two-way travel time is in milliseconds. Horizontal scale is shown in the inset.

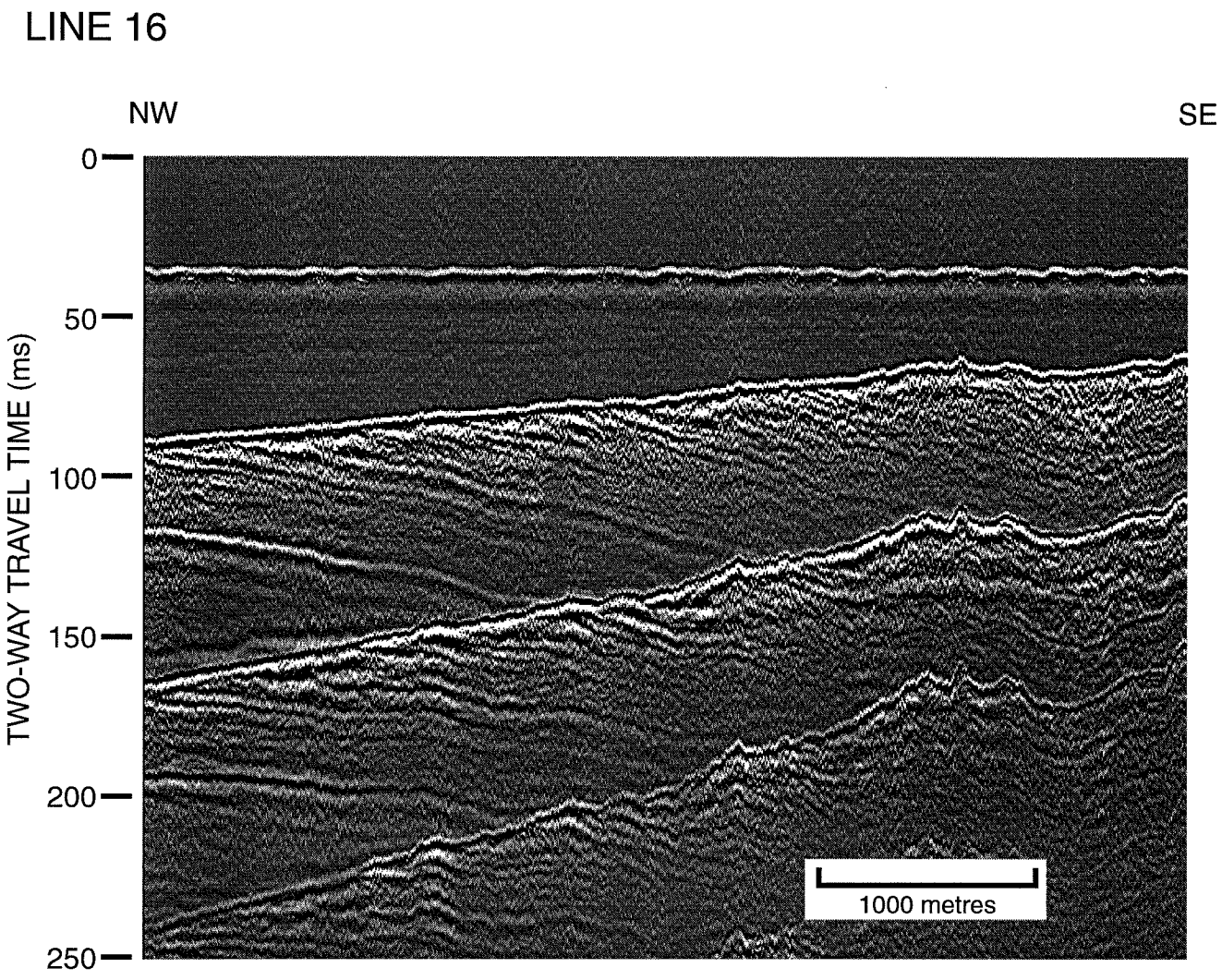

Figure 3.5 Seismic line 16 offshore from Point Aconi in two-way travel time. Two-way travel time is in milliseconds. Horizontal scale is shown in the inset.

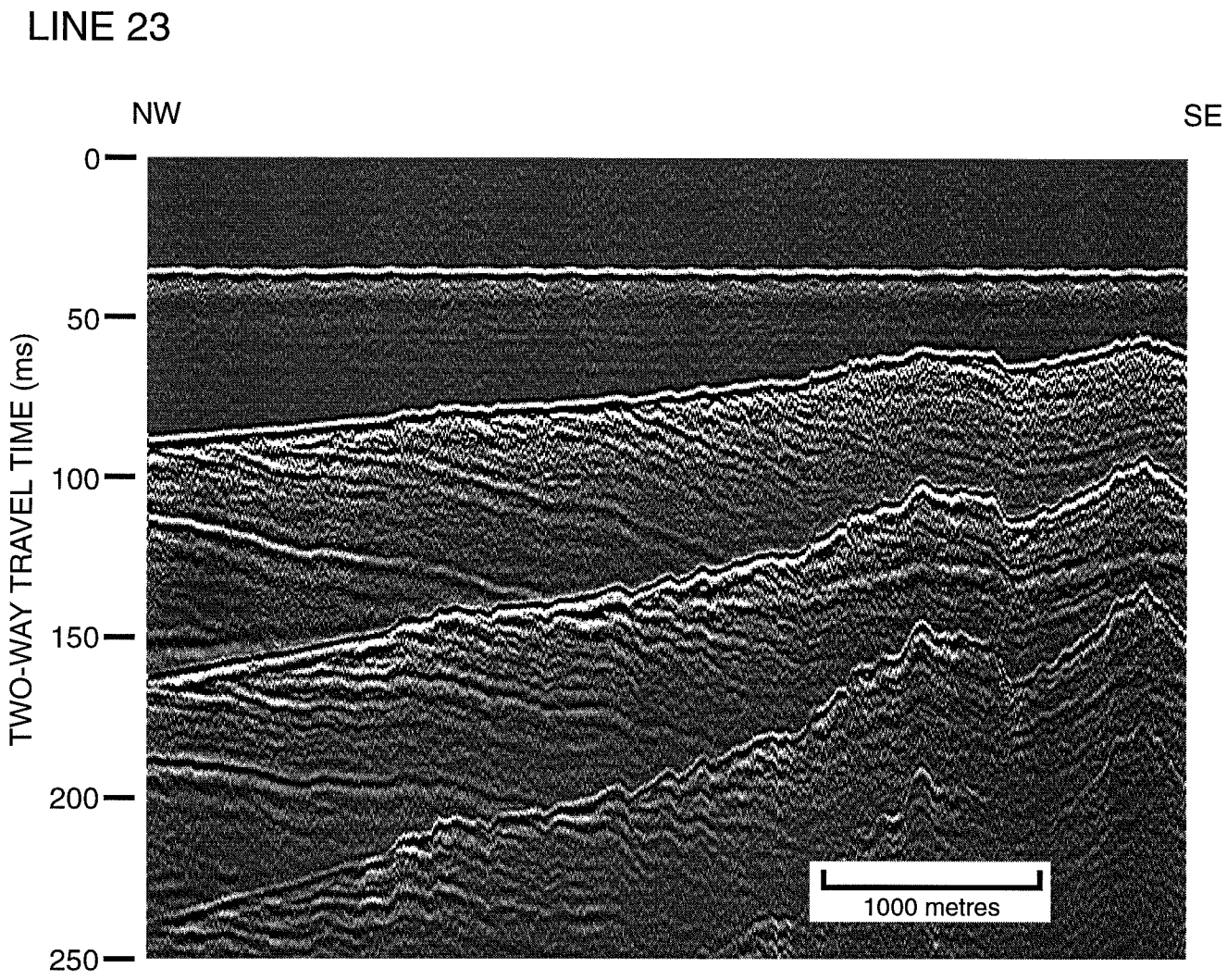

Figure 3.6 Seismic line 23 offshore from Point Aconi in two-way travel time. Two-way travel time is in milliseconds. Horizontal scale is shown in the inset.

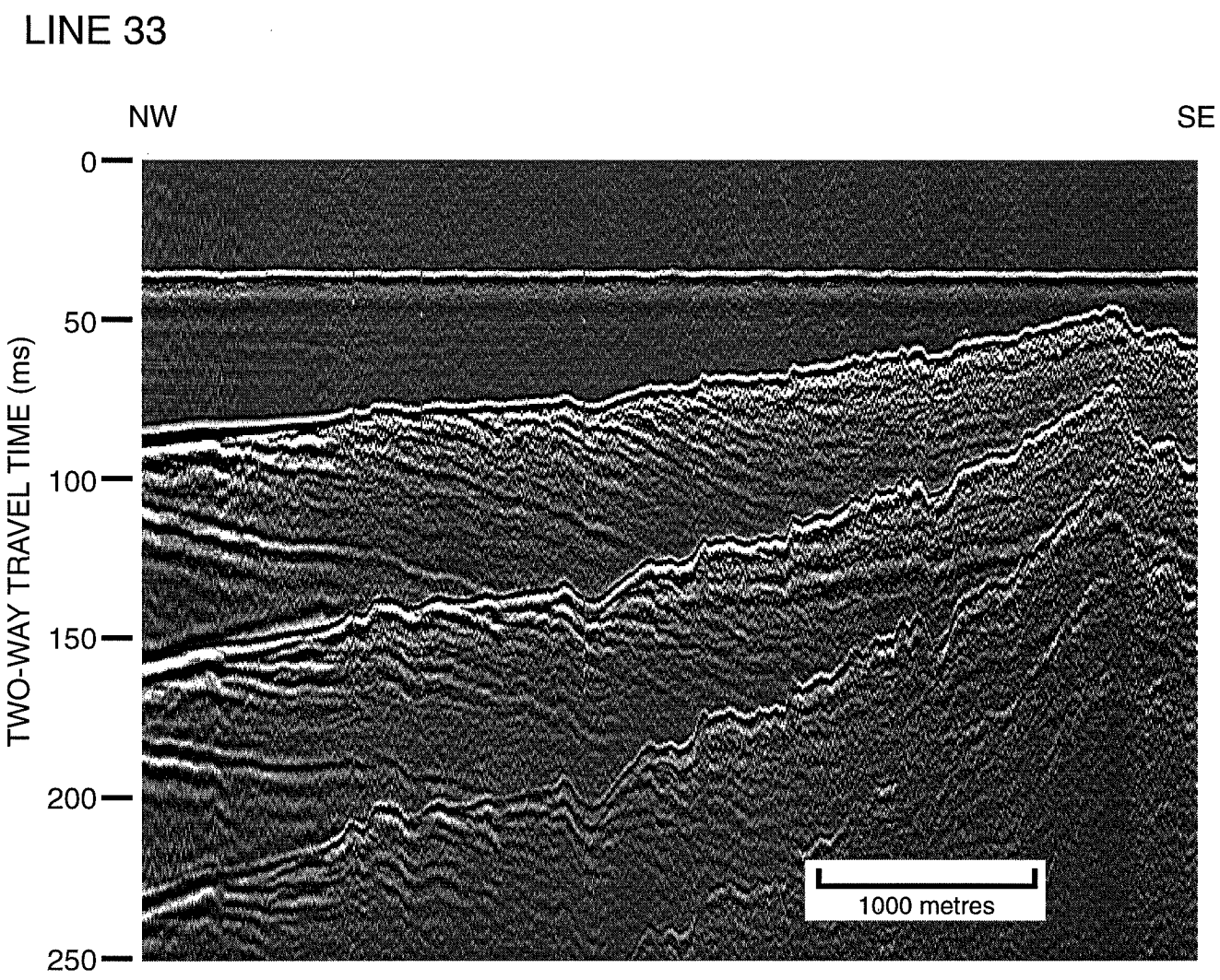

Figure 3.7 Seismic line 33 offshore from Point Aconi in two-way travel time. Two-way travel time is in milliseconds. Horizontal scale is shown in the inset.

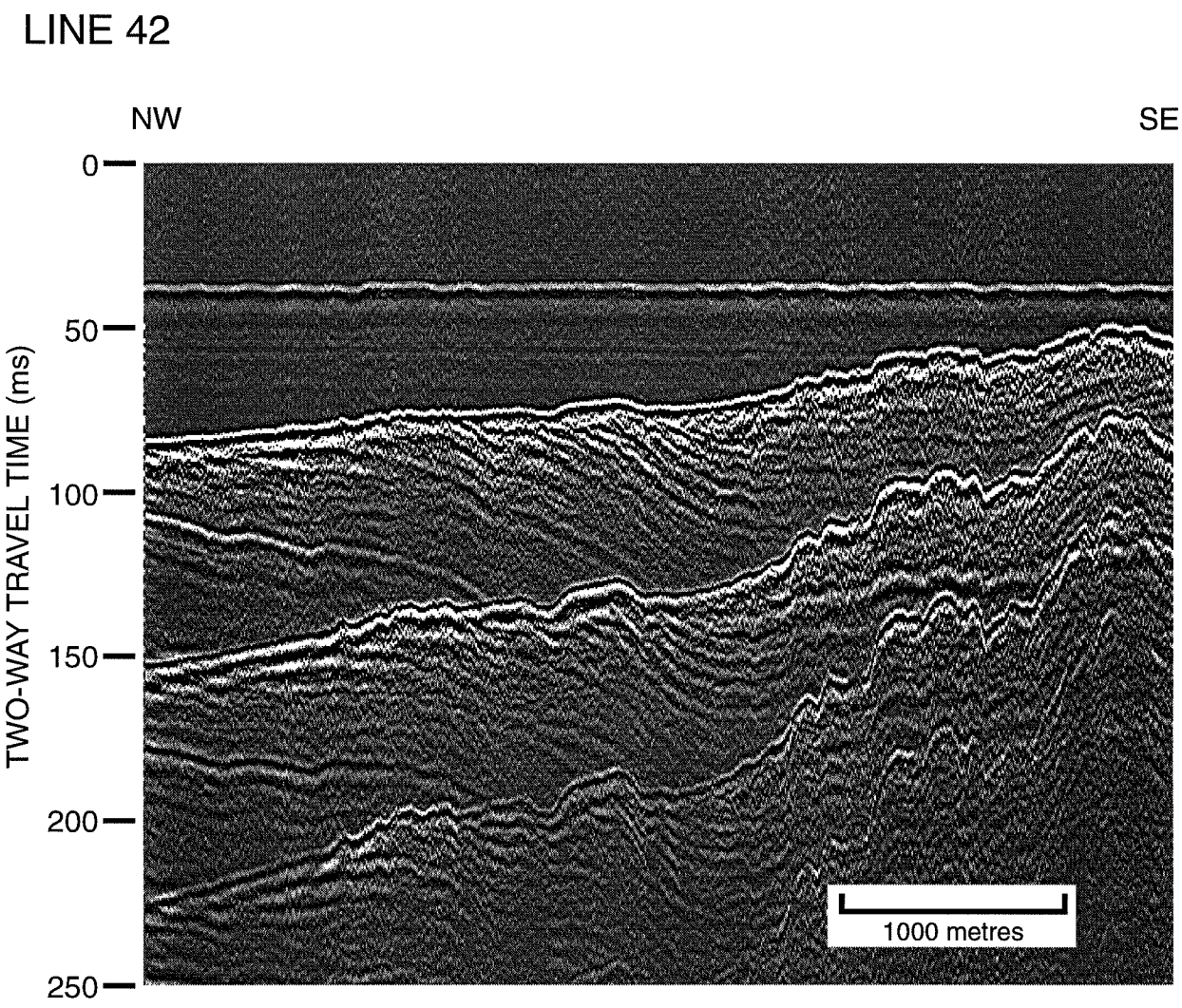

Figure 3.8 Seismic line 42 offshore from Point Aconi in two-way travel time. Two-way travel time is in milliseconds. Horizontal scale is shown in the inset.

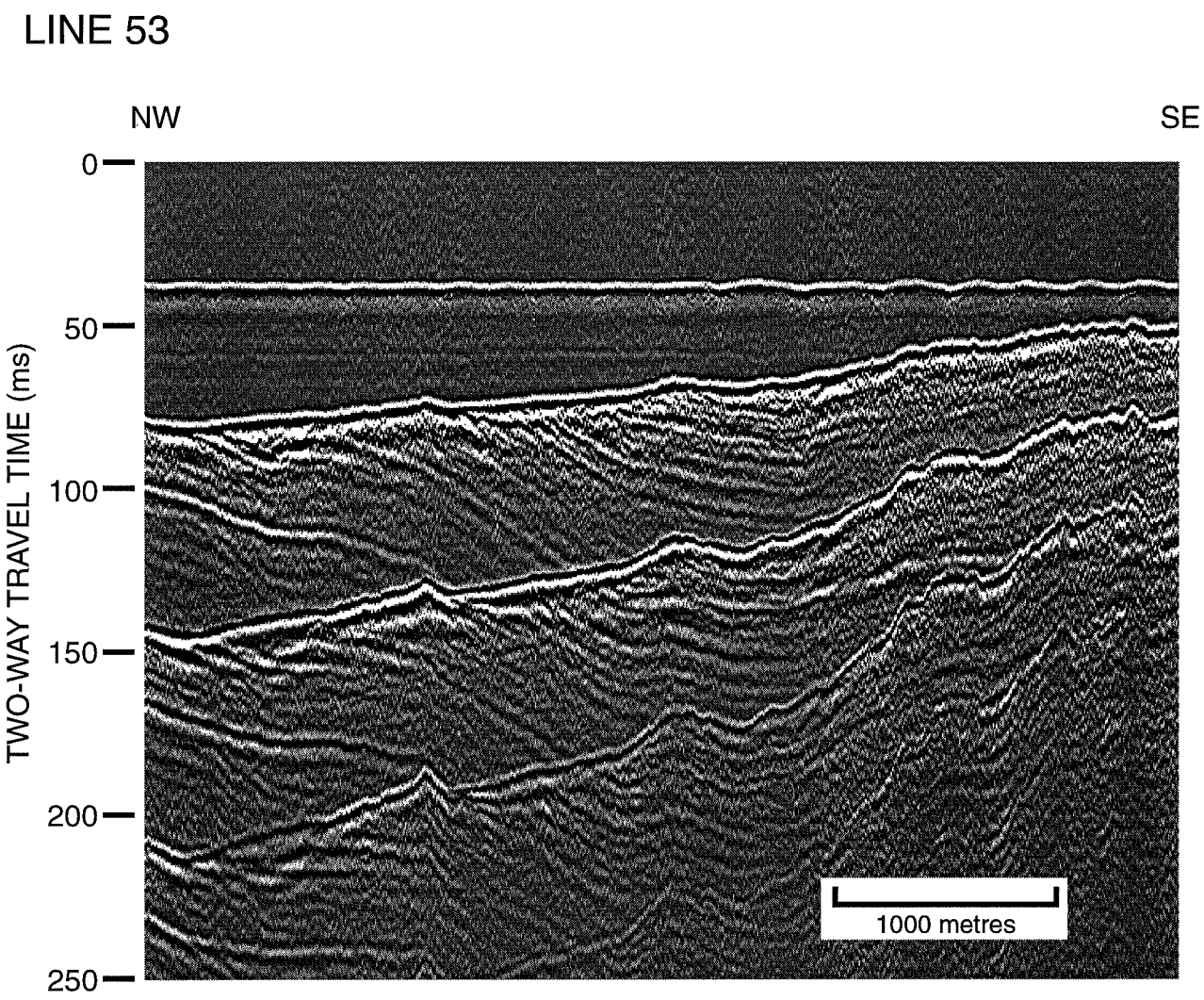

Figure 3.9 Seismic line 53 offshore from Point Aconi in two-way travel time. Two-way travel time is in milliseconds. Horizontal scale is shown in the inset.

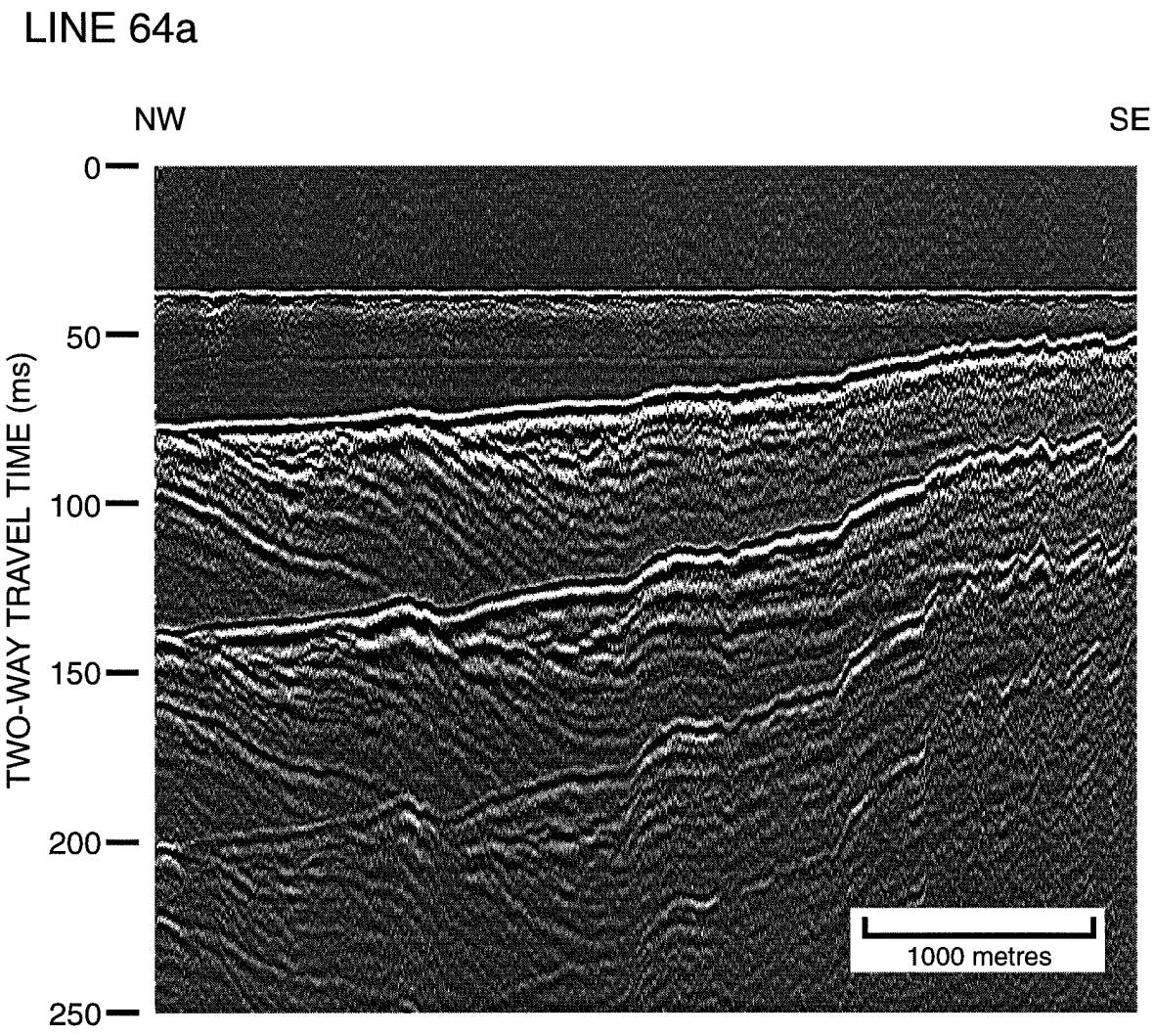

Figure 3.10 Seismic line 64a offshore from Point Aconi in two-way travel time. Two-way travel time is in milliseconds. Horizontal scale is shown in the inset.

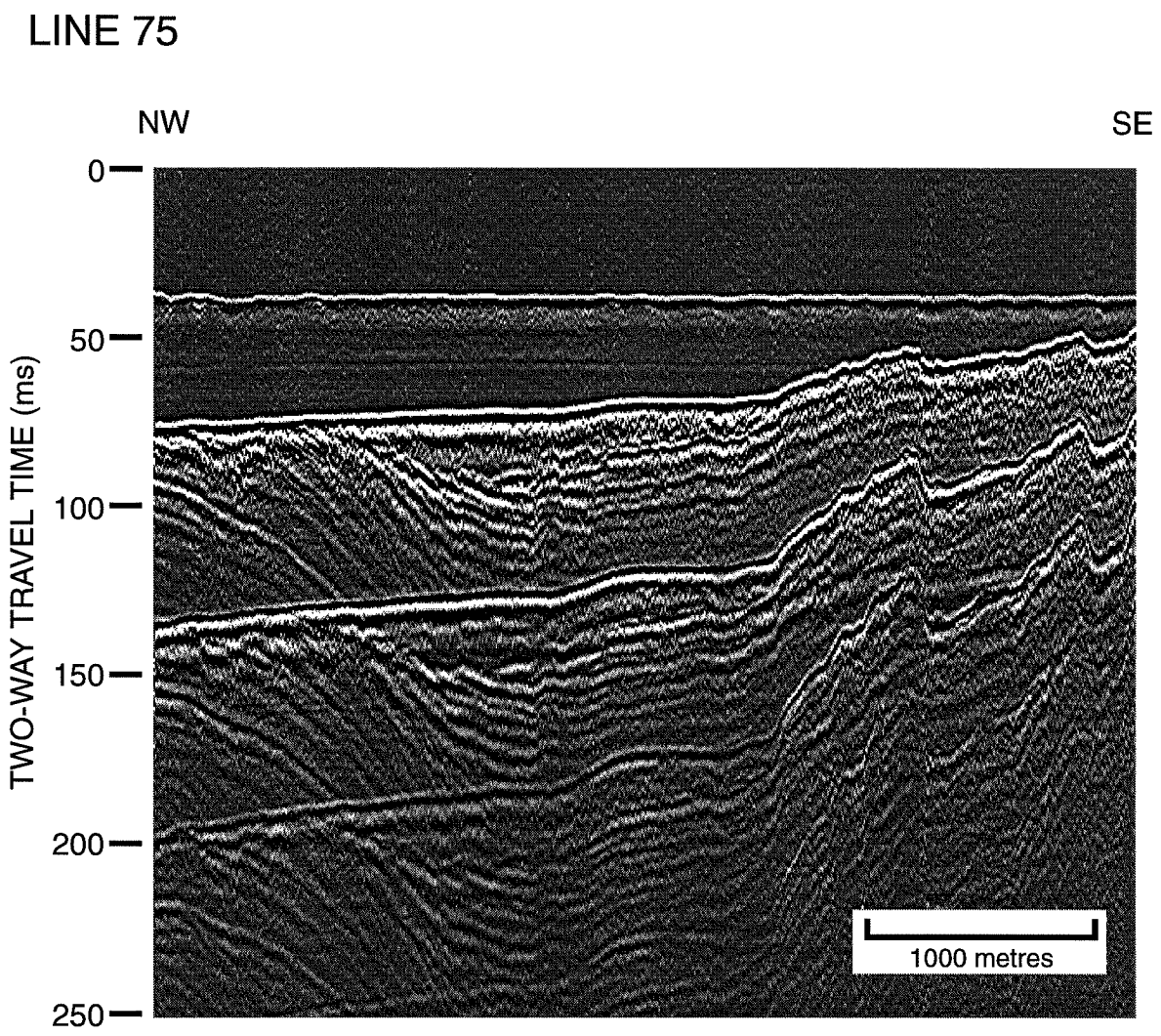

Figure 3.11 Seismic line 75 offshore from Point Aconi in two-way travel time. Two-way travel time is in milliseconds. Horizontal scale is shown in the inset.

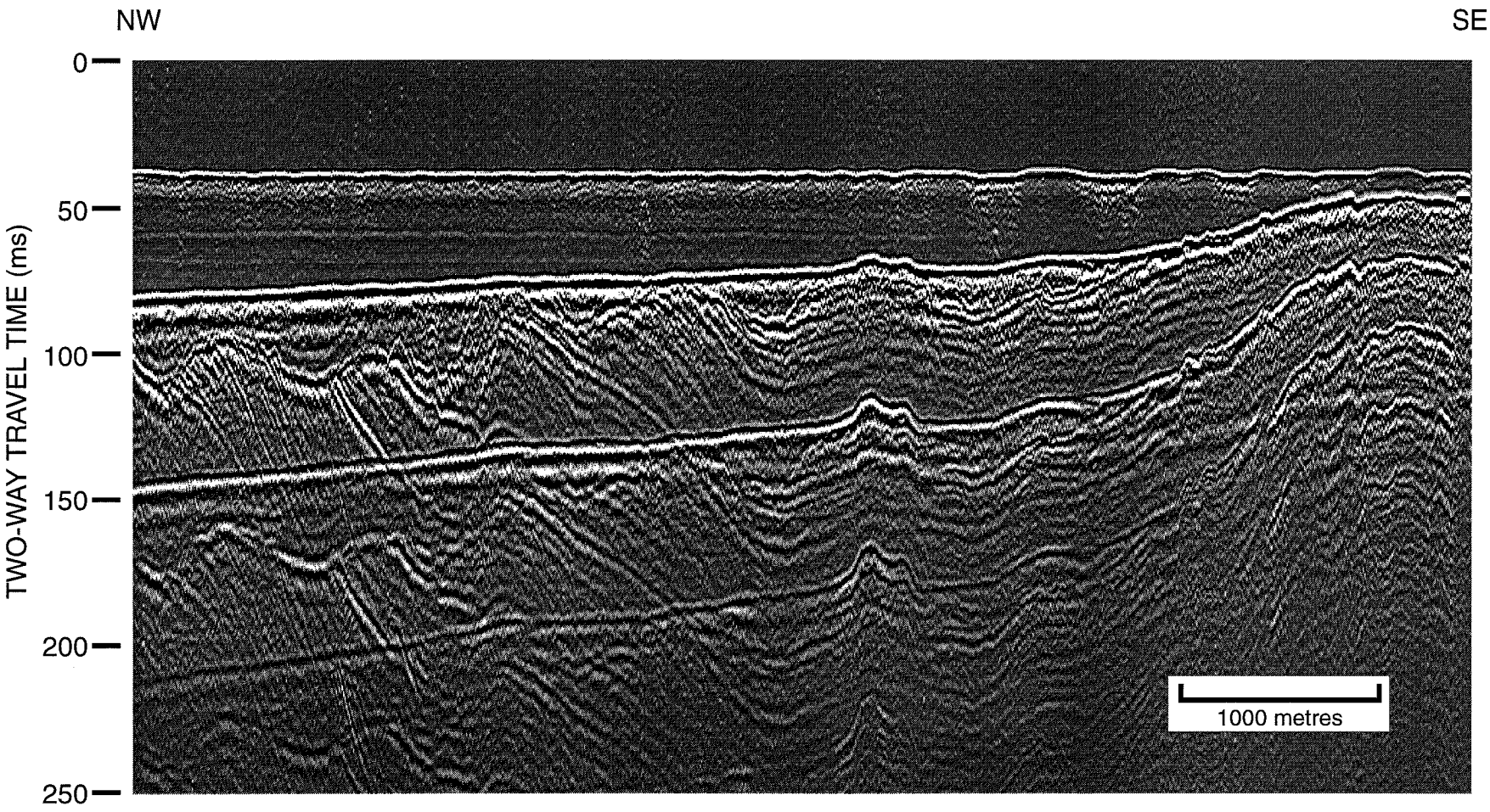

Figure 3.12 Seismic line 88 offshore from Point Aconi in two-way travel time. Two-way travel time is in milliseconds. Horizontal scale is shown in the inset.

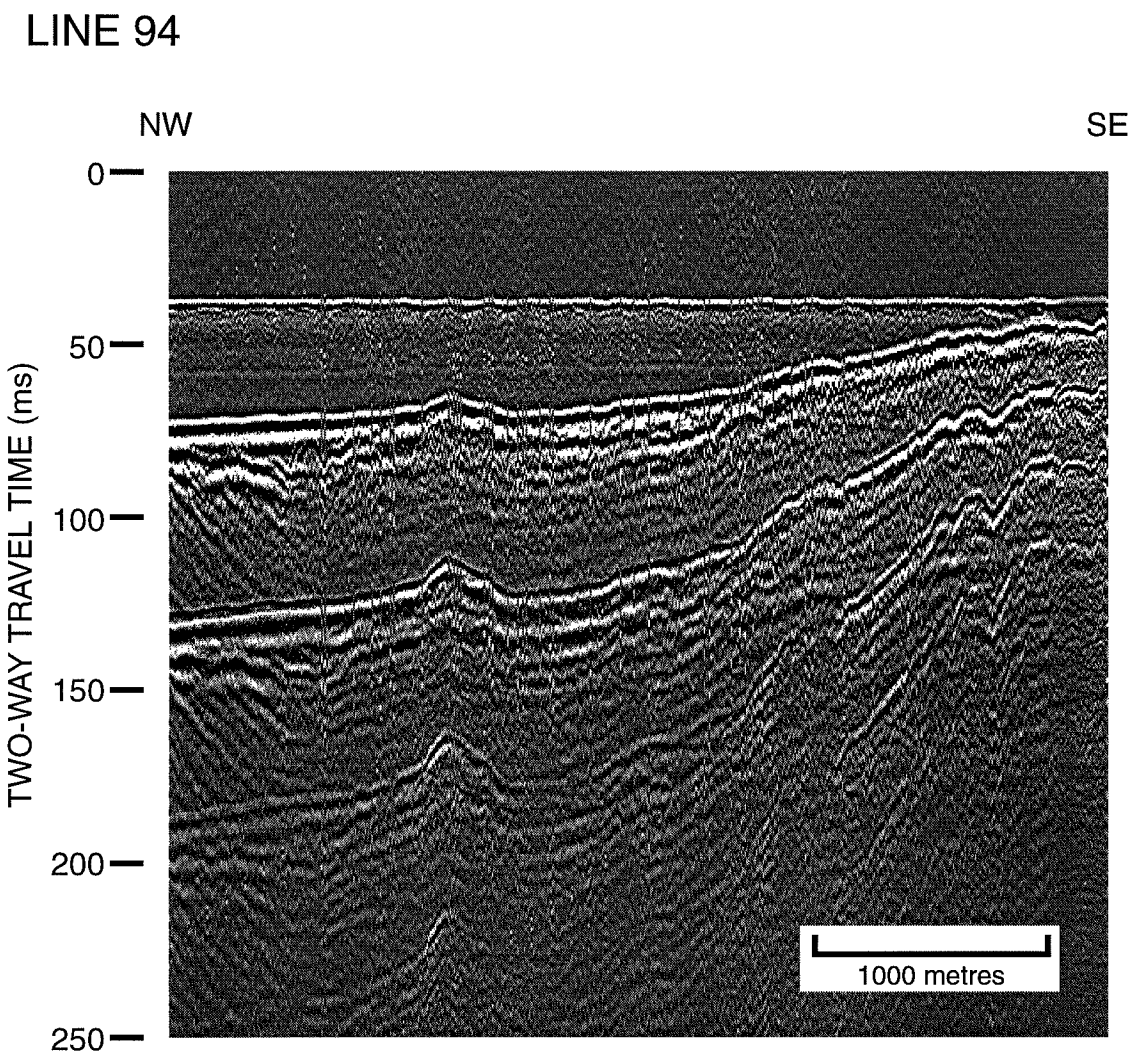

Figure 3.13 Seismic line 94 offshore from Point Aconi in two-way travel time. Two-way travel time is in milliseconds. Horizontal scale is shown in the inset.

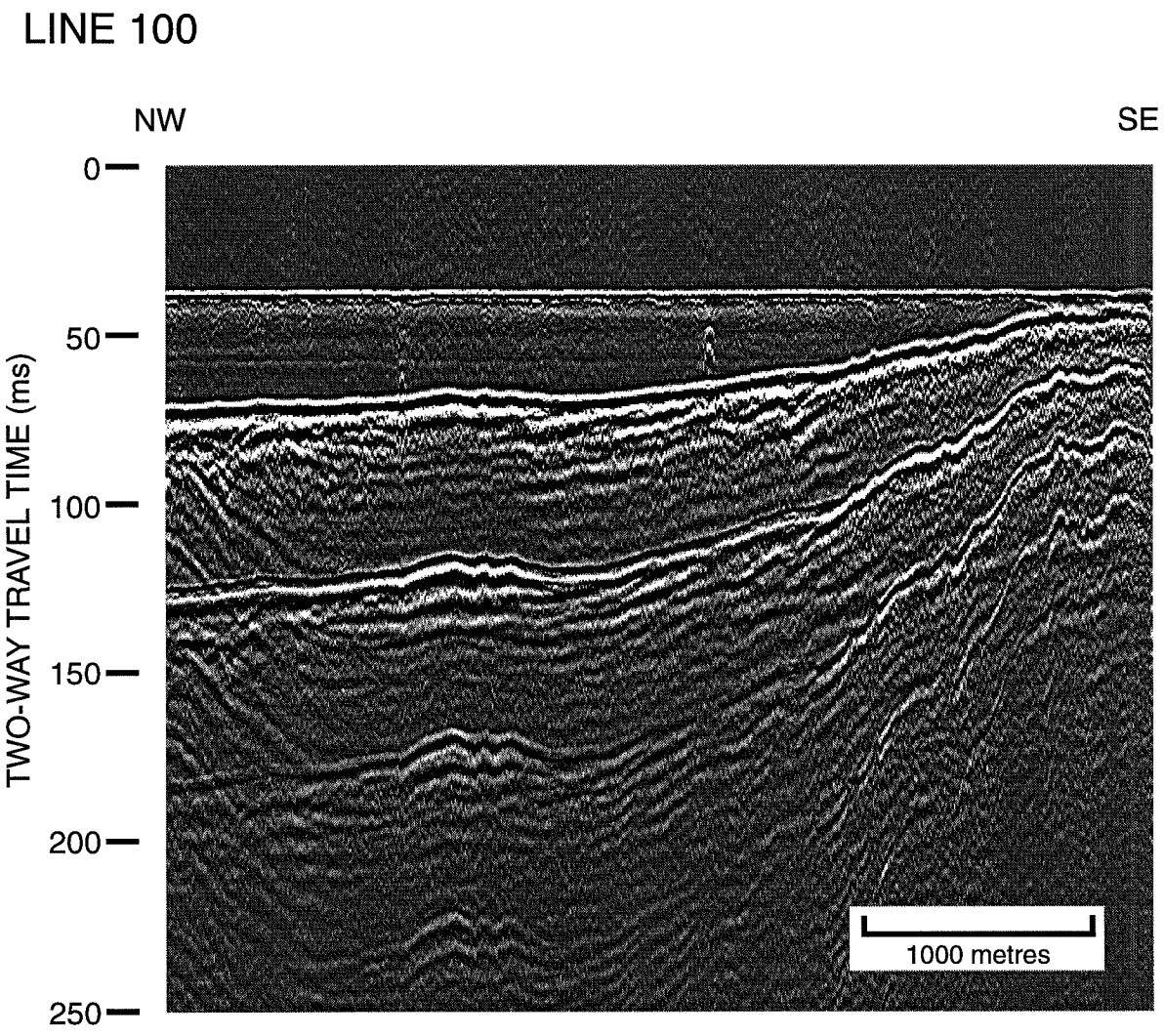

Figure 3.14 Seismic line 100 offshore from Point Aconi in two-way travel time. Two-way travel time is in milliseconds. Horizontal scale is shown in the inset.

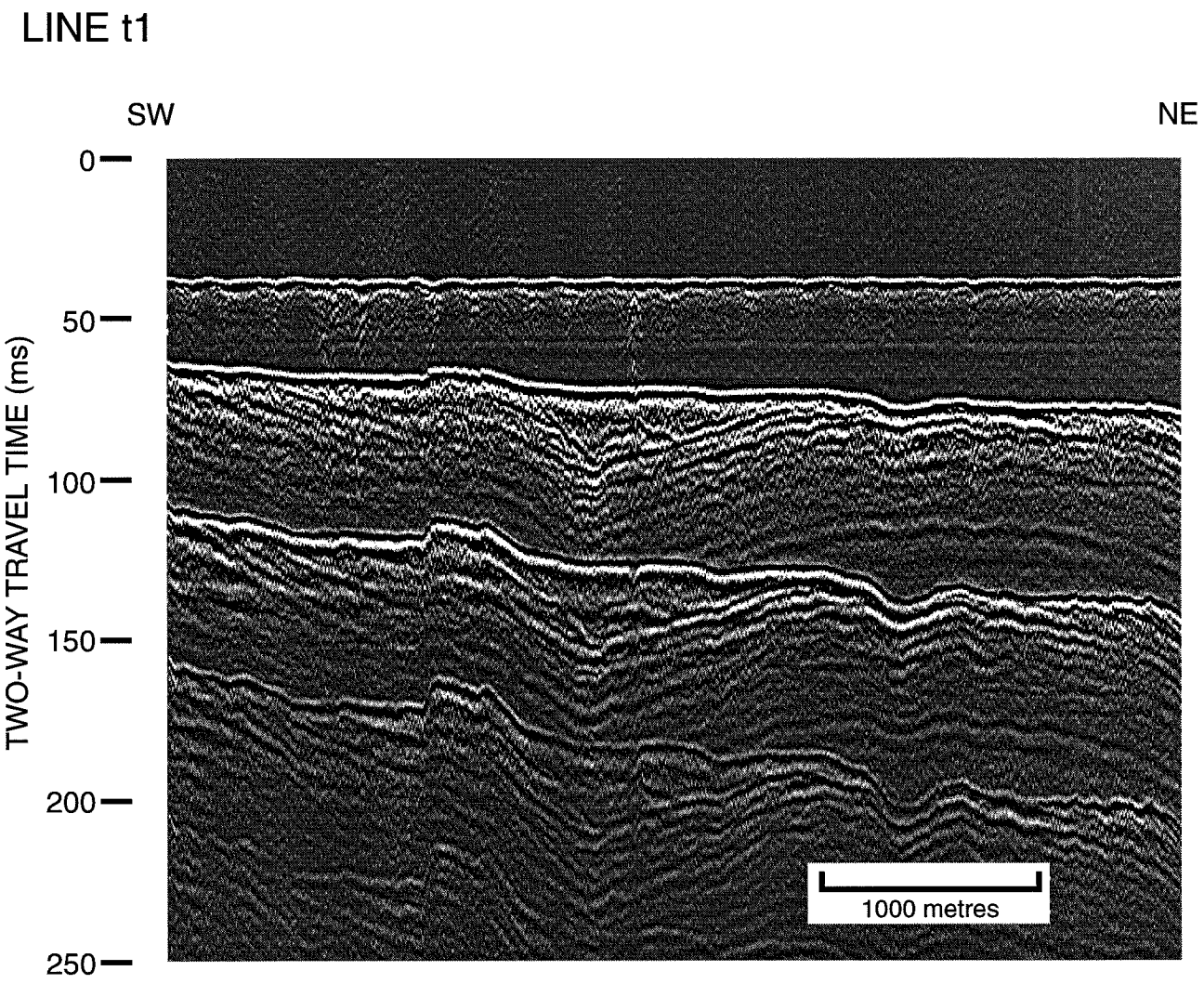

Figure 3.15 Seismic line t1 offshore from Point Aconi in two-way travel time. Two-way travel time is in milliseconds. Horizontal scale is shown in the inset.

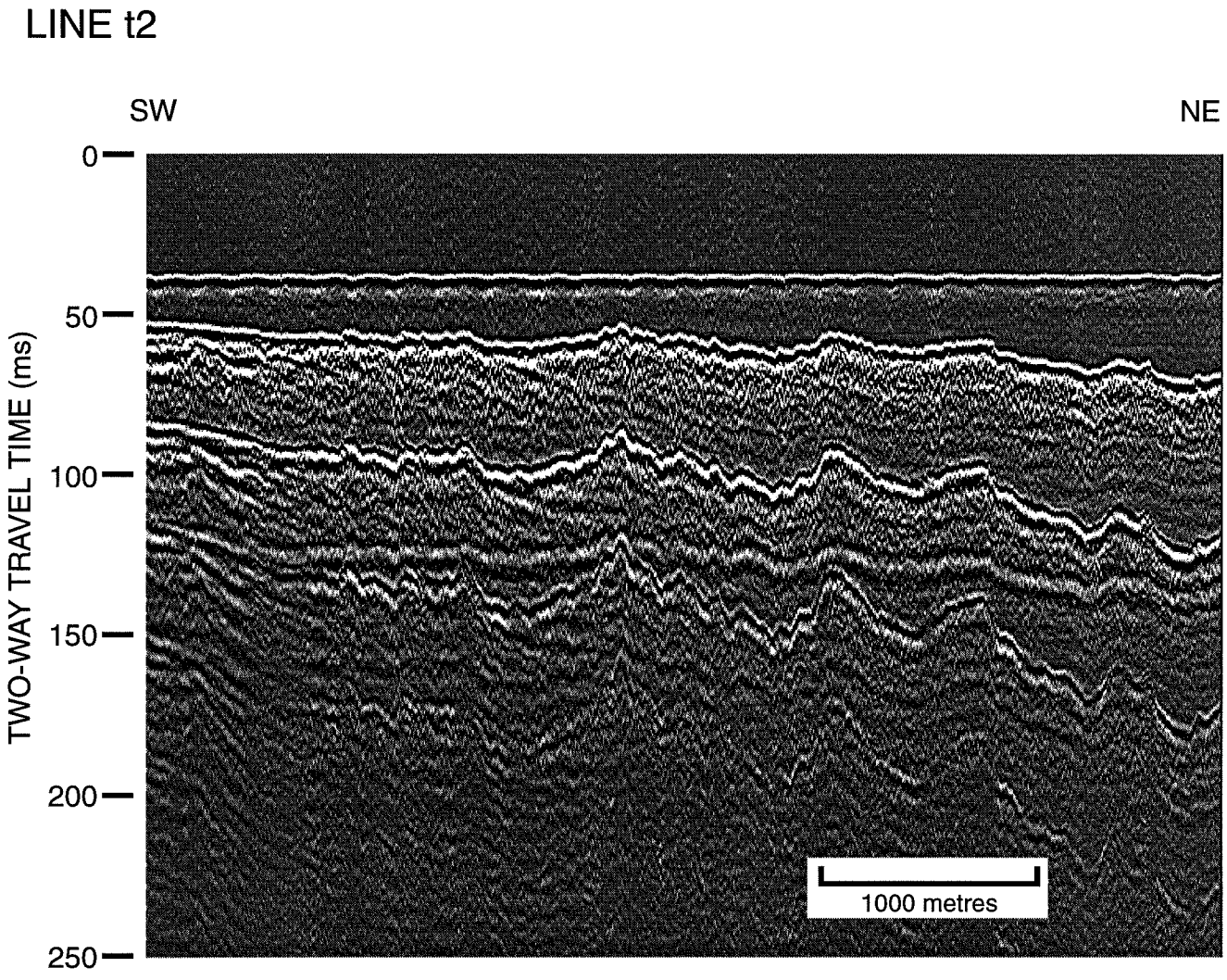

Figure 3.16 Seismic line t2 offshore from Point Aconi in two-way travel time. Two-way travel time is in milliseconds. Horizontal scale is shown in the inset.

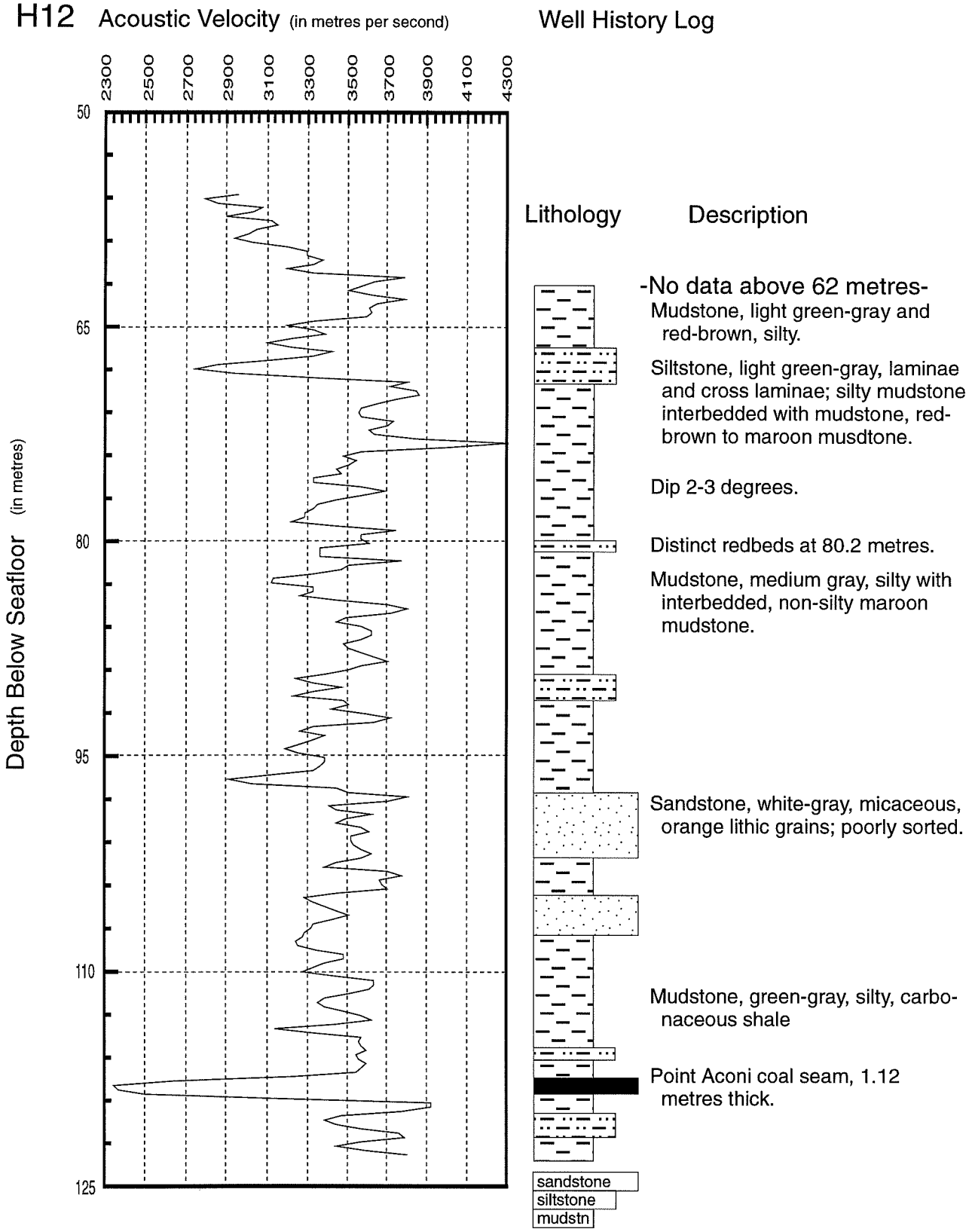

Figure 3.17 Acoustic velocity profile and corresponding well history log for offshore borehole H12. Depth is in metres below seafloor. No acoustical data exist for the 0-55 metre interval, and no lithological data exist for the 0-62 metre interval (data from Nova Scotia Department of Mines 1978 offshore borehole program).

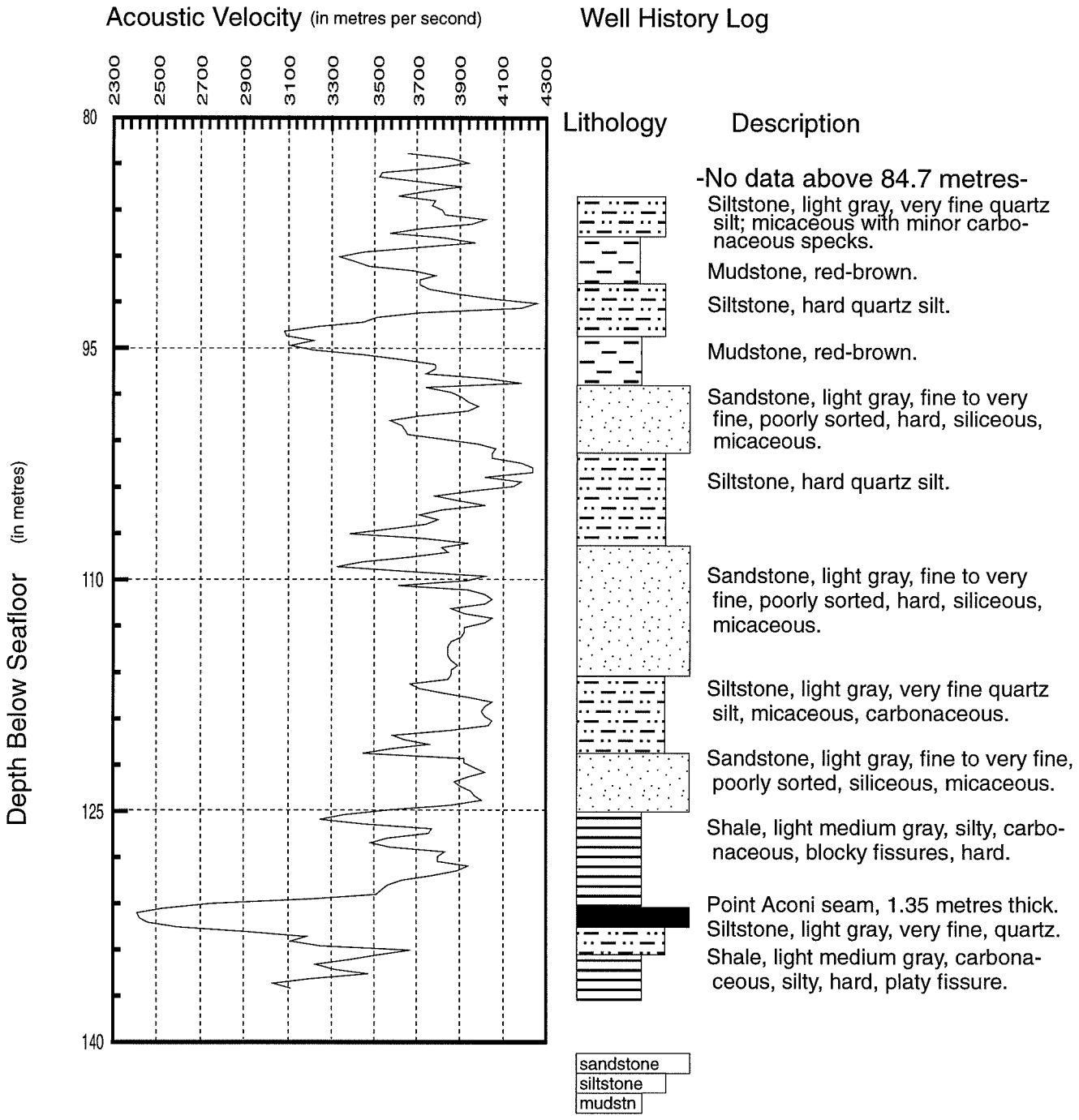

Figure 3.18 Acoustic velocity profile and corresponding well history log for offshore borehole H12A. Depth is in metres below seafloor. No acoustic data exist for the 0-82 metre interval, and no lithological data exist for the 0-84.7 metre interval (data from Nova Scotia Department of Mines 1978 offshore borehole program).

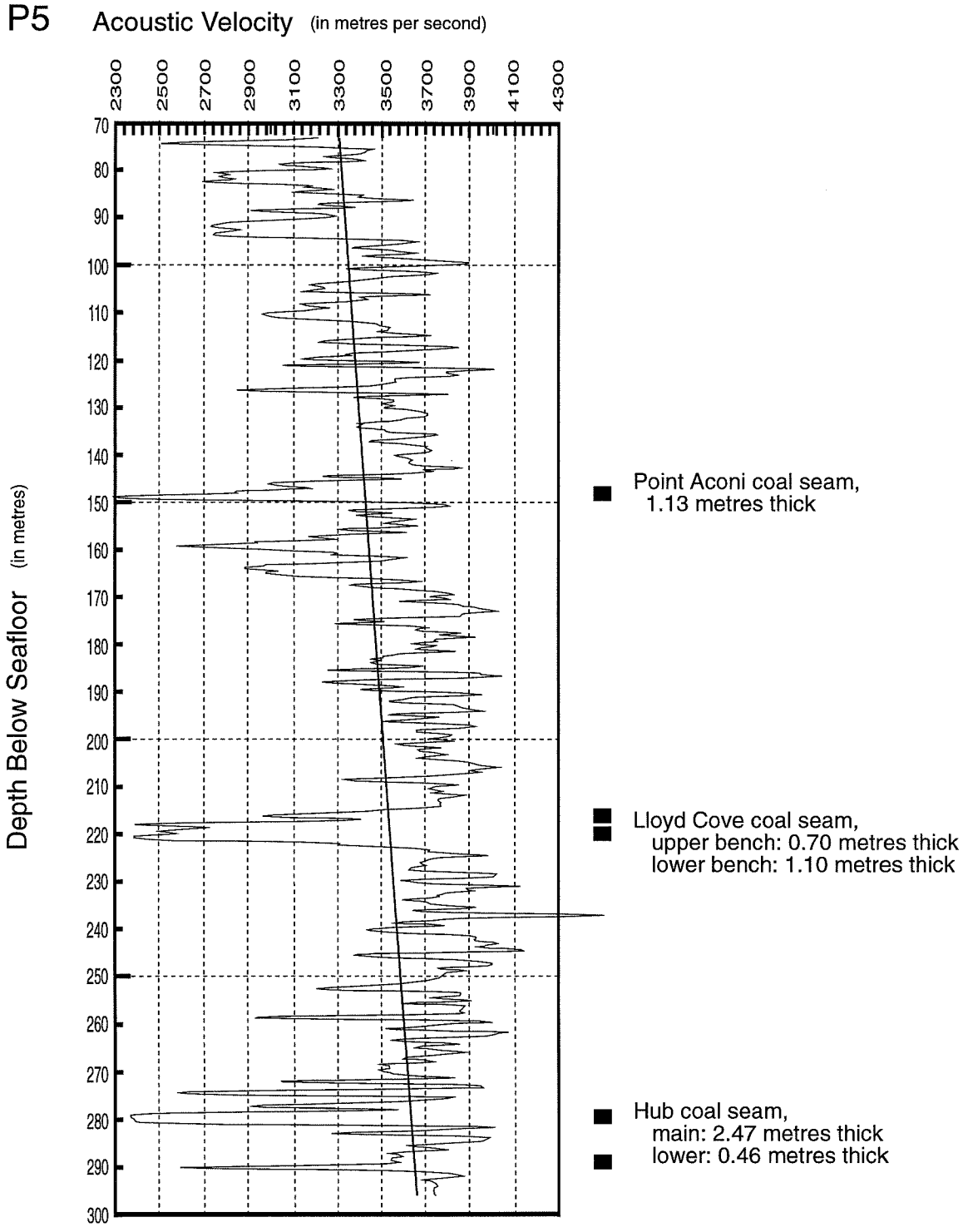

Figure 3.19 Acoustic velocity profile for offshore borehole P5, with least squares line Depth is in metres below seafloor. No data exist for the 0-72 metre interval (data from Nova Scotia Department of Mines 1978 offshore borehole program).

Figure 3.19 shows the acoustic velocity profile for borehole P5 to the level below the Hub coal seam. No data exist for the top portions of the three boreholes because, while drilling, a well casing supported approximately the top 100 metres below sea level.

3.4.2 Sonobuoy Velocity Data

Sonobuoy 71-1 (60°08.7 W, 46°24.7 N; AGC, 1971) recorded acoustic velocity of water, unconsolidated sediments, and bedrock (Table 3.1). Sonobuoy equipment uses refraction seismology. Unless strata are horizontal, refraction seismology requires that velocity measurements be in pairs (with each of the two measurements in opposite direction), and an average of the two providing the velocity. Because the Sonobuoy survey in 1971 was shot in one direction only, measurements should be considered approximate (A. Grant, pers. comm. 1995). Sonobuoy 71-1 is the only velocity data available for unconsolidated sediments and for outcropping bedrock.

3.4.3 Summary of Velocity Data

At the H12 borehole site, acoustic velocity varies between 2350 and 4300 m/s for the interval at and above the Point Aconi coal seam (Fig. 3.17). At the H12A borehole site, acoustic velocity varies between 2400 and 4260 m/s for the interval at and above the Point Aconi coal seam (Fig. 3.18). At the P5 borehole site, acoustic velocity varies between 2300 and 4546 m/s for the interval at and above the Hub coal seam (Fig. 3.19). Table 3.1 summarises acoustic

velocity for Sonobuoy 71-1, and boreholes H12, H12A, and P5. In addition, Table 3.1 includes the Point Aconi and Hub seams for comparison purposes.

Table 3.1 Summary of Acoustic Velocity Data Collected in the Study Area

Material	Depth Below Sea Level (m)	Acoustic Velocity (m/s)
Water	0 to 54.9 (Sonobuoy 71-1)	1500
Seafloor	37 (H12 site)	-
Seafloor	25 (H12A site)	-
Seafloor	42 (P5 site)	-
Unconsolidated Sediments	54.9 to 57.9 (Sonobuoy 71-1)	1828
Bedrock	57.9 to 69.8 (Sonobuoy 71-1)	3419 (avg.)
Bedrock	55.0 to 123.0 (H12 site)	3433 (avg.)
Bedrock	82.0 to 136.5 (H12A site)	3554 (avg.)
Bedrock	113.2 to 315.8 (P5 site)	3450 to 3750 (grad.)*
Point Aconi Coal Seam	117.4 to 118.5 (H12 site)	2350
Point Aconi Coal Seam	130.0 to 131.4 (H12A site)	2400
Point Aconi Coal Seam	155.2 to 156.3 (P5 site)	2283
Hub Coal Seam	243.2 to 245.6 (H12 site)	2381
Hub Coal Seam	247.2 to 249.2 (H12A site)	2427
Hub Coal Seam	298.7 to 301.2 (P5 site)	2540

* Acoustic velocity is presented as a range; see Figure 3.19 (acoustic profile of borehole P5)

CHAPTER 4 INTERPRETATION

4.1 Introduction

This chapter presents an interpretation of the multibeam swath bathymetric chart and the single-channel seismic records. The bathymetric chart shows the general structure of bedrock on the seafloor, and thus it complements the interpretation of the seismic data in which only three horizons define structure in much of the survey area. This chapter also presents two synthetic seismograms to help in the correlation of bedrock reflectors with coal seams.

4.2 Seafloor Morphology

4.2.1 Distribution of Bedrock Outcrop

The seafloor occurs as zones of smooth topography and zones of irregular topography. Zones of smooth topography represent thick (i.e., greater than approximately 3 metres) accumulation of unconsolidated sediments (Pleistocene sediments) (Fig. 4.1). Zones of irregular topography represent bedrock outcrop, and correspond to topographic highs in the study area (Fig. 4.1). A thin veneer of unconsolidated sediments covers bedrock in some parts of the study area, and represents the transition between zones of smooth topography and zones of irregular topography. This veneer of unconsolidated sediments, up to approximately 3 metres thick, is thickest in the deep-water part of the study area (i.e., 50 to 60 metres).

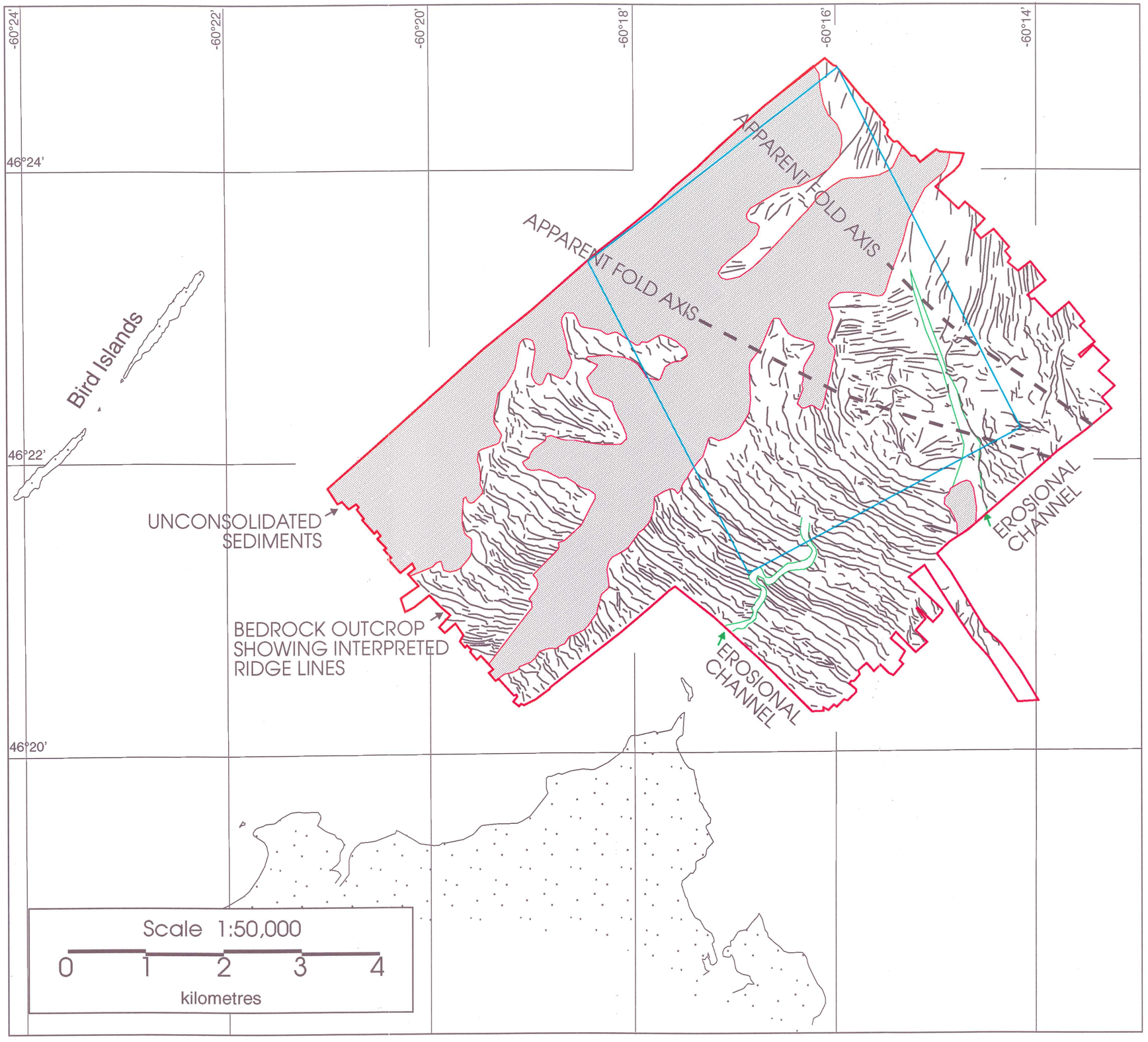

Figure 4.1 Bedrock outcrop offshore from Point Aconi with interpreted ridge lines and erosional channels. Ridge lines are sub-parallel and generally define bedding planes. Erosional channels were likely formed during low stands of sea level during Pleistocene times.

4.2.2 Ridge Lines

Several sub-parallel ridges occur in areas of bedrock outcrop. As a result of false-shadowing, bedrock ridges with elevations as little as 15 centimetres are visible in shallow areas; ridges rise an average 1.5 metres above surrounding seafloor (B. Courtney, pers. comm. 1995) to a maximum 3 metres above surrounding seafloor. Slopes on either side of ridges are commonly asymmetrical, and the steep side is narrower than the shallow side (Fig. 3.1). This thesis does not consider apparent change in dip with position of the ridge on the seafloor.

Ridges, and other linear features that are of length greater than 50 metres, appear on the map as ridge lines. Figure 4.1 shows ridge lines, which vary in length up to 2000 metres and can be straight or curved. Ridge lines in the southern part of the study area tend to be long and linear with northwest orientation. In the central part of the study area, the orientation of ridge lines varies between north and east. Orientation changes abruptly at the northern part of the study area, changing from east to north over a relatively short distance.

Ridges commonly represent the intersection of bedding planes with the seafloor (Stea et al. 1994), and generally show bedding dip (i.e., the shallow side of the ridge dips approximately in the direction of bedding dip). However, where ridge lines are short (less than about 250 metres), ridge lines may not be good indicators of bedding. Because bedding dip is shallow (less than 11 degrees), any local variation in surface topography might affect the orientation and continuity of bedrock ridges. Ridges in areas of shallowest dip (e.g., at an axial plane) are most affected by local variation in seafloor topography and, therefore, ridges will be shorter and less continuous at the axial plane. It follows that areas of abundant, short ridge lines define the general area of axial planes, but are only useful in the approximation of the location of fold axes.

Ridge lines that are longer than approximately 250 metres generally define two fold axes (or the intersection between axial plane and seafloor) on the seafloor. One fold closes to the west, is approximately symmetrical, and is at the centre of the seismic survey area. Ridge lines on the fold limbs are almost parallel. A second fold closes to the southeast and is located in the northeast part of the study area. Ridge lines on the two fold limbs are approximately perpendicular to each other. Figure 4.1 shows the estimated location of the two fold axes.

4.2.3 Erosional Channels

Two large, curvi-linear features occur as visible features on the seafloor where bedrock crops out (Figure 4.1). One feature occurs in the southeast part of the study area on a topographic high, at water depth between 5 and 25 metres. The feature is sinuous, runs in a northeasterly direction with relatively abrupt north and south termini, and does not follow ridge lines preferentially. The west and east edges are sharply defined and approximately 4 to 5 metres high, and the feature width (distance between east and west edges) is approximately 50 metres.

A second large, curvi-linear feature occurs in the eastern part of the study area and trends in a northerly direction. This second feature lies in a local topographic low at water depth 30 to 40 metres, is straighter than the first, has a gradual, tapered north terminus, does not follow ridge lines preferentially, and extends beyond the southeastern limit of the study area. The feature width is approximately 50 to 100 metres for much of its length, and narrows out in the northern section. The feature edge on the west side is not well defined, and is less than 1.5 metres high relative to surrounding seafloor. The feature edge on the east side is well defined and up to 10

metres high relative to the surrounding seafloor. The feature approximately coincides with the abrupt change in orientation of ridge lines for about 1500 metres along the length of the feature.

The two curvi-linear features are probably erosional channels, resulting from a low-stand in sea level following the last ice age. Stea et al. (1994) identified similar features on a multibeam swath bathymetry chart of the inner continental shelf offshore from Halifax Harbour, Nova Scotia.

4.3 Seismic Interpretation

4.3.1 Features on the Seismic Record

Figure 4.2 shows an example (line 80) of the interpretation of features on the seismic record. Features include:

1) **Da**: the direct arrival (seismic ray propagates directly to the receiver);

2) **Sf**: the seafloor (reflection at the water/seafloor interface);

3) **S**: unconsolidated sediments (reflection at the sediment/bedrock interface);

4) **FWBM**: first water-bottom multiple;

5) **C**: horizon C (a succession of bedrock reflectors);

6) **B**: horizon B (a distinct bedrock reflector); and

7) **A**: horizon A (a distinct bedrock reflector).

4.3.2 Distribution of Unconsolidated Sediments

Figure 4.3 shows the distribution of unconsolidated sediments in the seismic survey area, according to the seismic interpretation. Because of the limit of resolution is a quarter wavelength

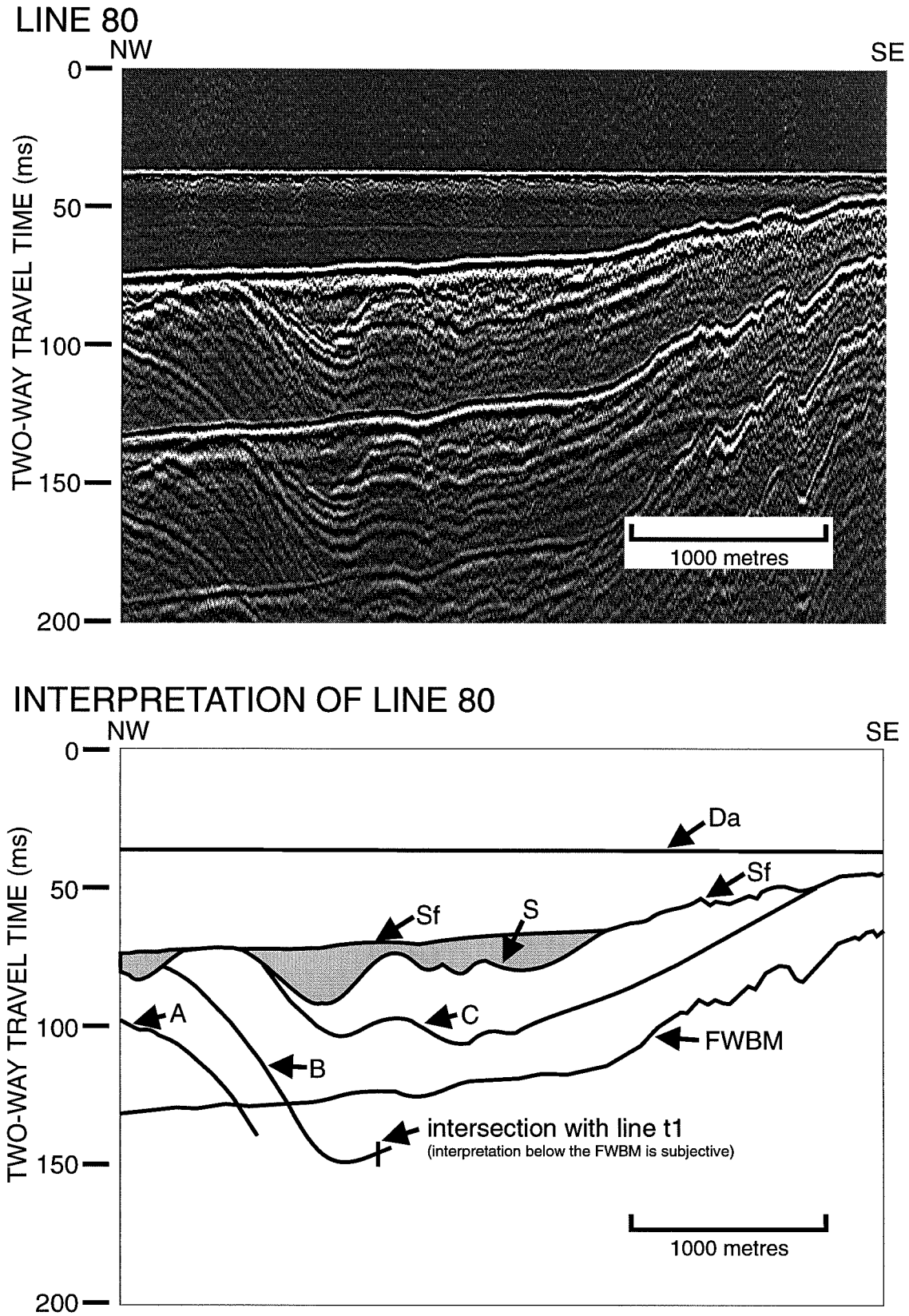

Figure 4.2 Example of seismic interpretation showing direct arrival (Da), seafloor return (Sf), sediment/bedrock interface (S), first water bottom multiple (FWBM), and horizons A, B, and C. Two-way travel time is in milliseconds. The inset shows the horizontal scale.

DISTRIBUTION OF UNCONSOLIDATED SEDIMENTS

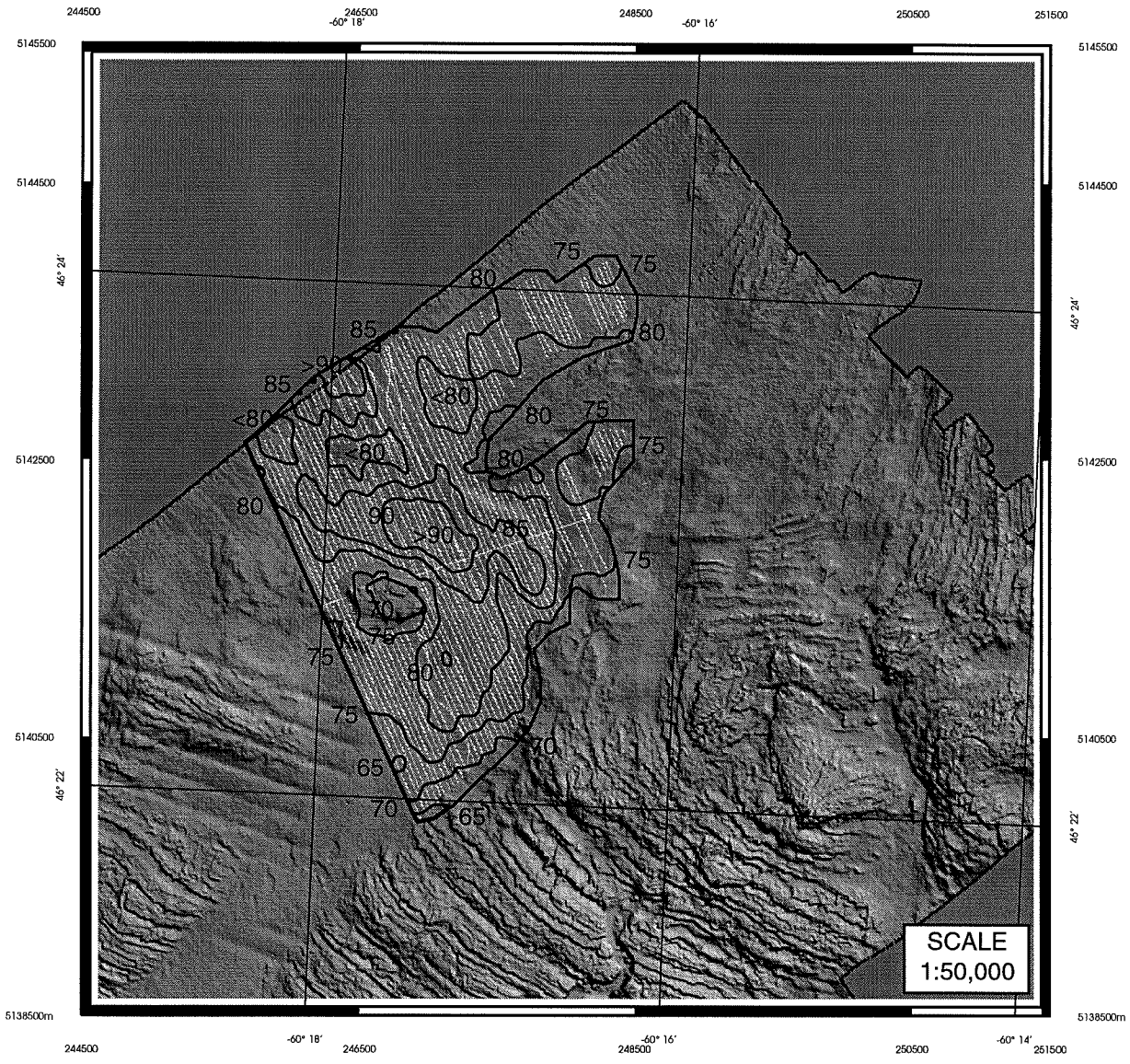

Figure 4.3 Contour map of unconsolidated sediments, with overlay of seismic track lines. Contours are in 5 millisecond intervals (two-way travel time).

(Appendix B), sediments less than 2 metres thick cannot be measured. Thickness of sediments (in two-way travel time) varies from 0 to 20 ms, corresponding to a maximum thickness of approximately 15 ±2 metres (this is an estimate and is not based on a rigorous analysis of all the seismic records).

4.3.3 Structure of Bedrock

The onset of the FWBM limits the interpretation of sub-surface structure to a maximum fepth of approximately 80 ms; interpretation below the FWBM is subjective. Three bedrock reflectors define structure below the seafloor (horizons A, B, and C) in the northern, central, and southern parts of the seismic survey area. Figures 4.4, 4.5, and 4.6 are contour maps of horizons A, B, and C, respectively, in two-way travel time. Horizon A defines the structure in the northern part of the survey area, covering a total of approximately 6.4 km^2. Contours show that dip varies and is generally to the south. Horizon B defines the structure in the central and northern parts of the survey area, covering a total of approximately 9.4 km^2. Dip varies and is generally to the south. Horizons A and B define an antiform (trend is east) in the northern part of the seismic survey area. Horizon C defines the structure in the central and southern parts of the survey area, covering a total of approximately 11.7 km^2. Horizon C defines a synform that trends eastward. The amount of overlap between horizons A and B is approximately 4.7 km^2 and the amount of overlap between horizons B and C is approximately 4.5 km^2. Horizons A and C do not overlap.

HORIZON A

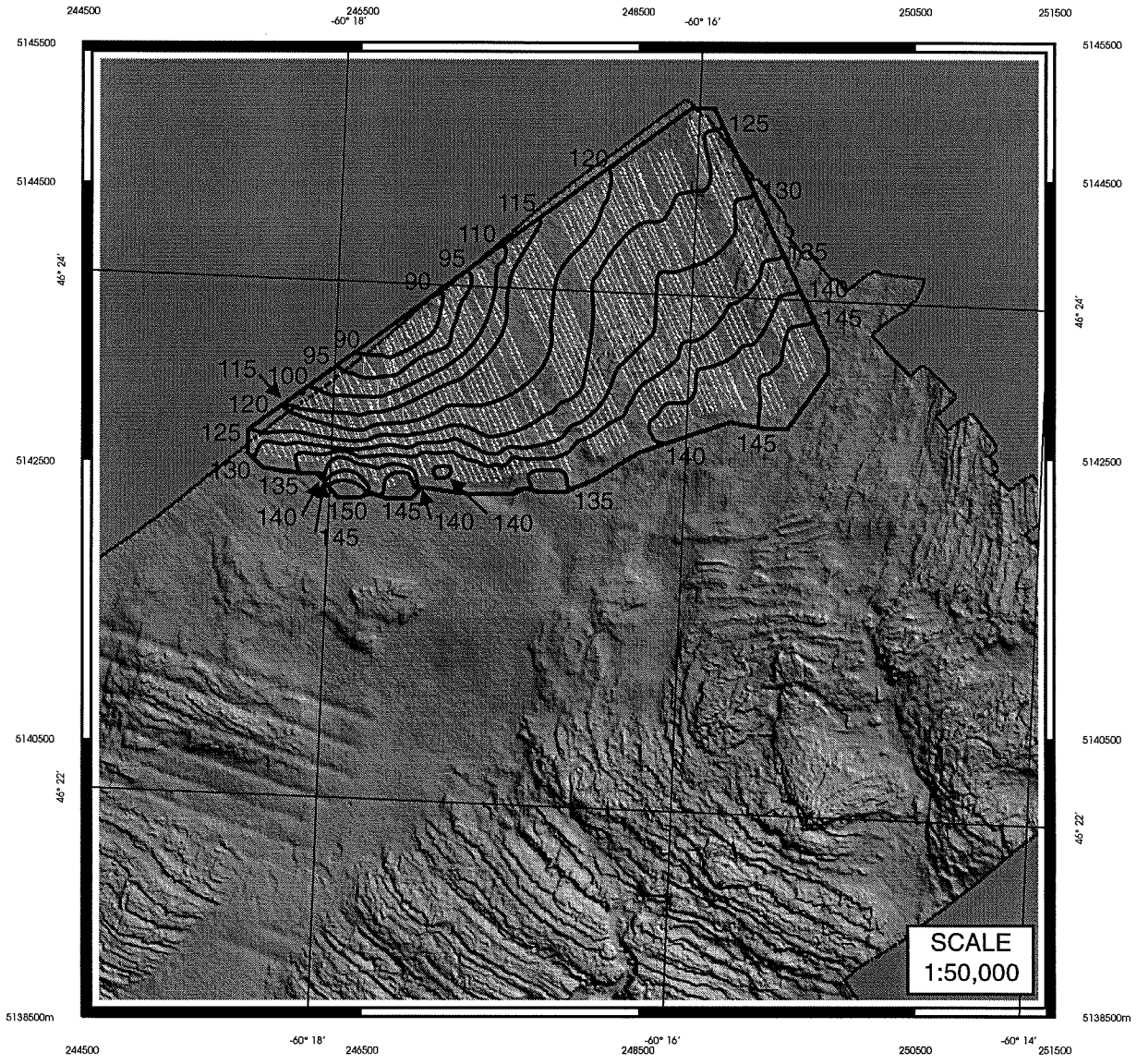

Figure 4.4 Contour map of horizon A, with overlay of seismic track lines. Contours are in 5 millisecond intervals (two-way travel time). Coordinates are in UTM and DEVCO grid (metric).

HORIZON B

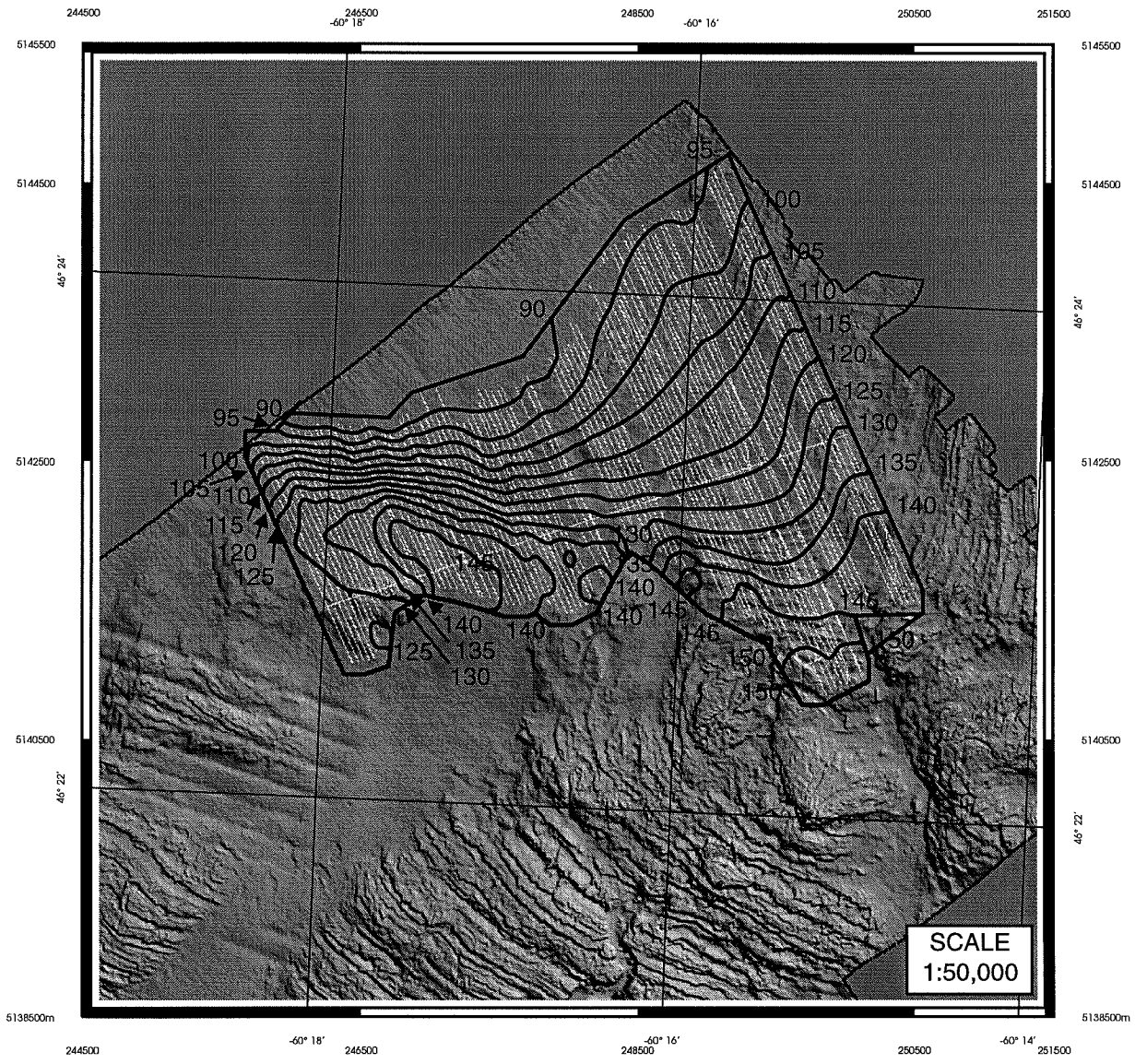

Figure 4.5 Contour map of horizon B, with overlay of seismic track lines. Contours are in 5 millisecond intervals (two-way travel time). Coordinates are in UTM and DEVCO grid (metric).

HORIZON C

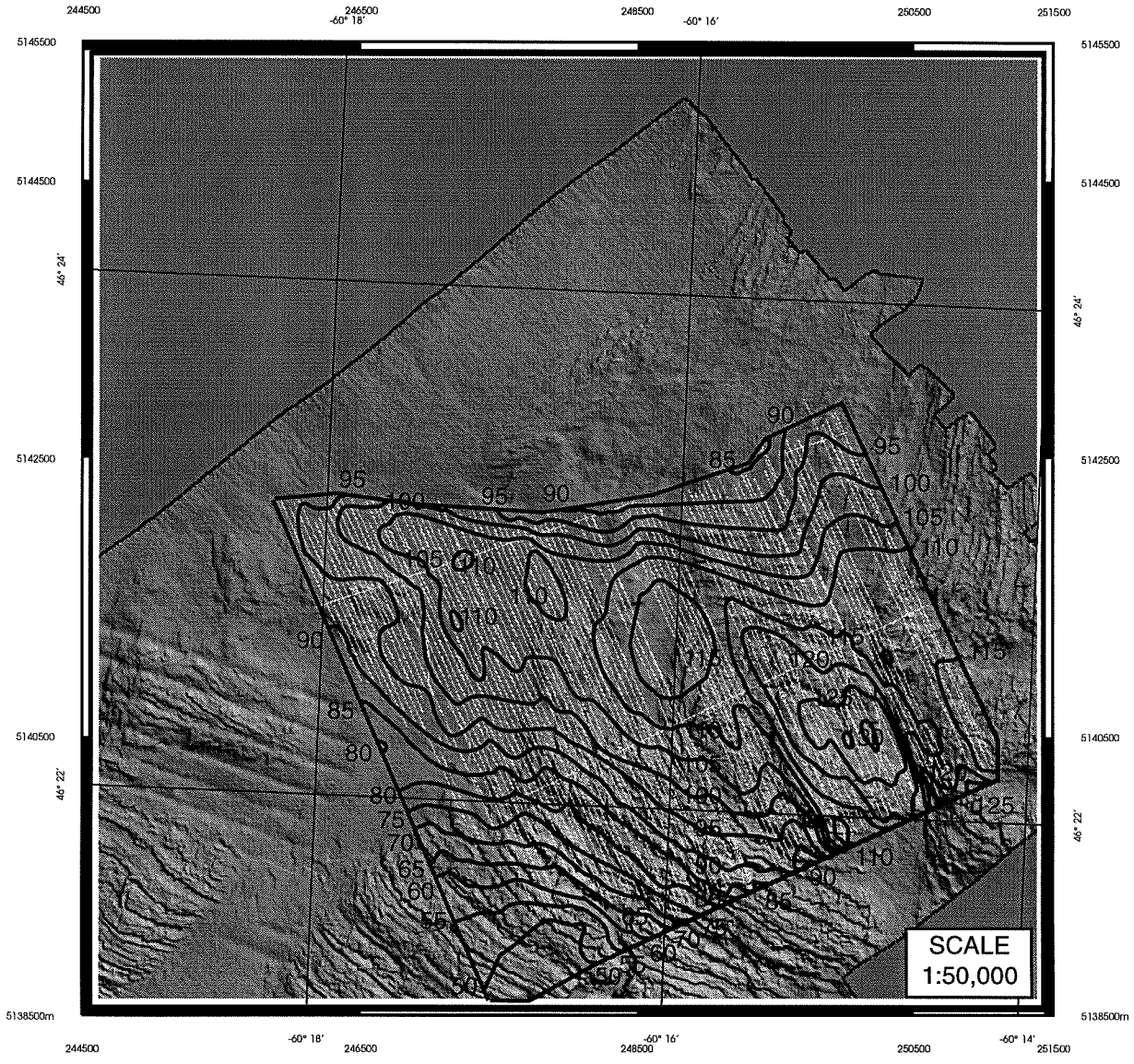

Figure 4.6 Contour map of horizon C, with overlay of seismic track lines. Contours are in 5 millisecond intervals (two-way travel time). Coordinates are in UTM and DEVCO grid (metric).

4.4 Correlation Between Bedrock Reflectors and Lithology

4.4.1 Potential for Correlation

Coal seams are useful for correlating lithology with bedrock reflectors. Three reasons for using coal seams for this purpose are: 1) coals have a sharp contrast in acoustic velocity and density, 2) coals are laterally extensive, and 3) boreholes identify coals by name. For these reasons, individual coal seams should have similar seismic signatures in much of the survey area, and boreholes indicate the depth of specific coal seams.

The correlation of bedrock reflectors with lithology relies on the intersection of seismic track lines with at least one borehole site. Figure 3.2 shows the location of boreholes H12, H12A, and P5. Line t1 intersects the location of boreholes H12 and P5. Line 61 intersects the location of borehole P5. No seismic line intersects the location of borehole H12A.

The conversion of the depth of the borehole casing shoe to two-way time allows the correlation of the seismic record (which is in two-way time) with boreholes H12 and P5 (which are in depth). Velocity data from Sonobuoy 71-1 (Table 3.1) constrains the borehole casing shoe to two-way time (below seafloor), corresponding to 33 ms (milliseconds) and 38 ms for boreholes H12 and P5, respectively.

At the H12 borehole site, the Point Aconi seam occurs at a two-way travel time of 71 ms below the seafloor, and the Lloyd Cove coal seam occurs at 100 ms. However, the onset of the FWBM (below which the record is overprinted with multiples) occurs at 50 ms. Therefore, direct correlation with lithology is feasible only for the interval above 50 ms and below 33 ms (depth of casing shoe). At the P5 borehole site, the onset of the FWBM occurs at about 54 ms,

and direct correlation with lithology is feasible only for the interval above 54 ms and below 38 ms (Fig. 3.19).

Because the bedrock is folded, and because the strata are laterally extensive, lithology may be correlated elsewhere at shallower depths on seismic lines t1 and 61. For example, the seismic data may image strong reflectors, such as the Point Aconi coal seam, where the Point Aconi coal seam occurs at shallower depth and above the FWBM (i.e., up-dip). Table 4.1 summarises the potential for correlating boreholes with bedrock reflectors. Table 4.1 compares the potential for boreholes H12, H12A, and P5, and shows that borehole P5 is the most appropriate of the three boreholes for correlating bedrock reflectors with lithology.

Table 4.1 Potential for Correlating Boreholes with Bedrock Reflectors

Borehole	**H12**	**H12A**	**P5**
Intersected by seismic line	line t1	not intersected	lines t1 and 61
Depth of Casing Shoe in Two-Way Time; b.s.f. (ms), approximate, based on 3419 m/s bedrock velocity	33	57	38
Depth of FWBM in Two-Way Time; b.s.f (ms)	50	not intersected	54
Depth of Horizon B in Two-Way Time; b.s.f (ms)	not interpreted	not intersected	70
Depth of Horizon A in Two-Way Time; b.s.f. (ms)	not interpreted	not intersected	not interpreted
Depth of Point Aconi coal seam in Two-Way Time; b.s.f. (ms), approximate, based on 3419 m/s bedrock velocity	71	79	100
POTENTIAL FOR CORRELATION (i.e., up-dip from intersection with the borehole site)	FAIR; no strong reflectors above the FWBM	POOR; not intersected by any seismic line	GOOD; elsewhere and up-dip on lines t1 and 61

4.4.2 Boreholes H12 and P5

From velocity profiles H12 and P5, Courtney (in prep.) produced two synthetic seismograms (SS-H12 and SS-P5; Figs. 4.7 and 4.8) by convolving the seismic pulse with the reflectivity function (Yilmaz 1987). The resulting synthetic seismograms approximate the seismic trace in the vicinity of the two borehole sites. The reflectivity function consists of a series of spikes, and each spike has an amplitude that is related to the reflection coefficient of a boundary. Courtney (in. prep) estimated acoustic impedance (density x velocity) with velocity (Appendix B), which assumes that change of density with depth is negligible compared to the change of velocity with depth. Synthetic seismograms usually also account for acoustical noise and intrinsic attenuation, which is a more accurate approximation of the seismic trace (Yilmaz 1987). However, for the purpose of this thesis, synthetic seismograms SS-H12 and SS-P5 are good approximations of the seismic trace in the vicinity of the two borehole sites.

4.4.3 Correlation on Line t1

Where seismic line t1 intersects the H12 borehole site, no strong reflectors occur above the FWBM. In addition, strong bedrock reflectors do not occur above the FWBM up-dip along line t1. Therefore, SS-H12 does not correlate with bedrock reflectors (Fig. 4.9).

Where seismic line t1 intersects the P5 borehole site, the casing shoe corresponds approximately with the FWBM; however, the interpretation of horizon B continues below the FWBM, at which depth it corresponds with a strong reflector on the synthetic seismogram. Translated elsewhere on line t1 (based on the intersection of horizon B at the P5 borehole site), SS-P5 corresponds with two strong reflectors, one unnamed reflector, and horizon B (Fig. 4.9).

SYNTHETIC SEISMOGRAM SS-H12

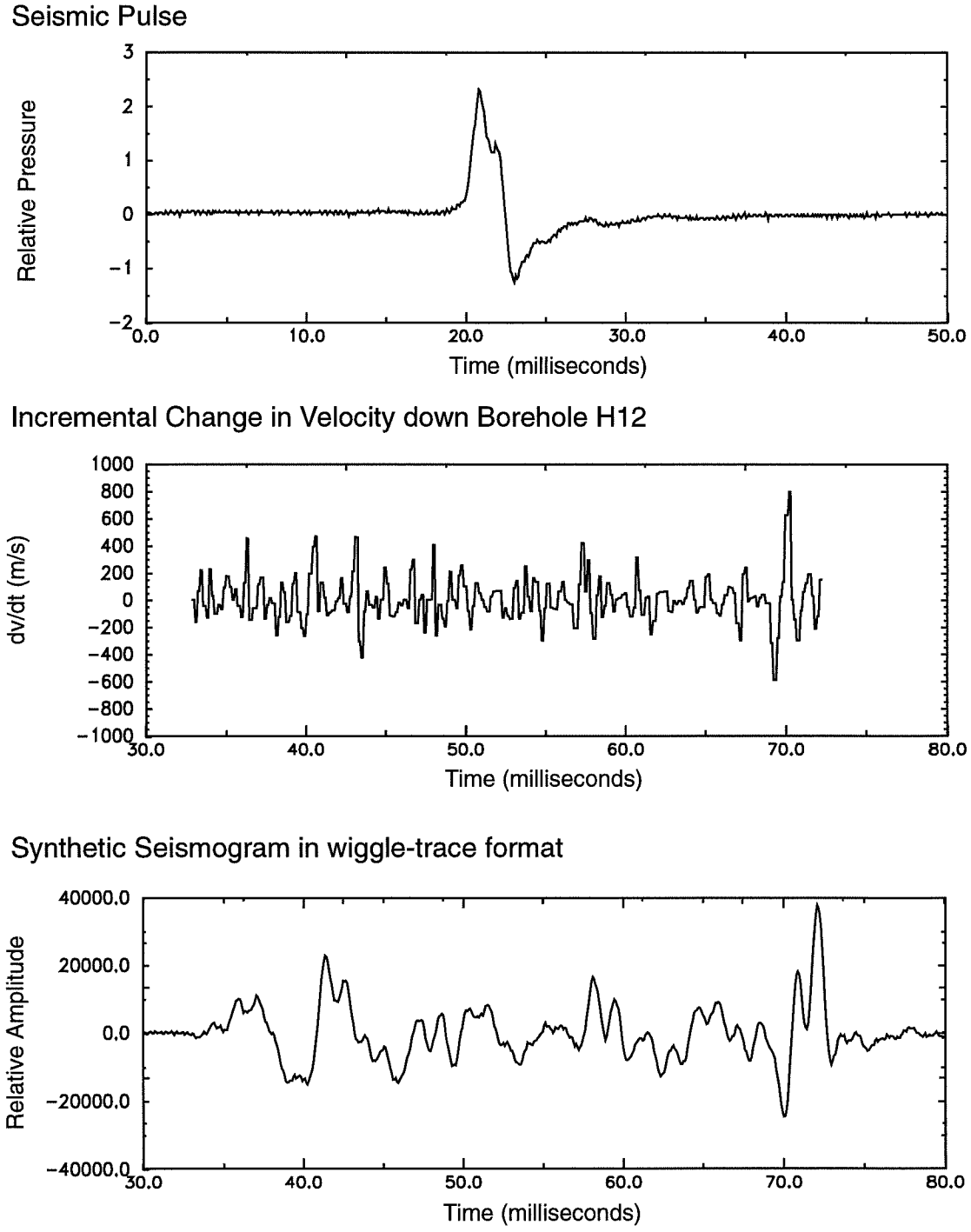

Figure 4.7 Synthetic seismogram SS-H12 is produced by convolving the seismic pulse with incremental change in velocity down borehole H12. The doubling of time approximates two-way travel time.

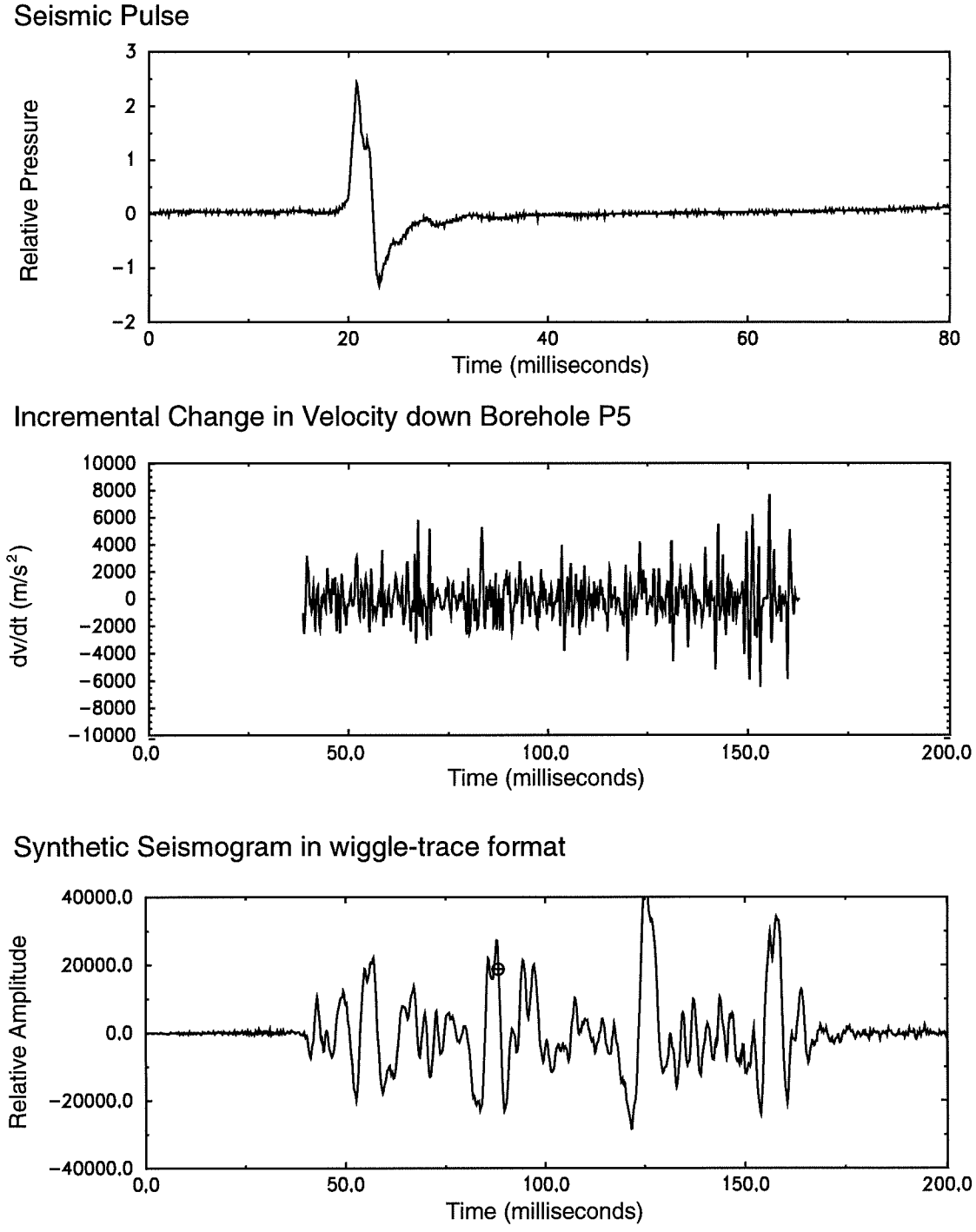

Figure 4.8 Synthetic seismogram SS-P5 is produced by convolving the seismic pulse with incremental change in velocity down borehole P5. The doubling of time approximates two-way travel time.

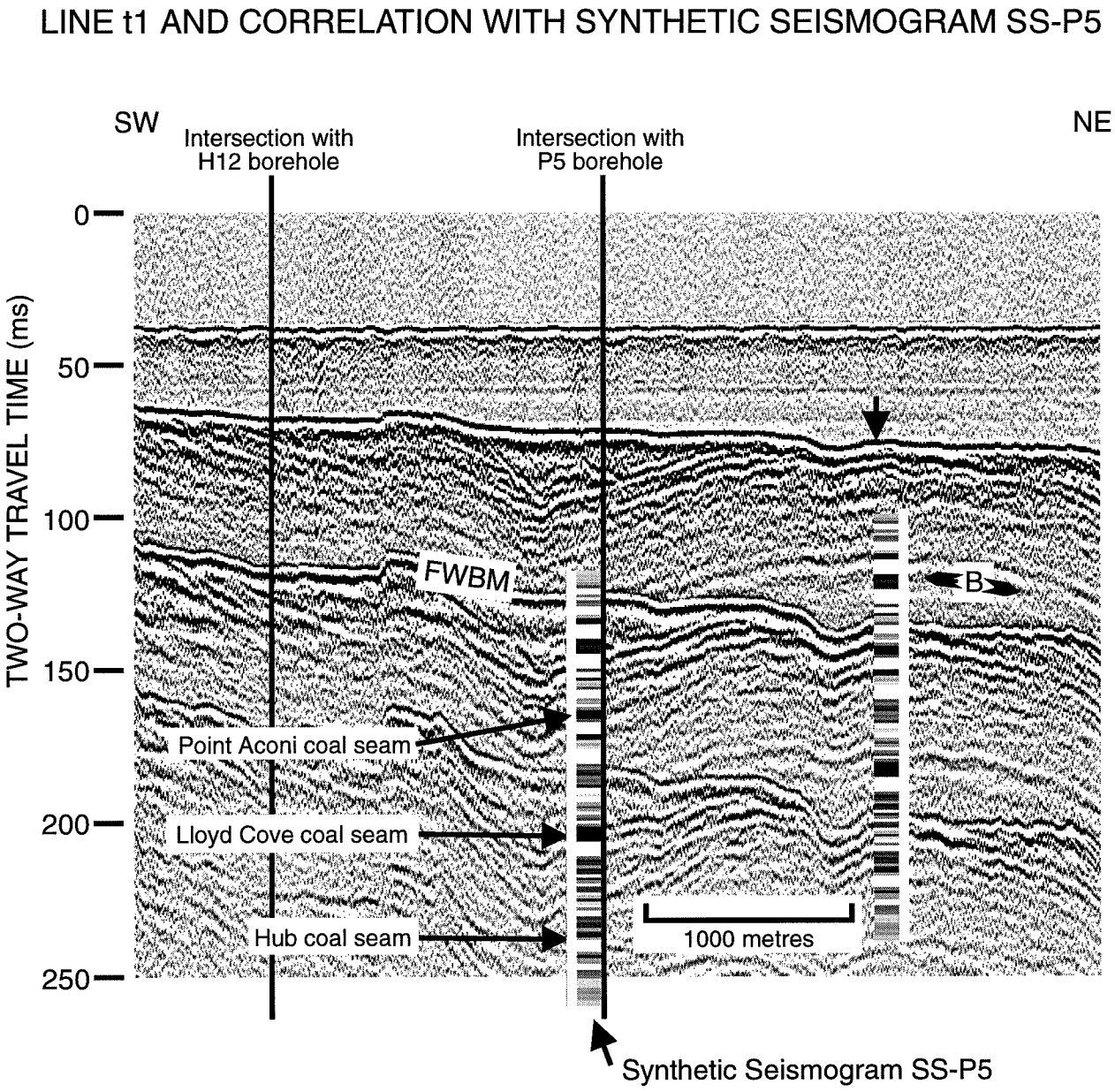

Figure 4.9 Correlation of bedrock reflectors with synthetic seismogram SS-P5. Seismic line t1 intersects the site of boreholes H12 and P5. Synthetic seismogram SS-P5 is based on the borehole P5 acoustic profile. Two negative peaks on the synthetic seismogram correlate to bedrock reflectors, and one of the two reflectors is horizon B. Two-way travel time is in milliseconds. Horizontal scale is shown in the inset.

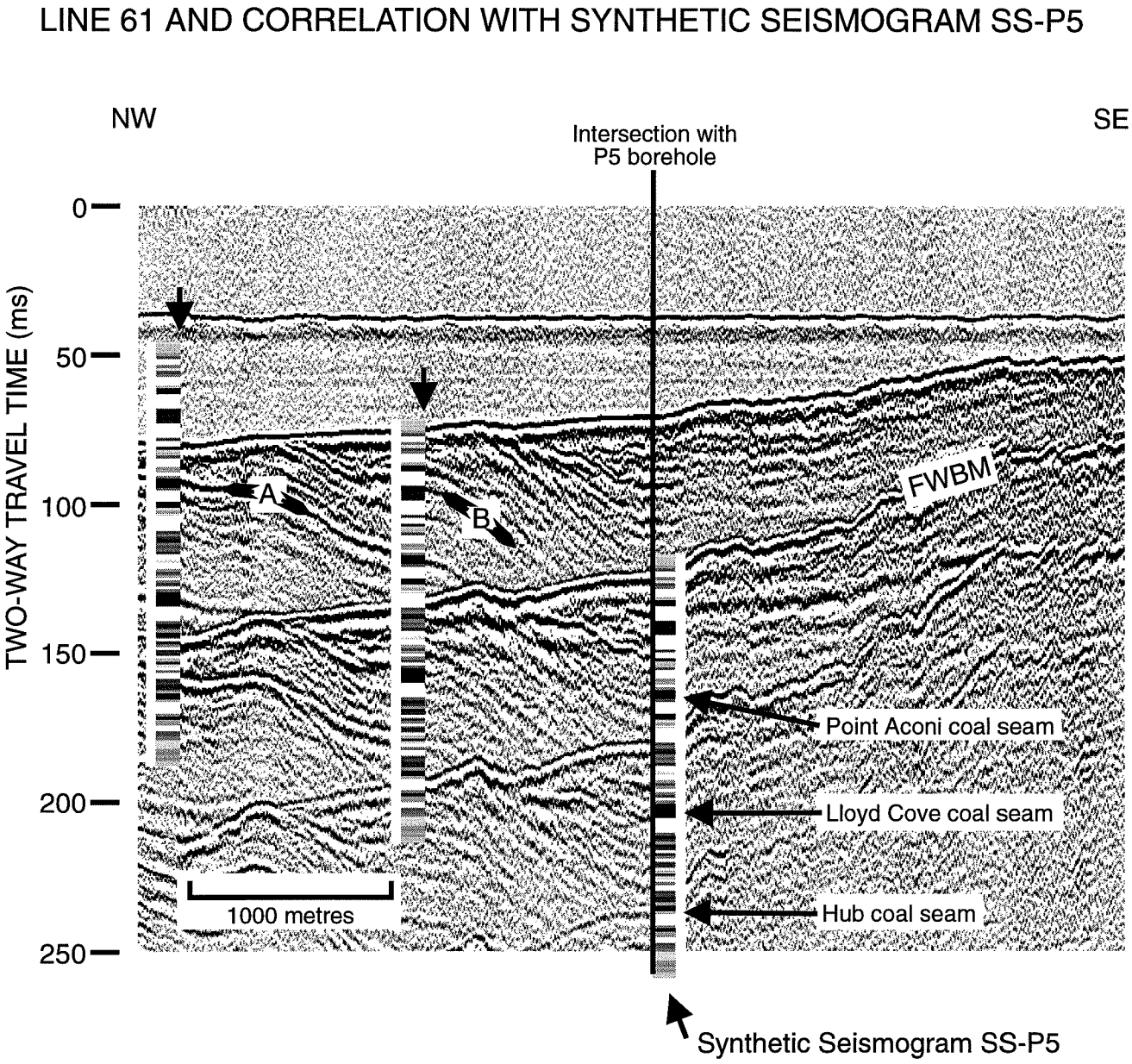

Figure 4.10 Correlation of bedrock reflectors with synthetic seismogram SS-P5. Seismic line 61 intersects the site of borehole P5. Synthetic seismogram SS-P5 is based on the borehole P5 acoustic profile. Five negative peaks on the synthetic seismogram, including those from the Point Aconi and Lloyd Cove coal seams, correlate to bedrock reflectors. In addition, horizon A correlates to the Point Aconi coal seam. Two-way travel time is in milliseconds. Horizontal scale is shown in the inset.

4.4.4 Correlation on line 61

Where seismic line 61 intersects the P5 borehole site, the direct correlation with bedrock reflectors is not feasible for the same reason as on line t1. However, as on line t1, horizon B is interpreted below the FWBM and corresponds with a strong reflector on the synthetic seismogram (Fig. 4.10). Translated 2250 metres up-dip on line 61 (translation is based on the intersection of horizon B at the P5 borehole site) (translation is performed in two steps of approximately equal distance), SS-P5 corresponds with five strong, negative reflectors. These five reflectors include: an unnamed reflector 7 ms above horizon B (unidentified lithology on borehole log), horizon B (unidentified lithology on borehole log), horizon A (Point Aconi coal seam on borehole log), an unnamed reflector 8 ms below horizon A (unidentified lithology on borehole log), and an unnamed reflector 39 ms below horizon A (Lloyd Cove coal seam on borehole log).

4.5 Summary

The areal distribution of unconsolidated sediments greater than 3 metres and bedrock outcrop is based on the multibeam bathymetric chart. Bedrock crops out in much of the study area and outcrop topography is irregular, consisting of several sub-parallel ridges. In some areas, a veneer of unconsolidated sediments (less than 3 metres thick) overlies bedrock, but ridges are visible despite the veneer. Ridges represent the intersection of bedding and the seafloor (Stea et al. 1994), and show the general location of two fold axes. In addition, the bathymetric chart shows two erosional channels that are probably remnant from a low-stand in sea level following the last ice age (Stea et al. 1994). The distribution of unconsolidated sediments, according to the

seismic data, is restricted to the western part of the seismic survey area and attains a maximum thickness of approximately 15 metres. Three horizons (horizons A, B, and C) define structure in the sub-surface. The onset of the FWBM limits the interpretation of the three horizons to a maximum two-way time of less than 80 milliseconds. Horizons A, B, and C define a synform and an antiform that trend eastward. Lines t1 and 61 intersect the site of borehole P5, where the FWBM corresponds with the borehole casing shoe. However, because bedrock is folded, bedrock reflectors occur at shallower depths elsewhere and up-dip along lines t1 and 61. A synthetic seismogram of borehole P5 serves as the tool for the correlation of bedrock reflectors with lithology, 2250 metres from the P5 borehole site along line 61. The synthetic seismogram correlates the Point Aconi and Lloyd Cove seams to horizon B and an unnamed bedrock reflector, respectively.

CHAPTER 5 DISCUSSION

5.1 Introduction

This chapter discusses some of the structural features in the study area (including the MacKenzie Syncline) as shown by the bathymetric and seismic data sets. Seafloor morphology influences the seismic record by producing drawdown effects and by disrupting reflector continuity. This chapter discusses the nature of the bedrock reflectors and compares the seismic record with the NSRF (1978) sparker-source data. Finally, this chapter outlines some theoretical implications for converting horizons from two-way time to depth and attempts to quantify the accuracy of the time-to-depth conversion.

5.2 Evidence of Structure on the Seafloor

The seafloor expression of structure is only general, because the seafloor topography affects the length and the degree of curvature of ridges (i.e., ridges are at the intersection between bedding plane and the seafloor and curve more where local variations in topography are significant). These ridge lines reveal two fold axes on the seafloor. One of these fold axes, which transects the centre of the seismic survey area, is the MacKenzie Syncline. The three-dimensional structure of the MacKenzie syncline is well defined on the seismic data. The other fold axis (an unnamed anticline) transects the northern part of the seismic survey area and the seismic data also defines this anticline. The two fold axes are sub-parallel at a spacing that

varies between 2500 metres in the west and 750 metres in the east. Figure 5.1 shows a perspective view of the sub-surface structure, as viewed from the west.

The identification of faults is one of the objectives of this thesis. The erosional channel in the northern part of the seismic survey area is a seafloor feature that has the appearance of a fault. The feature is relatively straight, is more than 3000 metres long, and coincides with an abrupt change in orientation of ridge lines. Thus, the bathymetric and seismic data suggest that the feature is a seafloor expression of a fault. One aspect of the seismic data is that track lines run approximately parallel to the channel and this coincidence in orientation made the interpretation more difficult. The seismic record, however, shows no features commonly attributed to faults (e.g., diffractions or abrupt vertical displacement of bedrock reflectors). Bedrock reflectors below the southern part of the channel change dip abruptly, similar to local variations in seafloor topography, but this change in dip may be the result of drawdown effects. In summary, these data support the interpretation of Stewart (1994) that strata are not faulted.

5.3 Relation between Seafloor Morphology and Continuity of Bedrock Reflectors

Two aspects of seafloor morphology may affect the continuity of bedrock reflectors: 1) the uneven topography of bedrock outcrop (e.g., the sound wave may scatter where outcrop is uneven and this scattering reduces the continuity of bedrock reflectors); and 2) the shallow water depth in the study area. Because hydrophone offset is constant, change in water depth affects the angle of incidence of the sound wave at the seafloor and at bedrock reflectors. The angle of incidence governs the proportion of the seismic signal transmitted as a refracted ray and the proportion reflected and, where the angle of incidence is large, the amplitude of the refracted ray

PERSPECTIVE VIEW of MacKENZIE SYNCLINE and UNNAMED ANTICLINE
(coloured according to two-way travel time)

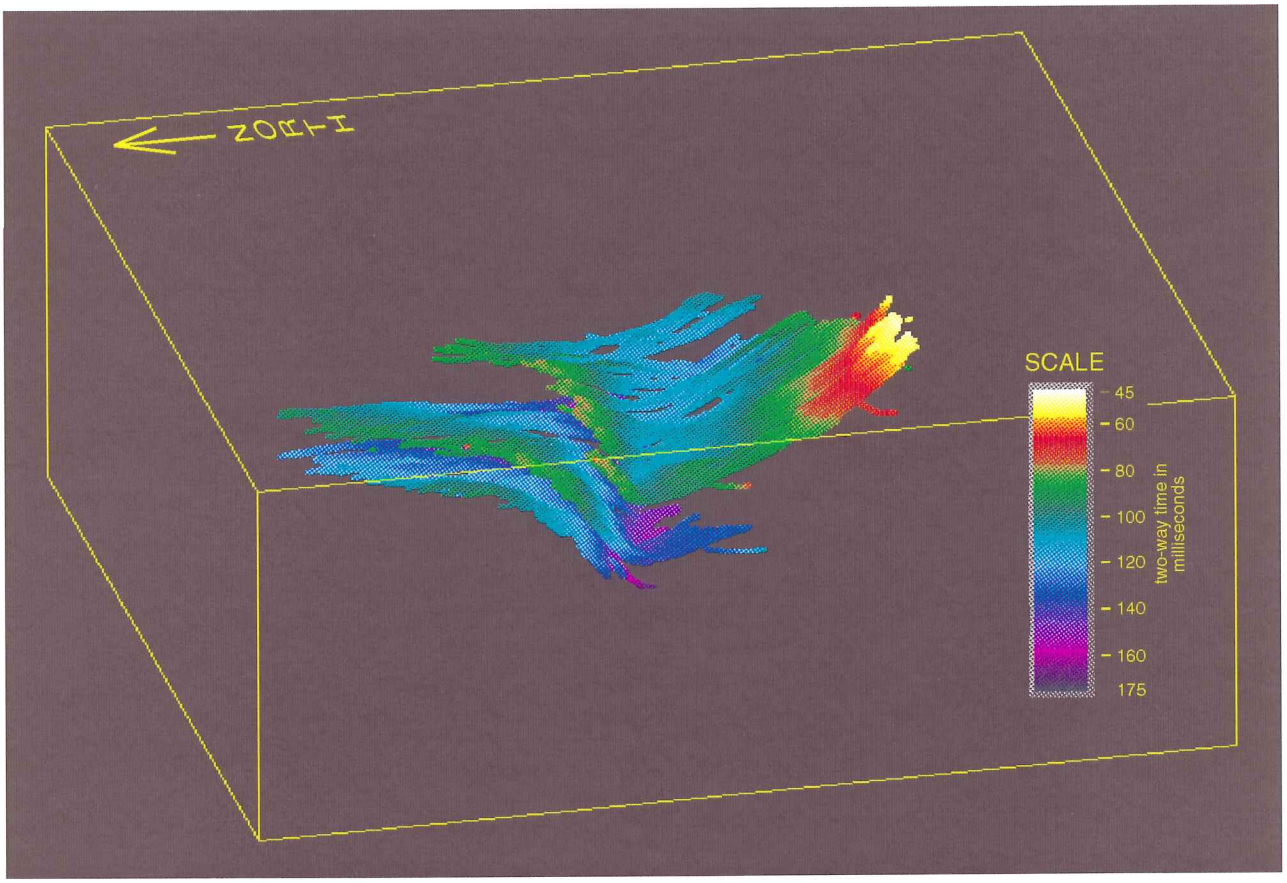

Figure 5.1 Perspective view of the MacKenzie Syncline and unnamed anticline. The sub-surface structure, based on the seismic data, is colour-coded to corresponding two-way travel time (vertical scale is shown in the inset). North is to the left of the page.

may be significant relative to the amplitude of the reflected ray (Kearney and Brooks 1991). In this situation the reflected ray may be indistinguishable from the refracted ray, therefore, reducing continuity. A lack of continuity in bedrock reflectors occurs almost exclusively in shallowest areas, including the eastern quadrant of the seismic survey area.

Outcrop topography may also be a factor in continuity of bedrock reflectors. Under normal conditions for marine reflection seismics, much of the seismic energy reflects when it reaches the seafloor. The amount reflected varies with angle of incidence (higher angle of incidence means that more acoustic energy reflects). Because bedrock outcrop is irregular in the study area, acoustic energy scatters. Changes in the proportion of reflected energy along track lines reduce continuity in bedrock reflectors. Variation in the angle of incidence may also mean different travel paths (i.e., scattering). Scattering implies a difference in return time between subsequent shots for the same bedrock reflector, thus reducing continuity in bedrock reflectors. Subsequent shots are approximately eight metres apart, close enough for significant differences in the returning signal between adjacent shots. Reduced continuity intensifies because areas of shallow water generally coincide with bedrock outcrop where topography is irregular.

5.4 Continuity of Bedrock Reflectors

The bedrock above the Lloyd Cove coal seam is a coal-bearing (coals are approximately one metre thick), mud/siltstone-dominated sequence with intervening sandstone (Figs. 3.17 and 3.18). On seismic records the coals appear as strong, negative reflectors with each reflector persisting laterally, generally with good continuity. Basic geophysical principles predict this type of response, given that the acoustic impedance of coal relative to adjacent sandstone presents

strong, negative acoustic contrasts, and that the coals are laterally extensive (Bird 1987). In terms of vertical resolution (approximately 3.5 metres; Appendix B), coal seams are not visible as individual reflectors. However, the contrast in acoustic impedance is sufficient to produce strong reflectors despite the relatively small thickness of coal seams. Strong reflectors that are not identified as coals on the borehole logs also show on the seismic record. Although these reflectors could represent coals that were simply overlooked during borehole logging (e.g., drill cuttings provided the basis for borehole logging for much of the length of the borehole, and cuttings were sampled approximately every 3 metres), they need not be coals.

5.5 Comparison With NSRF (1978) Seismic Data

The sleeve-gun record of this thesis is a particular seismic data set that is the basis for the interpretation of horizons A, B, and C, and the nature of bedrock reflectors will differ in other seismic surveys. The Nova Scotia Research Foundation (NSRF) shot a single-channel reflection survey in 1978. The 1978 survey used a sparker source, which meant that vertical resolution was approximately 1.2 metres. Figure 5.2 compares NSRF line NE-4 (line classification according to Stewart, 1994) with line t2. Line t2 is an example of poor continuity of bedrock reflectors. The sleeve-gun (1994) and sparker (1978) records show many reflectors; however, on the NSRF record, reflectors are more abundant and continuous. The vertical resolution of the sparker survey assures the appearance of abundant reflectors in the Sydney Mines strata. Reflector continuity is also better in the sparker data. Folds appear clearly on the sparker record and not on the sleeve-gun record. The survey aboard the Moresby (i.e., the 1994 seismic survey) also deployed a sparker source, but because of equipment malfunctions, the 1994 survey collected no

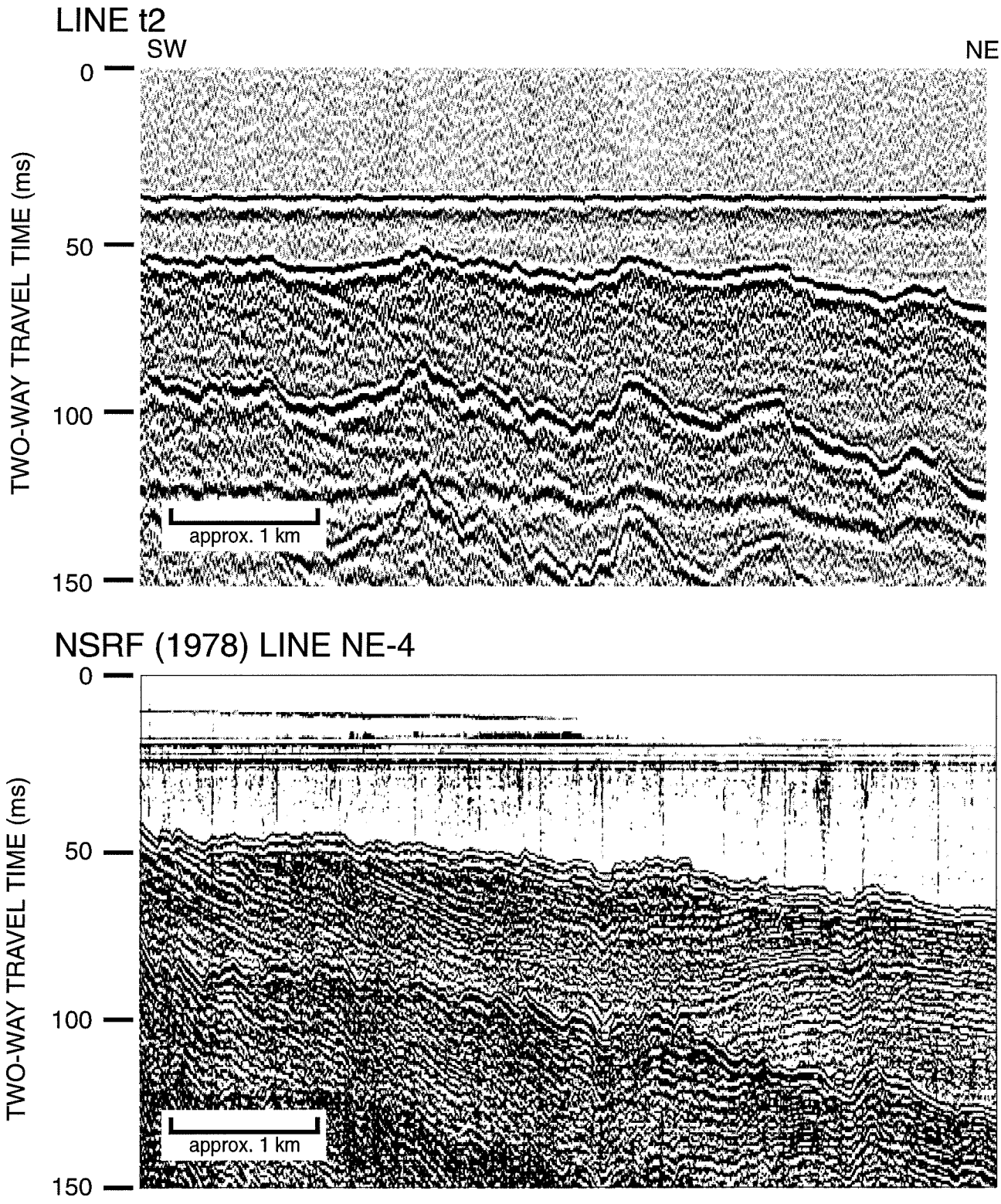

Figure 5.2 Comparison between line t2 (sleeve-gun source) and line NE-4 (the Nova Scotia Research Foundation used a sparker source). Line t2 is an example of poor continuity of bedrock reflectors. Line NE-4 has good continuity between bedrock reflectors and shows a synform and an antiform. The two survey track lines are almost coincident.

sparker data. However, the sleeve-gun record is still considered high resolution (Ziolkowski et al. 1979; Palmer 1987) and, as this thesis demonstrates, it can image coal.

5.6 Time-to-Depth Conversion: Future Work

5.6.1 Introduction

The ultimate goal of defining the structure is to aid in mine planning at the Prince Colliery. This section summarises a possible method of converting the interpretation of the seismic section, which is in two-way travel time, into depth below sea level. The method accounts for survey geometry, average velocity of various media, and refraction at the water/bedrock interface, but does not account for bedding dip. The dips are shallow enough (i.e., less than 11°) to ignore this effect. The conversion of the interpretation to depth is the groundwork for the extrapolation of structure to the level of the Hub coal seam (approximately 240 to >370 metres below seafloor) in the area of anticipated development by the Prince Colliery.

5.6.2 Effect of Survey Geometry

The distance from source to receiver for the seismic survey is 52 metres, which is approximately equal to the maximum water depth, and more than twice the minimum depth in the seismic survey area. This wide-angle reflection at the water/sediment interface and at lithological boundaries means that reflective boundaries may produce refracted ray paths, especially where water depth is shallowest. Therefore, the survey geometry greatly affects the interpretation of seismic data and must form part of the conversion of two-way time to depth.

5.6.3 Thickness of Unconsolidated Sediments

Mine planners at the Prince Colliery add the thickness of unconsolidated sediments to bathymetry to estimate bedrock thickness over prospective workings. The thickness of bedrock overlying prospective workings affects the width of mine workings; therefore, the ability to determine the thickness of unconsolidated sediments aids in mine planning at the Prince Colliery (B. McKenzie, pers. comm. 1995).

The calculation of thickness of unconsolidated sediments need not account for refraction effects. When the seismic signal travels through a boundary, the transmitted ray refracts by an amount governed by Snell's Law, but the velocity of the unconsolidated sediments is only 22% greater than the velocity of water. In the area of thickest accumulation of unconsolidated sediments (i.e., at 40-45 metres water depth, where the thickness of unconsolidated sediments is a maximum of 15 metres), the estimated error (obtained by comparing the calculation that accounts for refraction with the calculation that does not account for refraction) that results from ignoring refraction is approximately 2 metres (over-estimate of unconsolidated sediments). Over-estimating the thickness of unconsolidated sediments is preferable, because it implies that the calculation of thickness of bedrock overlying mine workings will be a conservative estimate. Figure 5.3 shows the calculation of thickness of unconsolidated sediments.

5.6.4 Depth to Horizons A, B, and C

The position of horizons A, B, and C on the two-way interpretation (Figs. 4.4, 4.5, and 4.6) can be converted to depth in the same way as unconsolidated sediments; however, this conversion accounts for changes in ray path that result from refraction at media boundaries.

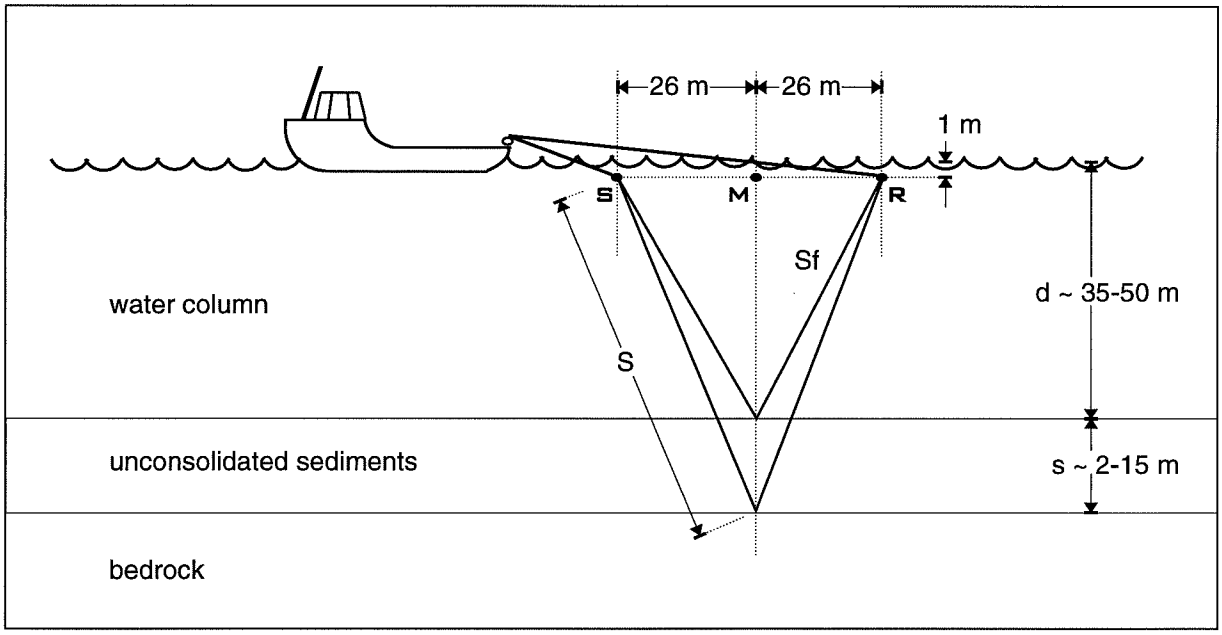

S = seismic source
M = mid-way point between seismic source and receiver
R = receiver

Let: Sf = one-way seafloor return in milliseconds, as interpreted from the seismic record
S = one-way bottom of sediments return in milliseconds, as interpreted from the seismic record
a = vertical travel time from mid-way point to seafloor in milliseconds
b = vertical travel time from mid-way point to bottom of sediments in milliseconds
o = offset/velocity of water = 26/1.5 = 17.3 ms = offset in milliseconds
s = calculated thickness of unconsolidated sediments in metres

Calculation of thickness of unconsolidated sediments:

$$a = (Sf^2 - o^2)^{1/2}$$

$$b = (S^2 - o^2)^{1/2}$$

s = velocity of sound in sediments x difference in travel times
= 1.8 x (b - a)

NOTE: This model gives an estimate of thickness of unconsolidated sediments. Two aspects arise from this estimate: 1) the model ignores refraction at the water/sediment interface, which has the effect of over-estimating the thickness of sediments (e.g., at water depth of 40 metres, the model over-estimates by approximately 12 %); and 2) the ray that reflects from the sediment/bedrock interface intercepts the seafloor at a different location than the ray that reflects from the seafloor, and this has the effect of under-estimating the thickness of sediments (e.g., at water depth of 40 metres, the model over-estimates by approximatel 6 %). The net effect is an over-estimate (e.g., at water depth 40 metres the model over-estimates by approximately 6%).

Figure 5.3 Model for the calculation of thickness of unconsolidated sediments. The model uses basic physical and geometric principles to convert two-way time to depth. Sediments occur at water depths between 35 and 50 metres and attain an estimated maximum thickness of 16 metres.

Refraction at the sediment/bedrock interface, as predicted by Snell's law, is significant because the velocity of bedrock is almost twice the velocity of the sediments. Also, refraction at the water/sediment interface is significant because this effects the angle of incidence at the sediment/bedrock interface. Figure 5.4 shows the effect of refraction on the conversion of horizons to depth.

Table 5.1 Possible Sources of Uncertainty Associated with the Conversion of Two-Way Time to Depth

POSSIBLE SOURCE OF UNCERTAINTY	EXPLANATION	APPROXIMATE ERROR IN METRES OR IN PERCENT OF CALCULATED VALUE
Interpretation of horizon C	Interpreter bias (see text), particularly in the eastern part of the seismic survey are	3.5 metres
Resolution of seismic data	The seismic data do not image coal seams as individual reflectors	3.5 metres
Bedding dip	The seismic data are not migrated, but dip is less than 11 degrees	less than 1 % calculated value
Accuracy of bathymetric data	See Appendix A	less than 0.60 metres
Accuracy of velocity data	The model uses average velocities; error associated with velocity may be more significant at shallower depth	not determined
TOTAL UNCERTAINTY*	A conservative estimate of possible error	4.5 - 9.5 metres for horizons A and B 8 to 13 metres for horizon C

* Additional error may be included for the extrapolation to the Hub coal seam

5.6.5 Quantifying Uncertainty

A number of possible sources of uncertainty exist in the conversion of two-way time to depth. Sources of uncertainty originate at the interpretation stage and at the conversion stage. At the interpretation stage, interpreter bias is a source of uncertainty that is not readily quantified. Continuity of horizons A, B, and C varies, and uncertainty of the interpretation may vary with

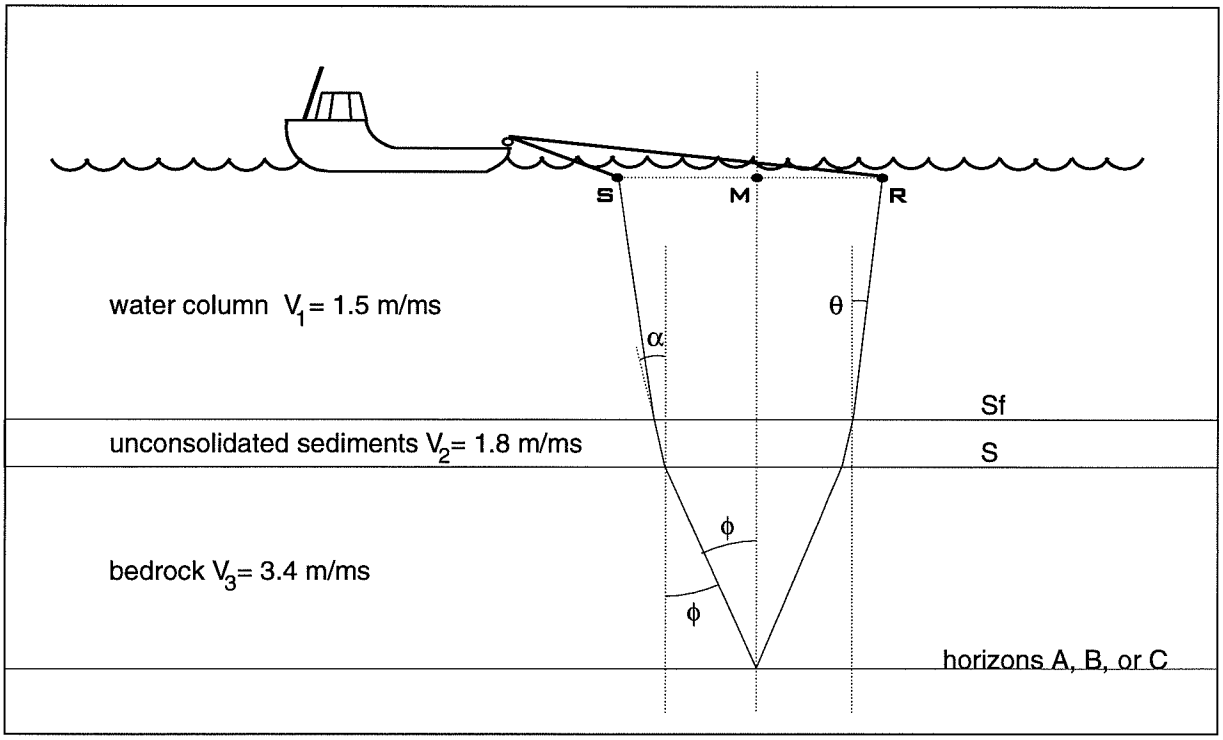

S = seismic source
M = mid-way point between seismic source and receiver
R = receiver

The seismic ray will refract at the water/sediment interface according to:

$$\frac{\sin\theta}{V_1} = \frac{\sin\alpha}{V_2}$$

The seismic ray will refract at the sediment/bedrock interface according to:

$$\frac{\sin\alpha}{V_2} = \frac{\sin\phi}{V_3}$$

The seismic ray will refract at the water/bedrock interface according to (not shown):

$$\frac{\sin\theta}{V_2} = \frac{\sin\phi}{V_3}$$

Figure 5.4 The effect of refraction on the calculation of depth to horizons. The model uses basic physical and geometric principles to convert two-way time to depth. For example, Snell's law predicts that the effect of refraction will be greatest at the water/bedrock and sediment/bedrock interfaces.

continuity of bedrock reflectors. Horizon A is a strong, continuous reflector and has a minimal associated uncertainty. Despite some lateral variation in continuity in horizon B, horizon B also has a minimal associated uncertainty. The vertical resolution of the seismic data will represent any uncertainty associated with horizons A and B. However, horizon C has an uncertainty that is related to the interpretation. Variations in continuity are most noticeable in horizon C, and horizon C defines a succession of reflectors that may or may not be confused with each other during the interpretation stage. This effect is more prevalent in the eastern part of the survey area, where uncertainty is estimated to equal vertical resolution. In addition, the interpretation of horizon C is subjective where variations in seafloor topography affect reflector continuity. Table 5.1 summarises possible sources of uncertainty associated with the conversion of time to depth. The total uncertainty is less than 9.5 metres for horizons A and B, and less than 13 metres for horizon C.

CHAPTER 6 CONCLUSIONS

6.1 Summary of Conclusions

This thesis has addressed the specific objective to provide an improved interpretation of bedrock structure in the area of anticipated development by the Prince Colliery. This study defines bedrock structure with a horizontal resolution previously not possible, and the relatively new approach of using multibeam swath bathymetry was also successful. Mine planning at the Prince Colliery makes allowance for the thickness of bedrock, which varies laterally with the depth of the Hub coal seam below the seafloor. This new interpretation is, therefore, of benefit to mine planning activities at the Prince Colliery.

This thesis concludes the following:

- three horizons (horizons A, B, and C) interpreted from single channel reflection seismic records define the structure of bedrock in the area of anticipated development by the Prince Colliery;
- the seismic data set shows no evidence of faulting;
- the multibeam swath bathymetric chart shows the general structure of bedrock where bedrock crops out;
- seafloor morphology influences the interpretation of the seismic records because of acoustical scattering at the water/seafloor interface;

- a lack of continuity in bedrock reflectors occurs almost exclusively in shallowest areas, including the eastern quadrant of the seismic survey area;
- two coal seams (Point Aconi and Lloyd Cove coal seams) correlate to bedrock reflectors on the seismic record; and
- the seismic time sections could be converted into depth, and based on measured distances to the Hub coal seam at borehole sites and at mine exposures, could be extrapolated to the depth of the Hub coal seam.

REFERENCES

Beck, A.E. 1991. *Physical Principles of Exploration Methods 2nd Edition.* Wierz Pub. Ltd., Winnipeg, 292 pp.

Bird, D.J. 1987. The depositional environment of the Late Carboniferous, coal-bearing Sydney Mines Formation, Point Aconi area, Cape Breton Island, Nova Scotia. unpublished MSc thesis, Dalhousie University, 343 pp.

Boehner, R.C., and Giles P.S. 1986. Geological map of the Sydney Basin, Cape Breton Island. Nova Scotia. Nova Scotia Department of Mines and Energy, Map 86-1, scale 1:50 000.

Courtney, R.C. in prep. An investigation of seabed mine subsidence and sub-seabed geological structure using three dimensional acoustic imaging methods. Atlantic Geoscience Centre, unpublished report.

Courtney, R.C., and Fader, G.B.J., 1994. A new understanding of the ocean floor through multibeam mapping. B.I.O. Science Review, May 1994, pp. 9-14

Gibling, M.R., Boehner, R.C., and Rust, B.R. 1987. The Sydney Basin of Atlantic Canada: an Upper Paleozoic strike-slip basin in a collisional setting. Canadian Society of Petroleum Geologists, Memoir 12, pp. 269-285.

Grant, A.C., Aspects of seismic character and extent of Upper Carboniferous coal measures, Gulf of St. Lawrence and Sydney basins. Palaeogeography, Palaeoclimatology, Palaeoecology, 106:271-285

Hacquebard, P.A., 1979. A geological appraisal of the coal resources of Nova Scotia. Canadian Mineralogy and Metallurgy Bulletin, 72: 76-87.

Hacquebard, P.A., 1993. The Sydney coalfield of Nova Scotia, Canada. International Journal of Coal Geology, 23: 29-42.

Kearney, P., Brooks, M., 1991. *An Introduction to Geophysical Exploration,* 2nd Ed.. Blackwell Scientific Publications, London, 254 pp.

Loncarevic, B.D., and Scherzinger, B.M., June 1994. Compensation of ship attitude for multibeam sonar surveys. Sea Technology, June 1994, pp. 10-15

Palmer, D. 1987. High resolution seismic reflection surveys for coal. Geoexploration, 24: 397-408.

Shaw, J. Parrott, D.R. and Courtney, R.C. 1994. A survey of Argentia Harbour, Newfoundland. Report to Public Works Canada, 14 pp., 5 Figures, 2 Charts.

Stea, R.R., Boyd, R., Fader, G.B.J., Courtney, R.C., Scott, D.B., and Pecore, S.S. 1994. Morphology and seismic stratigraphy of the inner continental shelf off Nova Scotia, Canada: Evidence for a -65 m lowstand between 11,650 and 11,250 C^{14} yr B.P. Marine Geology 117: 135-154.

Stewart, J. April 1994. Review of existing marine seismic data, Prince Colliery, Point Aconi, Nova Scotia. MacGregor Geoscience Ltd., Halifax, Nova Scotia, project 93-31, 18 pp.

Tibert, N.E. 1994. The geometry and depositional setting of the Late Carboniferous Mullins Coal in the South Bar Formation, Sydney Basin, Nova Scotia. unpublished BSc (Hon.) thesis, Dalhousie University, 73 pp.

Yilmaz, Ö. 1987. Seismic Data Processing, Investigations in Geophysics no. 2. Edited by E.B. Neitzel. Society of Exploration Geophysicists, 526 pp.

Ziolkowski, A. 1979. A simple approach to high resolution seismic profiling for coal. Geophysical Prospecting, 27: 360-393.

APPENDIX A MULTIBEAM SWATH BATHYMETRY SURVEY OPERATIONS

A.1 Introduction

The conventional method of bathymetric surveying (i.e., correlating echo-sounder profiles) yields low spatial resolution. Seafloor features are imaged in echo-sounder profiles only where the profiler is directly above the feature. Bathymetric data collected with conventional echo-sounder systems in areas of irregular topography are, therefore, general (Courtney and Fader 1994). Recent advances in the integration of multibeam sonar with differential geographic positioning systems (DGPS) has led to the development of an improvement on multibeam swath bathymetry. Swath bathymetry provides 100% coverage of the seafloor with high accuracy bathymetry. Swath bathymetry charts are used for marine navigation and conform to the standards of the International Hydrographic Organization (Loncarevic and Scherzinger 1994). This appendix outlines the main aspects of multibeam technology and makes specific reference to the Simrad™ EM-1000 deployed from the M. V. Frederick G. Creed offshore from Point Aconi in July, 1994.

A.2 Cruise Aboard the M.V. Frederick G. Creed

The multibeam swath bathymetry survey is the first of two geophysical surveys in the region offshore from Point Aconi (AGC project No. 94-011). Bathymetric data was collected between July 17-20, 1994 aboard the M.V. Frederick G. Creed. The survey was headed by Robert Courtney of the Geological Survey of Canada (Atlantic Geoscience Centre, Dartmouth,

Nova Scotia), who also conducted all post-processing of the data to produce the bathymetric chart.

Weather during the entire survey was excellent. Wind was slight and sea state (a semi-quantitative descriptor of wave height, in which the sea state scale ranges from 0 to 5) usually varied between 0 and 1 (no visible white caps). Sea state during the final day of survey operations was 2 (with visible white caps), and wind was slight during that day.

The M.V. Creed is a double-hulled vessel, weighing 150 gross tons and measuring 20.4 metres in length. Vessel stability was very good, even at high survey speeds (e.g., 13 knots), in sea states experienced during the survey. Stability and speed make the M.V. Creed an ideal vessel for deploying multibeam swath bathymetry equipment.

A.3 Accuracy

Swath bathymetry data are digital and an area surveyed by swath bathymetry is arranged into a matrix of "pixels". Each pixel represents a position on the Universal Transverse Meridian (UTM) co-ordinate system with corresponding bathymetric value in metres. Accuracy depends on the orientation of sonar transducer resulting from ship motion (roll, pitch, heading, and heave), and the prediction of the sound path through the water column. Swath bathymetry charts meet the current bathymetry standards of the International Hydrographic Organization (i.e., accurate to within 1 % water depth).

A.4 Vessel Positioning

Positioning in *X-Y-Z* is done with a differential geographical positioning system (DGPS). Differential GPS is accurate to within 3 metres on the X-Y plane (Courtney, in prep.). Position varies in the long-term (resulting from vessel motion along track lines, measured in minutes) and short-term (resulting from vessel motion dynamics, measured in seconds) and both motions affect accuracy.

Ship motion dynamics - in particular roll, pitch, heading, and heave motions - cause short-term variations in the sonar transducer's orientation and position (Loncarevic and Scherzinger, 1994). Inertial data from accelerometers and gyros combine with the positioning and velocity data from the DGPS, hence the term DGPS-aided inertial navigation system (INS). In general, long-term accuracy is maintained by DGPS and short-term accuracy is maintained by INS. If DGPS is temporarily interrupted, INS acts independently with little degradation in accuracy. Loncarevic and Scherzinger (1994) explained the various components of the INS system.

A.5 Track Line Orientation

Track line orientation varies with location and most track lines are oriented northeast; however, track lines in the southeastern part of the survey area are oriented northwest. Track line spacing varied with depth (shallow water means closer track line spacing) and ranged from 100 to 250 metres. In addition, a high degree of overlap between adjacent survey sweeps (150-200 % coverage of the survey area) ensured that the sonar equipment over-samples bathymetric points on the seafloor.

The primary objective of the survey aboard the M.V. Creed was to study seafloor subsidence above Prince Colliery workings resulting from mine shaft collapse. Additionally, during the progress of the survey, bathymetric data also showed potential for imaging bedrock structure. The survey plan was, therefore, changed to include additional areas of outcropping bedrock in the eastern part of the survey area.

A.6 Measuring the Velocity of Sound in Water

The accuracy of bathymetric measurement depends on available data for the velocity of sound in water. Velocity of sound in water averages 1500 ms^{-1}; however, local variations are significant to a swath bathymetry survey and can produce errors. Local variations in velocity of sound are usually vertical, and can result from thermoclines and saliclines, therefore, velocity was measured at regular intervals down the water column (velocimeter casts) to a depth of up to 55 metres below seafloor. Velocimeter casts were performed at the beginning of each survey day; Courtney (in. prep.) assumes the velocimeter cast is representative of the entire day, and the site of the velocimeter cast is representative of the entire survey area.

A.7 EM-1000 Multibeam Sonar

The M.V. Creed is equipped with the Simrad EM-1000 multibeam swath bathymetry system. The EM-1000 is hull-mounted, and consists of a 120 transducer array (60 port and 60 starboard; shallow mode configuration). The system maps the seafloor by 120 soundings (fired in two pings) at regular intervals along track. Angular coverage is 150 degrees, corresponding to a width of 7.4 times water depth. The beams are aimed at equal horizontal distance on the sea

floor (i.e., with tighter angular spacing in the outer parts of the coverage sector than straight down). Frequency of operation was 95 kHz and pulse length is 0.2 milliseconds.

A.8 Equipment Test Prior to the Survey

Errors caused by inadequate compensation of dynamic motion were identified prior to the survey. Errors show up best on flat seafloor, appearing as corrugations parallel to track lines. Prior to the survey, a test line was conducted in water depth that varied from 10 to 70 metres, and over flat and uneven seafloor. The test line was then "re-shot" in the opposite direction and the two images were analysed. The test line showed a systematic error related to orientation of the sounding equipment (sounder array). This error provided a correction value that was applied to all data for duration of the survey.

APPENDIX B SEISMIC SURVEY OPERATIONS

B.1 Introduction

The seismic survey is the second of two geophysical surveys in the region offshore from Point Aconi. The seismic data were collected between July 25-30, 1994 aboard the H.M.C.S. Moresby. The survey was headed by Robert Courtney of the Geological Survey of Canada (Atlantic Geoscience Centre, Dartmouth, Nova Scotia; project No. 94-011). Weather during the survey was good. Sea state varied between 1 and 2 (with visible white caps).

B.2 Cruise Aboard the H.M.C.S. Moresby

The Moresby is a 65-metre vessel of the Royal Canadian Navy fleet dedicated to offshore surveys. Vessel speed during the survey was 3 knots and vessel stability was maintained because of vessel size and calm weather.

B.3 Survey Coverage

Figure B.1 shows the areal extent of survey coverage. Track lines are oriented northwest, spaced 40 metres apart. Five gaps in the northern half of the survey areas (up to 200 metres between successive lines) show where data were not recorded. Of one hundred lines intended for the main survey area, 87 lines were recorded. A number of smaller gaps occur where survey lines deviate from straight, and where track lines do not extend the length of the survey area.

SEISMIC SURVEY TRACK LINES

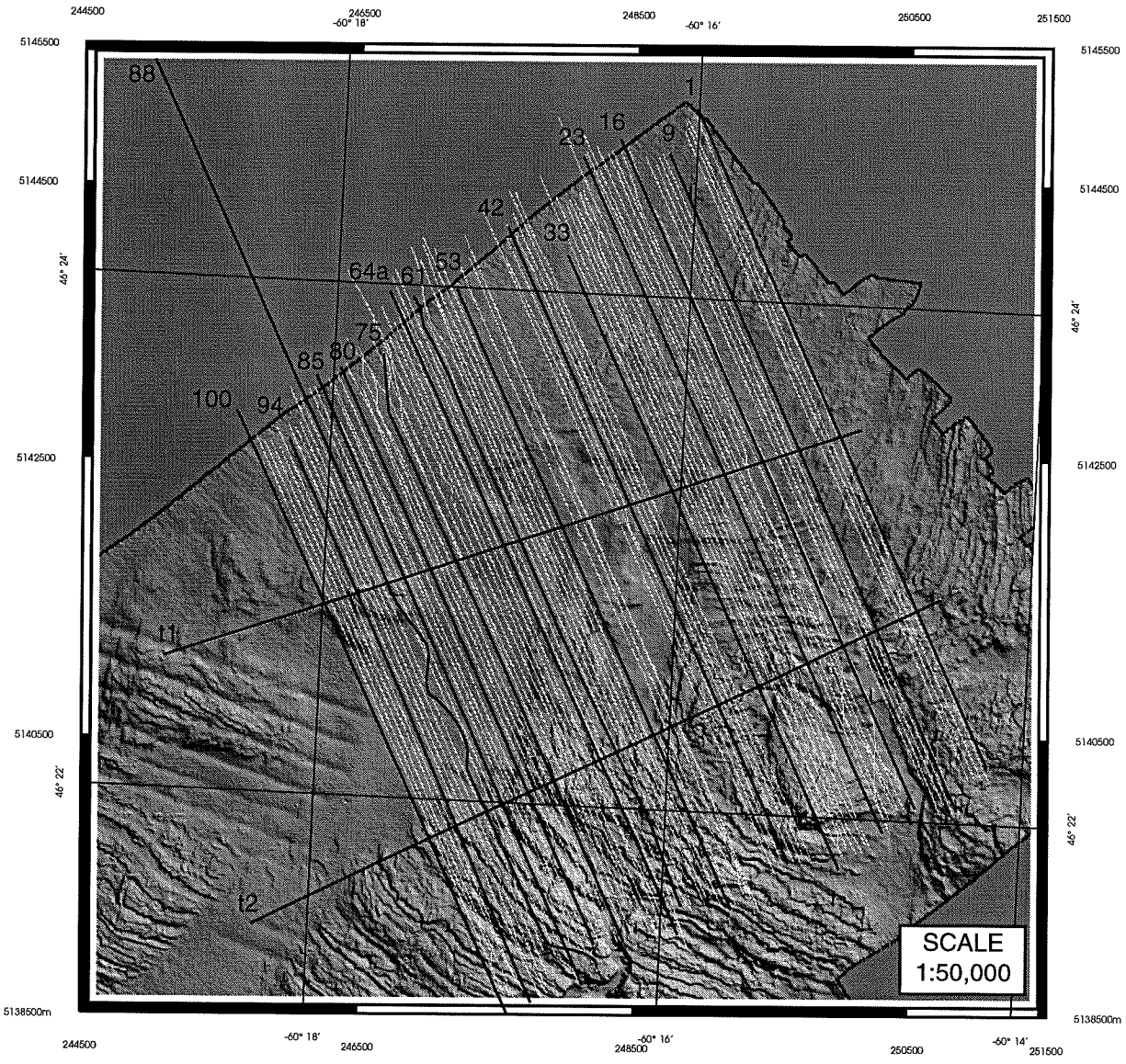

Figure B.1 The location of all seismic survey track lines that appear in this thesis. A total of 92 track lines cover the seismic survey area. Coordinates are in UTM and DEVCO grid (metric).

Two tie lines (t1 and t2) were shot perpendicular to the main track lines. Line t1 intersects offshore boreholes H12 and P5, Line t2 intersects borehole P6.

B.4 Seismic Source

This survey used a 40 cubic inch air gun (sleeve gun variety) seismic source (dominant frequency 250 Hertz). Pulse length is approximately 3 ms. An electronic signal triggers the air gun at regular intervals. Between shots, the air gun is charged with compressed air at 1600 p.s.i.. The seismic source was towed 18 metres from the stern and about 1 metre below sea level.

B.5 Hydrophone Receivers

The hydrophone receiver is part of a 24-channel streamer. Each channel of the streamer consists of an array of three hydrophones. This three hydrophone configuration is necessary for reducing noise that results from streamer motion while the vessel is underway. The total length of the streamer is 150 metres and, because of the length of the streamer, vertical motion was damped. A DGPS receiver at the tail of the streamer provided positioning data for the streamer. The distance from seismic source to hydrophone was 52 metres.

The streamer uses piezoelectric hydrophone receivers. A piezoelectric receiver measures changes in pressure in the vicinity of the hydrophone. During a change in pressure, such as passing sound wave, a piezoelectric crystal in the receiver produces an electric field which is converted to an electric signal and recorded on the survey vessel. The amplitude of the electric signal is proportional to the change in pressure at the hydrophone and is, therefore, a function of the amplitude of the sound wave.

B.6 Equipment Problems During the Survey

The survey encountered a number of equipment problems during the progress of the survey and these problems significantly affected the outcome. The survey was originally intended as a true 3-D survey (Yilmaz 1987), incorporating 24-channels. As a result of equipment failure, only four channels consistently recorded data (channels 2, 3, 4, and 5). Some channels only recorded usable data for short periods of time. The consequence of a four-channel data set is that it cannot be used for 3-D stacking and migration techniques; therefore, the data are best used as a single-channel set, using channel 2 because that channel has the lowest offset:water depth ratio.

B.7 The Nature of Bedrock Reflectors

Sound travels through different materials at different velocities. This concept underlies all aspects of reflection seismics, allowing layers to be imaged within the bedrock. Bedrock reflectors in well-stratified rocks represent the response of numerous layers (a reflector packet). The thickness of this reflector packet depends on the vertical resolution of the seismics (Section B.8). Within each reflector packet, an averaging effect takes place, and contrasts between individual layers within the packet will not be significant if the thickness of the layers is small relative to thickness of the packet. For this reason, thick layers of contrasting acoustical properties are more likely to be visible on the seismic record. However, this need not be the case, depending on constructive interference between reflector packets. Filtering effects of individual layers within packets (which will change as layer thickness and spacing changes) determine the continuity of the "interference reflectors". The appearance of the reflectors will be

further affected by the particular seismic equipment used, and the modes of shooting, recording and data processing (Ziolkowski 1979; Palmer 1987; Grant 1994).

B.8 Vertical Resolution

Vertical resolution is the ability to resolve individual, closely spaced reflectors. For two reflectors (one from the top and one from the bottom of a thin layer), the limit varies on how close they can be, yet still be separable on the seismic record. Vertical resolution is directly proportional to the dominant wavelength (λ) of the seismic signal. Dominant wavelength is:

$$\lambda = \frac{v}{f}$$

where v is the velocity of sound in the bedrock and f is the dominant frequency of the seismic signal. The acceptable threshold vertical resolution generally is a quarter of the dominant wavelength, although this can be subjective and depends on the noise level in the data (Yilmaz 1987). Vertical resolution VR then becomes:

$$VR = \frac{v}{4f}$$

Vertical resolution for the present data set is calculated as above. Velocity v is known from three offshore boreholes and Sonobuoy 71-1 (3419 to 3549 ms^{-1}), and dominant frequency for the seismic source is about 250 Hz. Vertical resolution in the seismic data is, therefore, between 3.4 and 3.6 metres.

B.9 Example of Converting Depth to Casing Shoe to Two-Way Time

The conversion of depth to the casing shoe to two-way travel time was necessary for the correlation of bedrock reflectors with lithology. The conversion accounted for survey geometry

and refraction at the sediment/bedrock interface, but does not account for refraction at the water/sediment interface. The following shows this conversion at the P5 borehole site:

Let D= depth of casing shoe below unconsolidated sediments in metres
(all other variables are defined on Figs. 5.3 and 5.4)
(s is calculated according to the model presented in Fig. 5.3)
(angles α and ϕ were estimated based on the survey geometry)

Time below seafloor $= 2((d\cos\alpha/V_1 + s\cos\alpha/V_2 + D\cos\phi/V_3) - Sf)$
$= 2((44\cos 9/1.5 + 7\cos 9/1.8 + 72\cos 17/3.4) - 33.5)$
$= 2((28.3 + 3.8 + 20.3) - 33.5)$
$= 104.8 - 67.0$
$= 37.8$ ms (two-way time)

B.10 Convolution Procedure for the Two Synthetic Seismograms

This thesis presented two synthetic seismograms that served as tools for the correlation of bedrock reflectors with lithology. Yilmaz (1987) summarises the convolution procedure as follows:

Definitions:

- ρ_k is the density at depth k
- v_k is the velocity at k
- c_k is the reflection coefficient for an interface at depth k
- w(t) is the established seismic impulse in time
- c(t) is the reflection coefficient for an interface at two-way time t (calculated from c_k based on v_k)
- x(t) is the synthetic seismogram in two-way time

Assumptions:

- $(\rho_{k+1} - \rho_k)$ is negligible compared to $(v_{k+1} - v_k)$
- source wave doesn't change as it propagates downwards
- no random noise

Reflection coefficient:

$$\bullet c_k = \frac{(\rho_{k+1}v_{k+1} - \rho_k v_k)}{(\rho_{k+1}v_{k+1} + \rho_k v_k)} \quad \text{becomes} \quad c_k = \frac{(v_{k+1} - v_k)}{(v_{k+1} + v_k)}$$

Convolution:

source wave * reflection coefficient = synthetic seismogram

$$w(t) * c(t) = x(t)$$